REPAIR OF IATROGENIC PRETERM PREMATURE RUPTURE OF HUMAN FETAL MEMBRANES

Dissertation

zur

Erlangung der naturwissenschaftlichen Doktorwürde

(Dr. sc. nat.)

vorgelegt der

Mathematisch-naturwissenschaftlichen Fakultät

der

Universität Zürich

von

Ajit Sankar Mallik

aus Indien

Promotionskomitee

Prof. Dr. Adriano Aguzzi(Vorsitz)

Prof. Dr. Urs Greber

Prof. Dr. Roland Zimmermann

PD Dr. Andreas Hugo Zisch (Leitung der Dissertation)

Dr. Martin Ehrbar (Leitung der Dissertation)

Zurich 2010

TABLE OF CONTENTS

SUMMARY

Preterm premature rupture of fetal membranes is a devastating complication of pregnancy with high risk of feto-maternal mortality and morbidity. Several attempts have been made to seal spontaneous and iatrogenic fetal membrane ruptures but none has made it to clinics. Persistent leakage of amniotic fluid following invasive surgical and diagnostic procedures jeopardize the benefit of such life saving interventions and draw the limits for the developing field of intrauterine fetal surgery. Efforts are directed to take action *before* the commencement of leakage of amniotic fluid rather than *after* the leakage in iatrogenic maneuver: one avenue of research focuses on prophylactic plugging of the fetoscopic lesion at the time of completion of the procedure, thus to increase the chance to prevent subsequent leakage of amniotic fluid. In order to design appropriate sealing strategies the knowledge of the mechanical and biological properties of intact and injured fetal membranes is indispensable.

The objective of this thesis is on the one hand to develop regimen that allow the repair of fetal membranes by plugging membrane lesions with fetoscopical interventions. On the other hand, we concentrate on the description of biophysical parameters of the fetal membrane by establishing biomechanical test regimen.

Towards a fetoscopic repair mechanism I have developed a method to decellularize amniotic membranes in order to produce a non-immunogenic material. These membranes proved to be stable enough for long term storage and for off-the-shelf use. In our animal trials using rabbit does, the material exhibited good handling properties as well as good sealing characteristics in absence of adverse biological effects. Although the plugs were at best marginally remodeled and populated with cells in these short term experiments in rabbits, the self locking features of the plugs and the predictably long term stability of the material might be a critically important for future clinical applications.

Towards the mechanical characterization of the fetal membranes I have together with the group of Prof. Edoardo Mazza, Department for Mechanics, ETHZ worked on the establishment of a novel device, which allows the measurement of mechanical properties and the testing of membrane sealing regimen under near to physiological

conditions. I have compared measurements of mechanical properties using this new generation device, which employs equibiaxial stretching with measurements performed with uniaxial stretching. These initial results indicate that the materials parameters can only be correctly estimated using biaxial stretching regimen and might add to the understanding of elastic and plastic features of biological membranes.

Collectively a thorough understanding of mechanical and biological properties and the design of materials platforms that can be adapted to the tissue requirements might only approach the complexity of this problem. Although much more research is needed, we think that our results on the membrane repair and the mechanical properties presented in this thesis are promising starting points towards the establishment of appropriate treatment regimen for PPROM of fetal membranes.

ZUSAMMENFASSUNG

Der frühe vorzeitige Blasensprung (PPROM) ist eine gravierende Komplikation während der Schwangerschaft und ist mit einem grossen Risiko für feto-maternale Morbidität und Mortalität verbunden. Verschiedene Versuche wurden unternommen um spontane und iaterogene Rupturen der fetalen Membran zu verschliessen, bisher konnte jedoch keine dieser Methoden in die Klinik eingeführt werden. Der anhaltende Verlust von Amnionflüssigkeit infolge invasiver chirurgischer und diagnostischer Eingriffe gefährdet den Erfolg von potentiell lebensrettenden Interventionen, und limitiert daher die Weiterentwicklung der intrauterinen fetalen Chirurgie. Gegenwärtige Anstrengungen fokussieren darauf zu handeln, *bevor* die Amnionflüssigkeit austritt, anstatt das Ausrinnen *nach* einem iaterogenen Eingriff abzuwarten. So gilt eine Forschungsrichtung dem prophylaktischen Verschluss der fetoskopischen Wunde im Anschluss an den Eingriff, um das Risiko eines nachfolgenden Flüssigkeitsaustrittes zu vermeiden. Um geeignete Verschlussstrategien entwerfen zu können, sind Kenntnisse hinsichtlich biologischen und mechanischen Eigenschaften von intakten und verletzten fetalen Membranen unabdingbar.

Das Ziel dieser Doktorarbeit ist einerseits eine Behandlung zu entwickeln, die die Reparatur von fetalen Membranen mittels Verstopfen der Membranläsion durch Fetoskopie erlaubt. Ein weiteres Ziel ist die Charakterisierung von biophysikalischen Parametern der fetalen Membranen, welches auch die Entwicklung einer biomechanischen Testprozedur beinhaltet.

Bezüglich fetoskopischer Reparaturmechanismen habe ich eine Methode zur Dezellularisierung von Amnionmembranen entwickelt, um daraus ein nicht immunogenes Material zu gewinnen. Diese dezellularisierten Membranen sind für die Langzeit-Lagerung geeignet und können daher serienmässig produziert und eingesetzt zu werden. In unseren Versuchen mit trächtigen Kaninchen zeigte das Material gute Handhabungs- und Verschlusseigenschaften ohne nachteilige biologische Effekte aufzuweisen. Obwohl die Verschlusspfropfen in diesen Kurzzeit-Experimenten nur geringfügig umgebaut und durch Zellen besiedelt wurden, dürften die selbstverschliessenden Eigenschaften der Pfropfen und deren voraussichtlich gute Langzeit-Stabilität wichtige Voraussetzungen für mögliche klinische Anwendungen erfüllen.

Um die fetalen Membranen mechanisch zu charakterisieren, habe ich in Zusammenarbeit mit der Gruppe von Prof. Eduardo Mazza, Departement für Mechanik, ETHZ an der Entwicklung eines neuen Gerätes gearbeitet. Dieses erlaubt die Messung von mechanischen Eigenschaften und das Testen von Verschlussmethoden der fetalen Membranen unter nahezu physiologischen Bedingungen. Ich habe in der Folge mechanische Parameter verglichen, die mit dem weiterentwickelten Testgerät unter equibiaxialer Dehnung oder mittels uniaxialer Dehnung erhoben wurden. Diese ersten Ergebnisse deuten darauf hin, dass die Materialparameter nur durch biaxiale Ausdehnung der Membranen korrekt erhoben werden können. Die in dieser Arbeit präsentierten Daten können unserem Verständnis für die elastischen und plastischen Eigenschaften von biologischen Membranen beitragen.

Insgesamt scheinen Lösungen zu diesem komplexen Problem nur durch das gründliche Verständnis der mechanischen und biologischen Eigenschaften sowie Materialien die den Bedürfnissen des Gewebes angepasst werden können, möglich zu sein. Obwohl weitere Untersuchungen benötigt werden, denken wir, dass unsere Resultate bezüglich Reparatur und Mechanik der fetalen Membran ein vielversprechender Anfang zur Etablierung von Behandlungsmethoden von PPROM darstellen.

ACKNOWLEDGEMENTS

The duration of my MDPhD in Zurich, has taught me the key to succeed in biological experimentation comes from constructive criticism, teamwork and self-organization. I would never have imagined coming to this point of my life without the support of following people:

Dr. Andreas H. Zisch has been the constant source of guidance, supervision and inspiration. The only reservation I carry along is that I am not fortunate enough to have him with me, while I am finishing my thesis. Dr. Zisch passed away on 2nd October 2009 after a long and brave battle against gastric carcinoma. He always advised me to consider every experiment important and deal with negative results with equal enthusiasm. In addition to his supervision, he gave me rare opportunities to review scientific articles, write grants and present my scientific work in an international environment. During his illness also he was never short of dedication towards science, which led to a significant publication even from his hospital bed. Rare are such great souls. I would like to dedicate my thesis to Dr. Zisch.

Prof. Adriano Aguzzi is the head of my MDPhD committee. I'm indebted to him for accepting me into the prestigious MDPhD programme. His critical guidance, review of my work from time to time and his brilliant ideas have shaped many of my thesis work.

Prof. Urs Greber is a member of my thesis committee. He has been constantly supportive in guiding various crucial experiments and designing them.

Prof. Roland Zimmermann is a member of my thesis committee. Being the director of the institute, he provided me with the opportunity to take part in one of the most difficult projects of tissue engineering. Despite his busy schedule, he has always taken personal interest in my project work and helped me connect to various crucial contacts that have been a valuable part of my work. His clinical inputs have shaped many of the experiments I have performed.

Dr. Martin Ehrbar is a member of my thesis committee. He substituted Dr. Zisch after his sad demise as my supervisor and since then has supported me in all possible ways. I'd specially mention his contribution towards correction of my thesis. I am also

thankful to Swiss National Science Foundation (SNSF) and Zurich center for Integrative Human Physiology (ZIHP) for their financial support during my PhD.

Dr. Grozdana Bilic needs a special mention for her relentless support during my thesis work. We have worked together on many interdependent projects and experiments. The scientific arguments with her have always stimulated me to get to know more.

Dr. Steffen Zeissberger has been a supportive lab member and good friend. I would acknowledge his critical discussions, support and suggestions in many experiments. It has been a pleasure to know and work with him all these years.

I can never thank my lab members and collaborators enough as they have provided me with their professional and personal support at all levels of my thesis work. I would like to acknowledge:

Prof. Edoardo Mazza, ETH for his excellent collaboration of the biomechanical evaluation of fetal membranes. He has introduced me to the biomechanics and brought me to a stage to understand this fascinating topic at tissue level.

Esther for her support in histology and her help in day-to-day lab work.

Claudia Haller for her help in collagen assay.

Dr. Mahmood Jabareen for his collaborative work in the uniaxial experiments on human fetal membranes.

Julien Egger has been an excellent co-worker in the biaxial analysis of fetal membranes. He has played the most important role in designing the ex vivo apparatus to evaluate fetal membranes. On personal front, he is a great friend.

Marc Hollenstein for his support in understanding and designing the uniaxial experiments.

Oleg Semenov and Algirdas Ziogas for being supportive in the lab.

During my stay in Zurich, many good friends have stood by me and supported me through out the phase of my PhD. I would like to acknowledge:

Payal, for her unconditional and relentless support both in scientific and personal front. She needs a special mention for constantly encouraging me during the downs of my PhD phase. Thanks for being there.

Annapoorna, for her personal support and care as a true friend.

Chitrangada, for her support, encouragement and discussions at length.

Raj for being a great friend in need.

I would also like to express my gratitude to Srini, Essai, Sarath, Naresh, Sowmini, Kalpana, Daalia, Leila and Marco for being such good friends during this phase of my life.

None of this would have been possible without the love and support of my parents who have been patient enough to bear with me in difficult times and encourage me whenever I felt low. It gives me immense pleasure to thank them for believing in me whenever I was preoccupied with thoughts of self-doubts. I would also like to thank my sister Liti and brother Pinu who have been more like friends and confidant and a continuous source of inspiration. My family has always made their presence so obvious despite the huge geographic distance between Zurich and India. Without their blessings, emotional support, encouragement, I would not have been where I stand in life now.

Last but not the least, I thank the Almighty for EVERYTHING.

Chapter 1

General Introduction

General Introduction

1.1 Human Pregnancy and Fetal Membranes

Human pregnancy and parturition are unique and complex events. The central theme of these biological events is a "developing human" which by convention is known as "fetus". The whole organization of the pregnancy is housed in a specialized extra-embryonic bilayered bio-sac, within the uterus. This extra-embryonic tissue collectively known as "fetal membranes" or "chorioamniotic membrane" contains the developing fetus and the amniotic fluid. The outer layer of this bio-sac is the vascular chorion and the inner layer is the avascular amnion. The Placenta, a specialized part of fetal membranes, establishes the feto-maternal circulation, hence the nutritional lifeline for the fetus. The unique features of the fetal membranes are, their limited tissue life span only for the duration of pregnancy and their physiological rupture as the fetus reaches term of pregnancy. As premature rupture of the chorioamniotic membrane is a serious problem associated with morbidity and mortality of the fetus, treatment options are highly demanded. In this thesis, the development of the chorioamniotic membrane, the spontaneous and surgically induced membrane failures as well as treatment regimens, which prevent the defect progression and the biomechanical evaluation of the tissue are discussed.

1.1.2 Development of Fetal Membranes

The initial documented drawings of fetus and fetal membrane goes back to Leonardo da Vinci during 15th century A.D. (Figure 1.1).

Figure 1.1: Drawing of a cut-open uterus with fetus inside it, by Leonardo da Vinci. Adapted from www.royalcollection.org.uk

Early in the process of implantation, the cells in the "Blastocyst" arrange themselves into an outer layer of cells known as "Trophoblasts" and a group of centrally located cell mass known as "Inner cell mass" or "Embryoblasts" (Figure 1.2). In the beginning, the inner cell mass is accumulated at one end of the blastocyst which is the embryonic pole, leaving one cavity inside the blastocyst known as blastocyst cavity. The trophoblasts differentiate into cytotrophoblast (lining the blastocyst) and the syncytiotrophoblasts that help the invasion of endometrium at the embryonic pole. With the gradual progress of implantation of the blastocyst, a small cavity develops in the inner cell mass, which is the primordium of the amniotic cavity. At this time point, the cells that line the inner surface of the trophoblasts in this cavity are called amniogenic cells or amnioblasts. The amnioblasts form the amnion that encloses the amniotic cavity (Figure 1.3). The human amnion is first identifiable at about the 7th or 8th day of embryonic development.

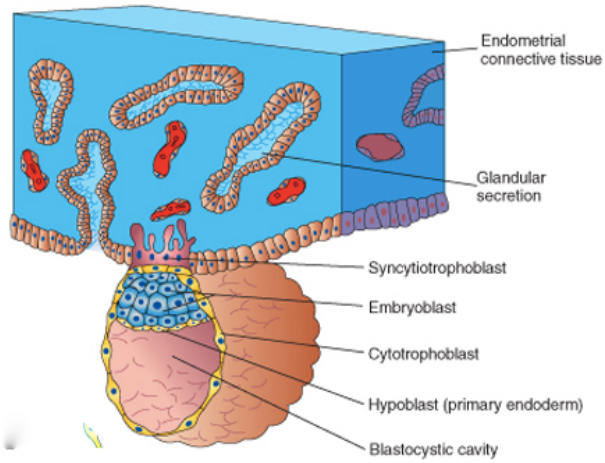

Figure 1.2: Attachment of blastocyst to the endometrial epithelium. In the early stage of implantation, the blastocyst cavity is formed. The trophoblast layer is differentiated into sycytiotrophoblast and cytotrophoblast.

As the formation of the amniotic cavity towards the embryonic pole of the blastocyst proceeds, further morphological changes in the inner cell mass bring about the formation of two new structures: the bilaminar "embryonic disc" and the "exocoelomic cavity". The embryonic disc forms the separation between the two

cavities i.e. the amniotic cavity and the exocoelomic cavity (Figure 1.3). The embryonic disc at this stage consists of two layers of the following cells namely the:

a) Epiblasts, a thick layer of columnar cells forming the floor of the amniotic cavity, which continues peripherally with the amnion (Figure 1.3).

b) Hypoblast or primary ectoderm, consisting of small cuboidal cells forming the roof of the exocoelomic cavity which continues with the exocoelomic membrane. The exocoelomic membrane cavity along with the lining hypoblasts soon becomes modified to be the primary umbilical vesicle (Figure 1.4).

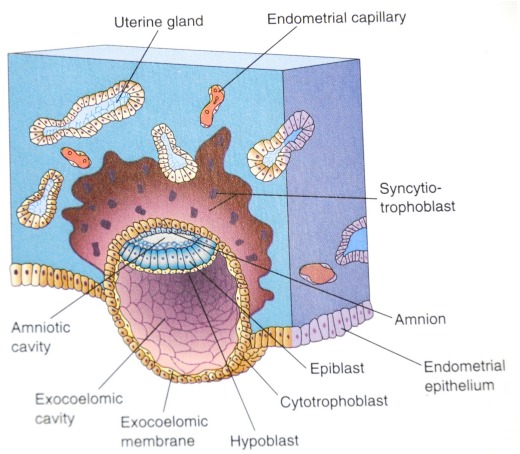

Figure 1.3: Drawing of an implanted blastocyst, showing the formation of the amniotic and the exocoelomic cavity. Adapted from Elsevier Moore and Persaud, The Developing Human 8e, www.studentconsult.com

Cells from the endoderm of primary umbilical vesicle form a layer of connective tissue known as “extra embryonic mesoderm” (Figure 1.4).

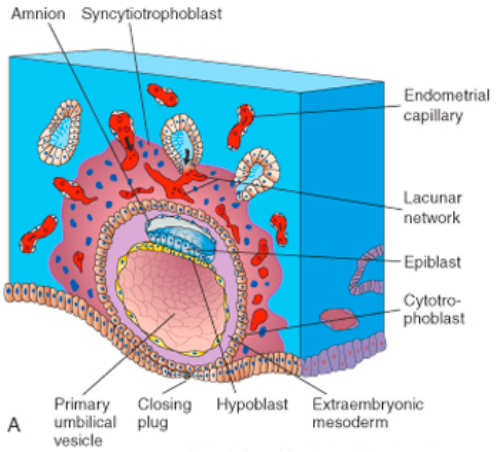

Figure 1.4: Formation of the extraembryonic mesoderm and the primary umbilical vesicle. Adapted from Elsevier Moore and Persaud, The Developing Human 8e, www.studentconsult.com

With the appearance of an isolated cavity known as "extra embryonic coelom", two new layers are created in the extra embryonic mesoderm (Figure 1.5). These layers are the:

1) Extraembryonic somatic mesoderm that lines the trophoblast and covers the amnion

2) Extraembryonic splanchnic mesoderm that surrounds the umbilical vesicle

The extra embryonic somatic mesoderm and both layers of the trophoblast form the chorion. The extra embryonic coelom becomes the chorionic cavity.

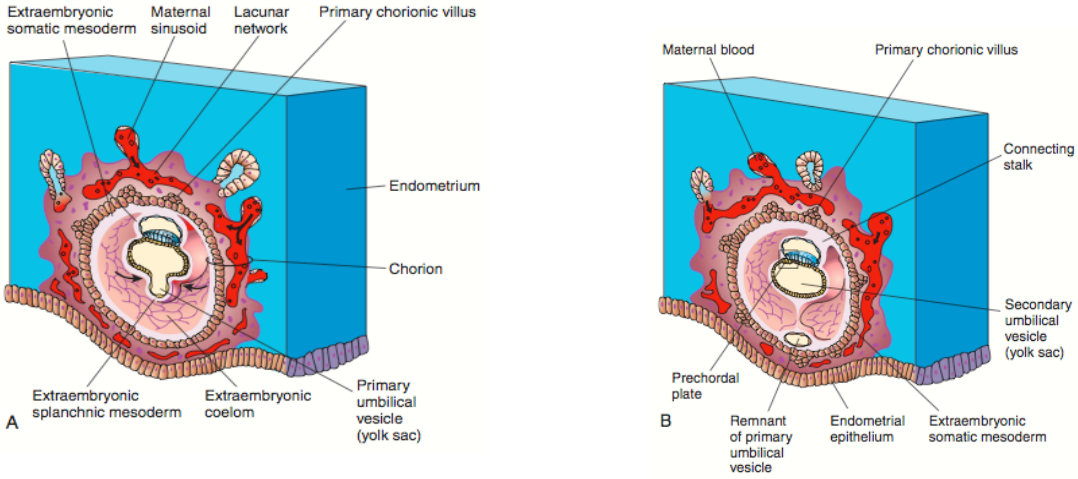

Figure 1.5: Sections through implanted human embryo. **A)** At day 13, the primary umbilical vesicle decreases in size and the primary chorionic villi appear. **B)** Newly

formed secondary umbilical vesicle. Adapted from Elsevier Moore and Persaud, The Developing Human 8e, www.studentconsult.com

The amniotic sac and the umbilical vesicle can be thought of as two balloons pressed together (at the site of embryonic disc) and suspended by a cord (connecting stalk) from the inside of a larger balloon (chorionic sac).

1.1.3 Structure of human fetal membranes

Fetal membranes are the reflected portions of the placenta and have two distinct layers apposed upon each other. The inner layer is amnion and the outer layer is chorion. Both layers show marked regional variations in term of parenchyma, thickness, and mechanical properties across the surface.

The fetal membranes do not have innervations. The inner amnion layer is avascular, whereas the outer chorion layer has small numbers of blood vessels (Figure 1.6). As the thickness of both the layers together come out between 0.5mm to 1mm, they get the nutrition by diffusion from amniotic fluid and uterine wall vessels. Although only 20% of the thickness of fetal the membranes, amnion is described to provide the majority of the tensile strength of the membrane(Oyen et al., 2004). Even though both amnion and chorion act as a single unit, there have been postulations that both layers can slide over each other. This sliding phenomenon can have important implications on natural defect closure and healing approaches(Gratacos et al., 2006).

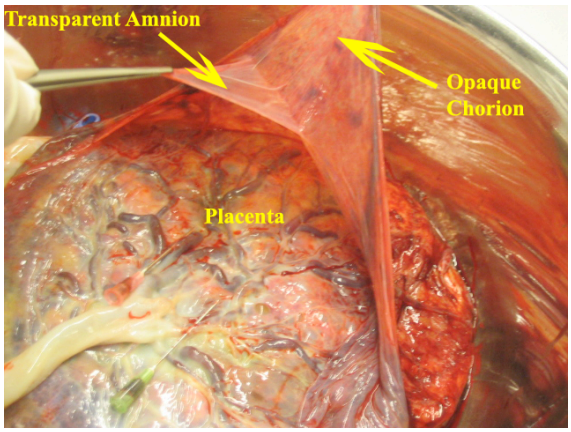

Figure 1.6: Separation of both amnion and chorion layers by blunt dissection of the fetal membranes. Here the fetal membranes are reflected from the border of the freshly collected placenta.

Histologically, the amnion and the chorion have been divided into distinct sub-layers as shown in (Figure 1.7). On the surface of the amnion, epithelial cells secrete collagen types III, IV and non-collagenous glycoproteins, which form the basement membrane. Mesenchymal cells in the amnion secrete collagens into the compact layer of the amnion. Interstitial collagens type I and III align in parallel bundles, which are responsible for mechanical integrity of the membrane, whereas type V and VI collagens form filamentous connections between interstitial collagens and the basement membrane. The thickest layer of the amnion i.e. the fibroblast layer is composed of type I, III, VI collagen. The spongy layer of the amnion is composed of mostly non-fibrillar type III collagen and this forms the interface between amnion and chorion.

The chorion stays apposed to the decidua of uterine cavity. The chorion has 3 layers, such as the inner reticular layer, the intermediate basement membrane and the outer trophoblast layer. The reticular layer is apposed to the spongy layer of the amnion and secretes collagen types I, III, IV, V and VI. The basement membrane consists of type IV collagen, fibronectin and laminin. The trophoblast layer marks the separation between fetal membranes and uterine decidua.

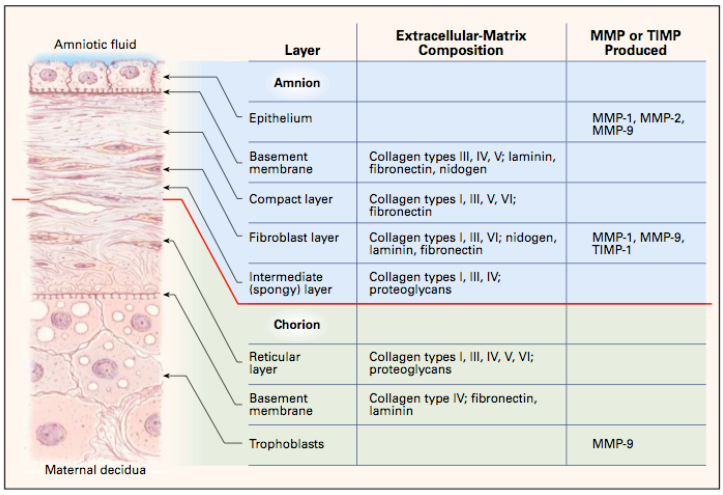

Layer	Extracellular-Matrix Composition	MMP or TIMP Produced
Amnion		
Epithelium		MMP-1, MMP-2, MMP-9
Basement membrane	Collagen types III, IV, V; laminin, fibronectin, nidogen	
Compact layer	Collagen types I, III, V, VI; fibronectin	
Fibroblast layer	Collagen types I, III, VI; nidogen, laminin, fibronectin	MMP-1, MMP-9, TIMP-1
Intermediate (spongy) layer	Collagen types I, III, IV; proteoglycans	
Chorion		
Reticular layer	Collagen types I, III, IV, V, VI; proteoglycans	
Basement membrane	Collagen type IV; fibronectin, laminin	
Trophoblasts		MMP-9

Figure 1.7: Schematic histological drawing to show different layers of amnion and chorion. Adapted from Parry et.al 1998

1.1.4 Physiological functions of the fetal sac

The fetal membranes create a highly specialized environment for the growing fetus throughout the duration of pregnancy. The dynamics of fetus and amniotic fluid are

well compensated by the elasticity and the tensile strength of the fetal membranes. Both layers of fetal membranes secrete substances to both directions and also allow passive diffusion of nutrients, water, oxygen and hormones while acting as a barrier to ascending infections from the urogenital tract of the mother during pregnancy.

The amniotic fluid contained in the fetal membrane sac increases gradually along the course of pregnancy, reaching about 30 ml at 10 weeks and 700-1000 ml by 37 weeks. It protects the fetus against injuries and also maintains body temperature, fluid and electrolyte homeostasis, provides space for development, and prevents the fetus to adhere to the amnion. Interestingly, the water content of the amniotic fluid gets changed every 3 hours by large volumes entering through the chorioamniotic membrane into maternal tissue fluid. The floating fetus swallows the amniotic fluid and the respiratory and digestive tracts of the fetus absorb it.

1.1.5 Normal outcome of a pregnancy

The normal successful pregnancy ends in childbirth at around term i.e. 37 completed weeks of gestation. Childbirth is the period from the onset of regular uterine contractions till the expulsion of the placenta through the birth canal of mother. The process by which childbirth normally occurs is known as labor in the obstetrical context. Human labor involves dynamic hormonal changes for its initiation and progression such as corticotropin-releasing hormone (CRH) from the fetal hypothalamus, pituitary adrenocorticotropin (ACTH), oxycitocin from the posteriorcerebral hypophysis and prostaglandin from decidua. The stages of labor include the expulsion of fetus, placenta, and fetal membranes from the mother's uterus by coordinated, involuntary uterine contractions. During the waves of contraction the positioning of the fetus along the uterine axis leads to simultaneous dilatation of the cervix, effacement of the fetus, and eventually rupture of the fetal membranes. Human labor is divided into four stages, such as dilation, expulsion, placental and recovery stage.

1.2. Rupture of fetal membranes

1.2.1 Physiological rupture of the membranes at term

The chorioamniotic membrane is perhaps the only tissue that ruptures physiologically. The rupture of the fetal membranes is coordinated with the physiological maturation

of the growing fetus and occurs in the second stage of active labor, which involves the expulsion of the fetus, following the complete dilation of the cervix in the first stage. A cascade of events ranging from mechanical modification, apoptosis in the fetal membranes, weakening of a zone of fetal membranes, remodeling of collagen and extracellular matrix components have been implied to play roles in the initiation of rupture of the fetal membranes (Osman et al., 2006). In normal pregnancy, labor starts between 38 to 42 weeks' gestation. Rupture of fetal membranes before 37 weeks' gestation, might result in premature birth and thus bears a large risk for serious clinical complications of the new born.

1.2.2 Premature Rupture of the fetal membranes

As defined by the World Health Organization (WHO), rupture of the fetal membranes at term (completed 37 weeks' gestation) but prior to the onset of labor is defined as "premature rupture of fetal membranes" (PROM). In consequence, PROM before 37 weeks of gestation is termed "preterm premature rupture of fetal membranes (PPROM). While PROM occurs in 8-10% of all pregnancies, PPROM affects 4-5% of all pregnancies and 30-40% of all preterm deliveries, and is the leading identifiable cause of preterm birth. Two types of PPROM i.e. **spontaneous (sPPROM) and iatrogenic (iPPROM)** are distinguished in Table 1.1.

1.2.3 sPPROM

In general, sPPROM is an irregular, difficult to heal, large dimension wound situated above the internal ostium of the cervix in 90% of all cases (Table 1.1).

sPPROM, as per definition, occurs at least 1 hour before the onset of contraction of uterus (Goldenberg et al., 2008). It is an unusual obstetric outcome in most species undergoing labor, except human. The reason for this outcome is sometimes attributed to the bipedal upright posture that compromises the mechanical properties of fetal membranes in the dependent part in humans (Bryant-Greenwood and Millar 2000) . sPPROM is the single most important etiology of all preterm births.

Table 1.1

	iPPROM	**sPPROM**
Schematic figure	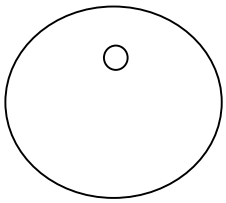	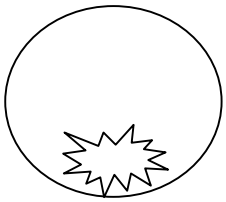
Etiology	Mechanically induced wound	Multifactorial weakness of the membrane
Size	Depends on the diameter of the used instruments in mm.	Supposed to be larger in terms of few centimeters
Shape	Round puncture wound with sharp demarcation	Irregular shape and poor demarcation
Status of the membrane	Clean and healthy without inflammation	Often associated with some form of inflammation
Incidence	0.1- 1% following amniocentesis 5-100% following open fetal surgeries and fetoscopy	4-5% of pregnancies
Time in gestation	Usually in the 2nd trimester Amniocentesis: 14th-16th week of gestation	Towards the later part of gestation (3rd trimester) and before 37 completed weeks.
Site	At the site of intervention	Above internal os of cervix in 90% cases
Outcome	Termination of pregnancy Serious maternal and fetal complications	Termination of pregnancy Serious maternal and fetal complications

1.2.4 Iatrogenic PPROM (iPPROM)

1.2.4.1 iPPROM: Achilles heel of fetal surgery

iPPROM occurs due to invasive interventions by the physician on the intact fetal sac. Since invasive diagnostic and therapeutic fetal interventions are integral part of modern obstetrics, the devastating aftermaths of such surgical procedures are of importance. Complications often associated with fetal surgery are amniotic fluid leakage, separation of both layers of fetal membranes and iPPROM. However, iPPROM with an incidence of 5-100% stands out as the most significant complication after injury of the fetal sac after such interventions.

Two major domains of invasive fetal interventions are open fetal surgery and its less-invasive counter part endoscopic or fetoscopic interventions. Even though both forms of fetal interventions have advantages and drawbacks, endoscopic surgery is gaining more and more acceptance for its less invasiveness and less postoperative complications.

In the case of open fetal surgeries, under general endotracheal anesthesia, the uterus is exposed by large laparotomy and opened with surgical staples. The fetus is partially exposed or exteriorized to follow the actual procedure to be performed on it. Two major conditions that are treated by open fetal surgical procedures are congenital cystic adenomatous malformation and myelomeningocele. None of these two conditions are amenable to fetoscopic interventions. The most important drawbacks of open fetal surgeries are high fetal mortality and significant maternal morbidity due to preterm labor and premature rupture of membranes. Other noteworthy complications are uterine rupture, chorioamnitis, life long need for cesarean delivery for subsequent pregnancies.

Boosted instrumental innovations in the form of video endoscopic surgery, miniaturization of cameras, fiber endoscopes have revolutionized the field of minimally invasive fetal surgeries. The first clinical fetoscopic surgeries were performed on umbilical cord and placenta, referred as “obstetric endoscopy”. Endoscopic or keyhole access to the fetal cavity definitely is advantageous compared

to open fetal surgery concerning preterm labor and maternal morbidity. Fetoscopic interventions can be classified as obstetrical endoscopy, which includes procedures like laser coagulation of placental or umbilical cord vessels, and fetoscopic surgery, where the procedure is performed on the fetus itself. The conditions or disorders amenable to intervention with minimal access surgical techniques are listed in Table 1.2.

Table 1.2: Conditions amenable to minimal access surgery, adapted from (Fowler et al., 2002)

Neonatal	Fetal
Gastoesophageal reflux	Congenital Diaphragmatic hernia
Pyloric stenosis	Urinary tract obstruction
Patent ductus arteriosus	Amniotic bands
Hirschprung's disease	Pleural effusion
Inguinal hernia	Sacrococcygeal teratoma
Malrotation	Diseases of monochorionic twins
Ovarian cyst	Discordant anomalies
Congenital Diaphragmatic hernia (CDH)	Twin reversed arterial perfusion
Cryptoorchidism	Twin-twin transfusion syndrome
Lung biopsy	
Cholecystectomy	
Nephrectomy	
Esophageal atresia	
Tracheoesophagela fistula	

In amniocentesis, the incidence of iPPROM is i.e. 0.5-1%. The incidence of iPPROM following diagnostic fetoscopy is 3-5%; following operative fetoscopy is 5-8%. In a

trial of fetoscopic endoluminal tracheal occlusion for severe CDH, the rate of iPPROM was reported to be 100% (Harrison et al., 2003).

Since such procedures are performed in the first or second trimesters of pregnancy at a pre-viable gestational age, the associated perinatal morbidity and mortality following iPPROM, definitely falls short of the expected benefits of the very procedure. Hence iPPROM remains the Achilles' heel of fetal surgery. It is not surprising for this reason that, rescue of pregnancy following iPPROM demands immediate sealing of the port of amniotic fluid leakage

1.2.4.2 Instruments used in minimally invasive fetal surgeries

Depending on the time of interference during gestation, the generic instruments for minimal invasive procedures on the developing human are named fetoscopes, or embryoscopes.

Embryoscopy defines the direct examination of the embryo through the amniotic membranes during 9-10 weeks' gestation by introduction of an endoscope through the exoceolomic space. Embryoscopy is performed either by transcervical or transabdominal route and does not injure the amnion membrane (Ville et al., 1997). Beyond 12 weeks' gestation, embryoscopy becomes difficult or impossible as the chorion layer of the fetal membrane fuses with the amnion layer.

Transcervical embryoscopy is performed by introduction of a rigid scope through the cervical canal. The rigid scope enters the exoceolomic cavity after delaceration of the chorion. While entering, the scope is kept perpendicular to the fetal membranes to avoid tenting, which may cause separation of the chorion from the uterine wall.

In case of transabdominal embryoscopy, local analgesia is used down to the myometrium, at the point of insertion of the trocar. A small skin incision is often required.

Fetoscopy is the examination of the fetus after 11 weeks' gestation. This is performed transabdominally in the amniotic fluid. It is to be noted that, physiological fusion of amnion and chorion beyond 11 weeks' gestation, does not allow exoceolomic embryo-fetoscopy. Thus the amniotic cavity is entered under the direct vision of the uterus using the "Seldinger technique" (Seldinger 1953).

Even though fetoscopy can be performed in the amniotic fluid environment, distension media is used to improve visualization and working space around the surgical field. The common distension media are warm ringer lactate solution and carbon dioxide gas.

1.2.4.3 Mortality and morbidity associated with PPROM

The devastating nature of PPROM is due to the fact that premature infants are at higher risk than their term counterparts and there exists no definitive treatment to arrest the course of both forms of PPROM. Preterm birth alone is responsible for 75% of all deaths in perinatal life (Michels 1950) of which two thirds are due to infants delivered before 32 weeks' gestation.

Surviving infants suffer from a broad range of morbidities such as respiratory distress syndrome (RDS), cerebral palsy, blindness, deafness, kernicterus, intestinal bleeding, patent ductus arteriosus (PDA), neuro-sensory deficits, subnormal heights, lower IQ. All the morbidities are directly linked with the prematurity, for example in case of RDS, the type II alveolar cells in the lining of alveoli of lungs are deficient. These cells secrete surfactants to reduce the surface tension across the alveoli and help the newborn to breathe. In premature infants the absence of type II alveolar cells makes the alveoli collapse and prevent breathing.

1.3 Management of PPROM

1.3.1 Medical management of PPROM

The **diagnosis of PPROM** is crucial in the management process. Expectant mothers complain of leakage of fluid either in the form of "gush of fluid" or steady trickle of small amounts of fluid per vagina. On physical examination, pooling of amniotic fluid is seen in a speculum examination in the posterior vaginal vault. In certain cases, frank pooling of amniotic fluid is not found, rather leaking is present at the cervix up on pushing of the fundus of uterus, cough or strains (Duff 1996). Two commonly used biochemical tests help to clear the confusion if physical examination is inconclusive along the history, such as nitrazine test and fern test. Following diagnosis, the major goal of management is to extend the period of latency aiming to maximize the gestational age at the time of delivery.

The **natural history of PPROM** is labor, which once started leaves no option for active interference to prolong the gestational period. However, prolonged rupture of membrane is associated with an increased risk of maternal and fetal morbidity due to infections, pulmonary hypoplasia, skeletal deformities and Potter's facies (Thomas and Smith 1974). Neonatal survival before 20 weeks' gestation is rare even though a period of latency is allowed from ruptured state up till delivery. When PPROM occurs between 20 and 24 weeks (Falk et al., 2004) the prognosis increases with increasing gestational age at the time of rupture. Remarkably, in three different studies, considering 20 to 36 weeks of gestation, time from PPROM to labor was 48 hours in 49% to 93% of the patients and only in 7% to 51%, pregnancy could be extended for 7 more days (Graham et al., 1982; Nelson et al., 1994).

Administration of steroids has been one of the main stay of management during the latency phase of PPROM. Steroids stimulate the synthesis of surfactants by the type II alveolar cells; hence the incidence of respiratory distress syndrome reduces significantly (Imseis and Iams 1996)

The **use of antibiotics** during the latency period following PPROM aims to prevent ascending maternal infection and reduces neonatal morbidity. In a randomized controlled trail (Lockwood et al., 1993) piperacillin was compared to a placebo and it was reported that there was significant increase in the latency period but no improvement in neonatal morbidity and mortality.

Clinical management of PPROM is symptomatic and there exists no treatment that targets the pathology i.e. ruptured fetal membranes. Actual management varies from Institution-to-institution and includes immediate delivery or termination of pregnancy versus a conservative approach with various combinations of tocolytics, steroids and antibiotics. However there has been tremendous pool of experimental approaches to heal or seal the actual lesion.

1.4 Repair of PPROM

1.4.1 Approaches to repair PPROM

The strategies to treat PPROM aims at restoring the continuity of the fetal sac and thereby prevent leakage of amniotic fluid prior to term pregnancy. In this context,

both sPPROM and iPPROM would need a common approach to secure the leaking amniotic fluid, leading to a "repaired" fetal sac that can carry the pregnancy up to term. If carefully noted, approaches to repair a ruptured fetal membrane must be distinguished:

a) Approaches after the leakage starts i.e. mostly in cases of sPPROM

b) Approaches before the leakage starts i.e. mostly in cases of iPPROM

There have been clinical attempts to secure the site of amniotic fluid leakage following sPPROM and iPPROM by physical plugging the cervix or the defect site with liquid sealants or solid biocompatible scaffolds. One of the very initial trials was inspired by natural blood clotting process, i.e. injection of clotting agents to form a blood clot at the lesioned membrane or at the cervix (Sener et al., 1997). In another example, sealing of sPPROM was approached by delivery of maternal platelets mixed with fibrinogen through fetoscopic application "amniopatch" (Quintero et al., 1999). W. Mulla et al (Sciscione et al., 2001) tried off-the-shelf fibrin sealant intracervically and Quintero et al reported a success rate of 50% with the "amniopatch" technique to seal iPPROM lesions (Quintero 2001). In an interesting trial with 4 human cases, Young et al., reported successful closure of post-amniocentesis rupture sites in 3 cases by sequential endoscopic delivery of platelets, fibrins and powdered collagen slurry (Young et al., 2004). In terminal cases, having high risk of pregnancy loss, biologically compatible scaffold materials have been tried. In one such case, at 17 weeks' of gestation, collagen plug was placed endoscopically over the internal ostium (Sener, Ozalp et al. 1997; Quintero et al., 2002) following sPPROM; this pregnancy continued till 30th week despite recurrence of amniotic fluid leakage after day 14 of the intervention to secure the same. In another attempt, gelatin sponges were used for sPPROM before 21 weeks' gestation, which resulted in survival of 8 fetuses out of 14. However some of the surviving fetuses were reported to have musculoskeletal anomalies (O'Brien et al., 2002). Despite their potential feasibility to secure the rupture site, none of the methods could make their ways to clinics. There exists a need to innovate new material strategies, which should have the combination of tissue-adhesives with long-term engraftments and low resorption nature under wet conditions.

Approaches to seal before the actual leakage takes place require good surgical skills, accurate localization of the lesion and exact delivery of biosealants and/or solid bioscaffolds. One avenue of research concerns prophylactic sealing of fetoscopy sites to stop amniotic fluid leakage before the final withdrawal of the fetoscope from the fetal sac. As mentioned earlier, the sequential injection of platelets, fibrin glue and powdered collagen slurry by Young et al (Young, Mackenzie et al. 2004) proved the feasibility of such an attempt. It is noteworthy, all trials so far along this line have been preclinical and the animal model for this has been midgestational rabbit. In 1999, Deprest et al. (Deprest et al., 1999) demonstrated technical feasibility to deploy collagen plugs by fetoscopic means, onto surgically exposed amnion sacs in the rabbit model. The important read out parameters in such attempts were integrity of the amnion sac, maintainance of amniotic fluid volume and fetal survival. Both solid scaffolds made of collagen and synthetic polymer plugs were used in such attempts , listed in Table 1.3.

Table 1.3: Plugs used for closure of fetoscopic access sites

Study	Plugging material	Animal	Improved amniotic integrity
Papadopulos et al. (1998) [16]	Collagen (Colgen®)	rabbit	No
Deprest et al. (1999) [24]	Collagen (Colgen®)	rabbit	No
Luks et al. (1999) [26]	Gelatin sponge (Gelfoam) + myometrial suture	sheep	All foetuses survived till the ewes were killed near term
Luks et al. (1999) [26]	Gelatin sponge (Gelfoam) + myometrial suture	rhesus monkey	3 out of 5 foetuses survived till spontaneous delivery
Gratacos et al. (2000) [25]	Collagen (Colgen®) + myometrial suture	rabbit	Yes
Gratacos et al. (2000) [25]	Matrigel + myometrial suture	rabbit	No
Devlieger et al. (2003) [36]	Porcine small intestine (bioSIS) contains transforming growth factor-β and basic fibroblast factor	rabbit	Yes
Papadopulos et al. (2006) [27]	Collagen (TissueFoil E®) + fibrin sealant + myometrial suture	rabbit	Yes
Papadopulos et al. (2006) [27]	Tissue banked human amnion membrane + fibrin sealant + myometrial suture	rabbit	No
Papadopulos et al. (2006), Mallik et al. (2007) [15, 27]	Collagen foil (TissueFleece®) + fibrin sealant + myometrial suture	rabbit	Yes
Mallik et al. (2007) [15]	Decellularized human amnion + fibrin sealant + myometrial suture	rabbit	Yes
Ochsenbein-Kölble et al. (2007) [32]	Decellularized rabbit amnion + myometrial suture	rabbit	Yes
Ochsenbein-Kölble et al. (2007) [32]	Polyestherurethane (Degrapol)	rabbit	Yes

Each such method did not exhibit any significant benefit for restoration of the amniotic fluid volume and fetal sac's integrity, but combination of collagen plugging along with myometrial suture showed it to be successful (Deprest, Papadopulos et al. 1999). In a noticeable report gelatin sponges were applied for long-term closure of fetoscopic access site in sheep and rhesus monkeys having gestational ages of 145 and 165 days respectively (Luks et al., 1999). Endoscopic evaluation showed swelling of inserted gelatin sponge as it absorbed fluid and this lead to self-locking of the sponge at the membrane defect. The common notion of low or absent anatomical repair and poor plug engraftment in fetal membranes has motivated researchers to seek local biological repair modules at the very site of the lesion by tissue engineering approaches. Graft materials were supplied with growth factors or amnion cells to enhance cell migration and graft colonization (Bilic et al., 2004; Papadopulos et al., 2006). Bilic et al. (Bilic et al., 2005) used collagen and fibrin gels seeded with amnion epithelial and mesenchymal cells to mimic native amnion tissue in vitro. Even though fibrin gels were more suitable in this in vitro study, the rate of resorption was too fast to envision an animal trial. Similarly, collagen plugs in this study contracted dramatically, which would result in sloughing of the plug material and rapid loss of plug at the site of application in vivo.

1.4.2 Why approaches to repair PPROM failed?

The strategy to repair PPROM has been to secure the leakage of amniotic fluid by "plugging" or "patching" the rupture site. The possible reasons for the failure of multiple attempts can be summarized as below.

1. Difficulty in localizing and accessing the site of rupture in the uterine cavity

2. Wet environment due to constant presence of amniotic fluid

3. Mismatch between the applied plug material and native fetal membrane. This could be due to biological and biomechanical factors.

1.4.3 Holistic approach to repair fetal membrane rupture: Insight gained from iPPROM

As noted in the previous sections, the repair strategies towards fetal membrane rupture should include a holistic approach that involves both bioengineering aspect of patching and gluing plus biomechanical matching of the external application methods with that of native fetal membranes.

Due to their pathophysiological differences, sPPROM posses a bleak chance to repair, where as the development and repair methodologies can be better studied in its well defined counterpart i.e. iPPROM. However, the repair of iPPROM is complimentary towards the repair of sPPROM. Hence, the reasons for which iPPROM is considered as the prototype model between 2 clinical categories of PPROM, to develop a repair approach are:

1. sPPROM usually denotes a larger undefined wound

2. sPPROM as an entity is difficult to realize and design in an ex vivo set up or in vivo animal model, as it always presents as final outcome in clinical domain

3. Due to its association with infection, sPPROM poses a greater challenge with respect to iPPROM

4. The strategies for repairing iPPROM may be translated for sPPROM

1.4.3 In vitro and ex vivo approaches for iPPROM repair:

One major lacuna in this field of experimental iPPROM repair is that there is no standard ex vivo platform for simulating the in vivo situation, before the whole module is translated either to animal model or humans. One major part of my thesis goes to establish an ex vivo device to mimic the physiology of fetal membrane in utero. The need for an ex vivo platform can be reasoned out as below:

1. Immediate biochemical, mechanical, biological examinations are feasible on an ex vivo platform to correlate findings before putting the approach in a complete in vivo situation

2. Validation of any technique on an animal model needs extensive screening in a simulated environment to repair iPPROM, as animal models are expensive.

3. An ex vivo platform can be used as training module for the surgeon as most "sealing" approaches need a learning curve.

1.5. Outline of the work presented in this thesis

Despite various attempts to repair iPPROM, no method has made it to clinics so far. It is well understood that fetal membranes do not show anatomical wound healing capacity. Keeping these points in mind, I attempted to prepare a surgically viable plug from human amnion itself, with the aim to deliver it fetoscopically to the site of lesion. Though this attempt showed the viability of the plug and method of application in a rabbit model, further confirmation will be necessary in a larger animal model. This work is presented in chapter 2 of my thesis.

Along this line, one major challenge is to find out candidate glue, which is ideal enough to polymerize from a fluid status to solid state in the wet environment of amniotic fluid. I tested many commercial types of glue on the basis of their biocompatibility and mechanical adherence to human fetal membranes. This work is presented in chapter 3 of my thesis.

In addition to the above bioengineering aspects, repair of ruptured fetal membranes, demands a thorough understanding of its biomechanical properties. Therefore, in collaboration with the Department of Mechanical Systems, ETH Zurich, I evaluated the base line mechanical behaviour of fetal membranes in a uniaxial set up. This initial study set the motivation for the establishing an ex vivo set up which could mimic the inflation of human fetal membrane. I also correlated the microcomponents of fetal membranes such as elastin and collagen to the obtained mechanical parameters in an attempt to establish a condition to predict the imminent rupture condition in a clinical set up where presumptive repair methods could be implemented. These biomechanical studies are presented in chapters 4 and 5.

Chapter 2

Fetoscopic Closure of Punctured Fetal Membranes With Acellular Human Amnion Plugs

This part of my thesis is a modified version of the publication:

Fetoscopic Closure of Punctured Fetal Membranes With Acellular Human Amnion Plugs in a Rabbit Model

Ajit S. Mallik[1*], Max A. Fichter[3], Susanne Rieder[2], Grozdana Bilic[1], Sofia Stergioula[2], Julia Henke[2], Karl-Theo M. Schneider[2], Juozas Kurmanavicius[1], Edgar Biemer[2], Roland Zimmermann[1], Andreas H. Zisch[1*] and Nikolaos A. Papadopulos[3]

[1]Department of Obstetrics, university Hospital Zurich

[*]Zurich center for Integrative Human Physiology

[2]Department of Obstetrics & Gynecology, Technical University Munich, Germany

[3]Department of Plastic and Reconstructive Surgery, Center for Preclinical research and Section of Perinatal Medicine, technical University Munich, Germany

2.1 Introduction

2.1.1 Outline of this work

Operative fetoscopy on fetus and placenta has become a therapeutic option. However, needle and fetoscopic punctures of fetal membranes for diagnostic or surgical interventions in the amniotic cavity lead to localized defects that carry significant risk for persisting membrane leakage and subsequent iatrogenic preterm premature rupture of fetal membranes (iPPROM). Such iatrogenic rupture of fetal membrane is a complication of pregnancy with a high risk for premature birth. Efforts must concentrate on taking action before rupture (prophylactic plugging) rather than reacting after obvious rupture.

Despite series of studies, in both humans and various animal models, no technique has made into clinics. Such attempts witnessed various combinations of bio-glues, bio-scaffolds and surgical methods. Most such trials of prophylactic plugging were performed in rabbit at midgestation for various reasons, one being the loose relationship of the membranes, making membrane sealing even more challenging (Ochsenbein-Kolble et al., 2007). Yet, the experimental situation in rabbits is entirely different from the human clinical situation, and primarily suited to judge technical feasibility.

One major issue for the failure of such studies could be the mismatch between the applied biomaterials and the natural fetal membrane tissue. To address this issue, I developed a surgical plug from the decellularized human amnion membrane (DAM). In this study, I evaluated the efficiency of the DAM to close the fetoscopically created iPPROM in a midgestational rabbit model. Amniotic integrity, fluid volume and fetal survival are the main parameters to measure the treatment performance in this rabbit model.

2.1.2 Decellularized amnion plug in the repair of iPPROM

Interventional options to reseal the entry wounds have remained very limited. Wounds in the fetal membranes are difficult to seal, and do not heal well, for technical as well as biologic reasons. An appealing strategy for closure of iatrogenic puncture wounds in the fetal membranes is to deploy biopolymeric plugs that

immediately seal, perhaps even help anatomic healing of leaky membranes. Pioneering experimental approaches to iatrogenic preterm PROM and spontaneous preterm PROM were intraamniotic injection at the puncture site of maternal platelets mixed with fibrin cryoprecipitate (amniopatch) (Quintero, Morales et al. 1999), endoscopic placement over the internal os of a collagen plug (amniograft for spontaneous preterm PROM) (Quintero, Morales et al. 2002), or intrauterine deposition of gelatin sponge (O'Brien et al., 2002). Early positive clinical experience with amniopatch sealant indicates feasibility of treatment of iatrogenic preterm PROM (Quintero 2001; Quintero 2003), but still no treatment has progressed to clinical routine.

Stable integration and low resorption of plugs grafted in fetal membrane defects are key requirements for long-lasting closure. Fetal membranes exhibit inherent low or even no wound healing capacity (Gratacos, Sanin-Blair et al. 2006), which complicates grafting of plugs in defective membranes. Rapid resorption limits the usefulness of fibrin-based sealants. We previously evaluated microsurgical solutions for closure of fetoscopic access sites in the midgestational rabbit model. Fetoscopic grafting of a commercial collagen matrix foil, TissuFleece E (Resorba Wundversorgung GmbH & Co. KG, Nuremberg, Germany), followed by its fixation with fibrin glue and myometrial suturing was effective (Deprest, Papadopulos et al. 1999; Papadopulos, Klotz et al. 2006). In the present study, we explored plugging of punctured fetal membranes with decellularized matrix directly produced from human amnion with the idea that such native-tissue matrix plugs might better integrate (Portmann-Lanz et al., 2007). Human amnion represents a unique, readily available source for production of human extracellular matrix (ECM) scaffold. Removal of cellular components renders allogeneic or xenogeneic tissue nonimmunogenic while leaving the complex mixture of structural and functional proteins that constitute natural ECM. Acellular ECM is resorbable and potentially capable of inducing constructive remodeling of injured tissues. Biologic scaffolds produced from decellularized tissues have been successfully used in both preclinical and in human clinical applications (Gilbert et al., 2006). We tested acellular human amnion plugs in the midgestational rabbit model that constitutes a well-accepted, very challenging model with a loose relationship between fetal membranes and the uterine wall. As stated by Ochsenbein-Kolble et al (Ochsenbein-Kolble, Jani et al. 2007), although in

rabbits the relationship of the fetal membranes to the decidua and myometrium is much different from that in humans or nonhuman primates, surgically induced membrane defects that are left uncovered will persist in most cases, leading to oligohydramnios and its consequences.

2.2 Results

I developed a devitalization protocol for production of a cell-free human amnion scaffold (Portmann-Lanz, Ochsenbein-Kolble et al. 2007). In the present study, I established a modified protocol that combines detergent extraction before dispase treatment and mechanical cell scraping to accomplish more rapid removal of cells. Electron micrographs of Figure 2.1 show top views of the epithelial lining of human amnion before and after decellularization. Removal of epithelium was complete and also the underlying stroma appeared cell-free. The natural collagen fiber architecture of the stromal compartment that underlies

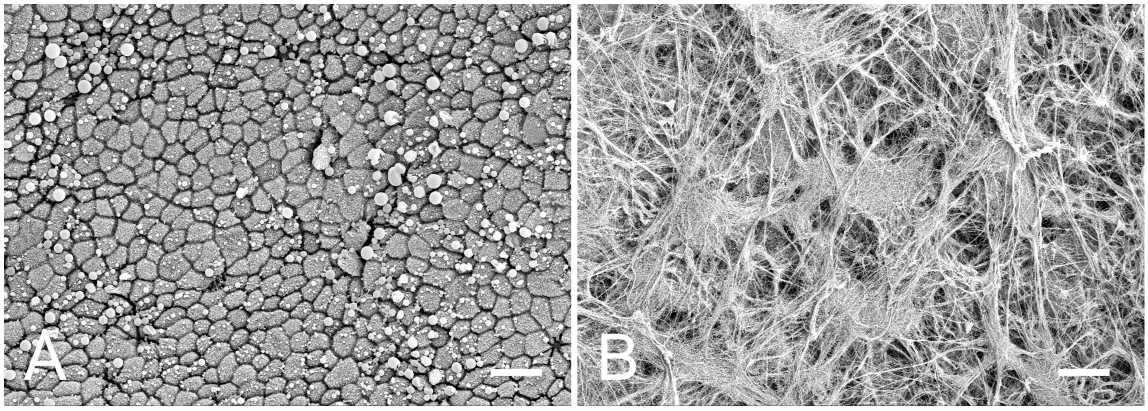

Figure 2.1: Scanning electron micrographs of human amnion tissue before and after decellularization. **A.** Before cell removal. The top view of the amnion shows the confluent lining of amnion epithelial cells. **B.** After cell removal. The network of collagen fibrils that builds the stroma of amnion was preserved. Bar size: 20 μm.

the amnion epithelial layer was retained (Figure 2.1B). Decellularized term human amnion membrane prepared with this new protocol was found to be a nontoxic substrate for adhesion and growth of cells. In cell-seeding experiments in vitro,

various cultured human cell types, including amnion epithelial and mesenchymal cells, endothelial cells, chondrocytes, and fibroblasts were plated on decellularized term human amnion membrane and cultured for 48 hours (Figure 2.2). Using a live or dead staining assay and side-by-side comparison with cells seeded on tissue culture plastic, we demonstrated that the great majority of cells adhering to decellularized term human amnion membrane remains vital and assumed the morphology of outgrowing cells. The decellularized term human amnion membrane material was found stable and suitable for storage and shipment (in this study shipped from Zurich to Munich). Decellularized term human amnion membrane kept in physiological saline buffer at 4°C for almost a 1-year period did not show any decomposition.

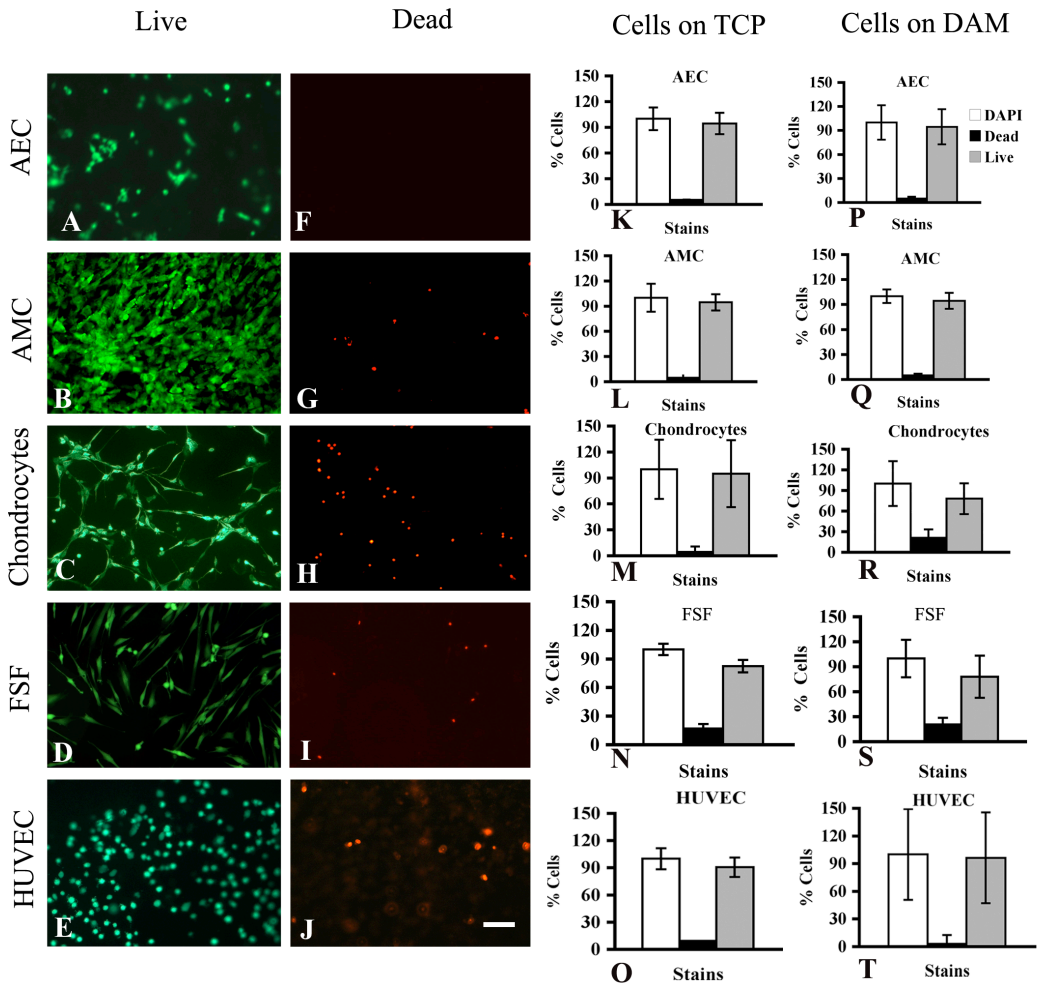

Figure 2.2: Decellularized term human amnion scaffold is nontoxic for cells and supports adhesion and outgrowth of multiple human cell types in vitro. Human cells were seeded on human amnion membrane and cultured for 48 hours. Then, live and dead cells on the decellularized term human amnion scaffold were identified by incubation with calcein (live cells; green fluorescence) and ethidium bromide (dead cells; red fluorescence). A-E. Representative fluorescence images of decellularized term human amnion scaffold stained for live cells. F-J. Representative fluorescence images of decellularized term human amnion scaffold stained for dead cells. K-O. Survival of cells seeded on decellularized term human amnion. Percentages of live (grey column) and dead cells (black column) in culture are given relative to total number of cells which was determined by 4′,6-Diamidin-2′-phenylindol-dihydrochlorid stain (white column). P-T. Comparative survival of cells on tissue culture plastic. Each experiment was performed in triplicate. Values are given as

mean±standard deviation. AEC, amnion epithelial cells; AMC, amnion mesenchymal cells; FSF, human foreskin fibroblasts; HUVE, human umbilical vein endothelial cells

We created fetoscopic punctures in 27 amniotic sacs in eight rabbit does and tested for fetoscopic plugging with small pieces of decellularized term human amnion membrane sheet (n=10) or commercial collagen matrix foil (n=10). Seven sacs were punctured but without further treatment. Decellularized term human amnion membrane was found much easier to deploy fetoscopically than commercial collagen matrix foil into the fetal membrane defect. The soft, pliable decellularized term human amnion membrane sheet could be readily pushed through the needle of the fetoscope, where it became compacted. The resulting decellularized term human amnion membrane could be released into the lesion with good precision to form a plug with a dimension in the 1-cm range (Figure 2.3). We encountered neither any plugging of the fetoscopic needle by decellularized term human amnion membrane nor a loss of decellularized term human amnion membrane from sudden release into the amniotic cavity. Decellularized term human amnion membrane's good surgical performance may be also attributed to natural stickiness of the material and the self-locking mechanism of relaxing decellularized term human amnion membrane sheets once they are released into the defect. In Figure 2.4, we detail features of decellularized term human amnion membrane compared with commercial collagen matrix foil

Experimental outcome was assessed 1 week after surgery by standard analysis of fetoscopy in the midgestational rabbit model(Papadopulos et al., 1998; Papadopulos et al., 1999; Papadopulos, Klotz et al. 2006). Surgeons' inspections of the treatment sites did not reveal any signs of inflammation. No amniotic bands or adhesions and no fetuses herniating into the maternal abdomen were detected. Table 2.1 summarizes the fetal outcome measures. Fetal survival rates in the decellularized term human amnion membrane and commercial collagen matrix foil study groups were 80% and 70%, respectively, compared with 71% in the unmanipulated and 57% in the left-open study groups. Amniotic integrity and fetal characteristics were determined for the 41 sacs with living fetuses. Amniotic integrity was 75% and 71.4% for sacs treated with decellularized term human amnion membrane and commercial collagen matrix foil,

respectively, compared with 25% in the left-open group (Table 2.1). In the unmanipulated study group, 95.5% of the amniotic sac groups were intact. Fetal body weight, fetal lung weight, and fetal lung/ body weight ratio were not different between the study groups.

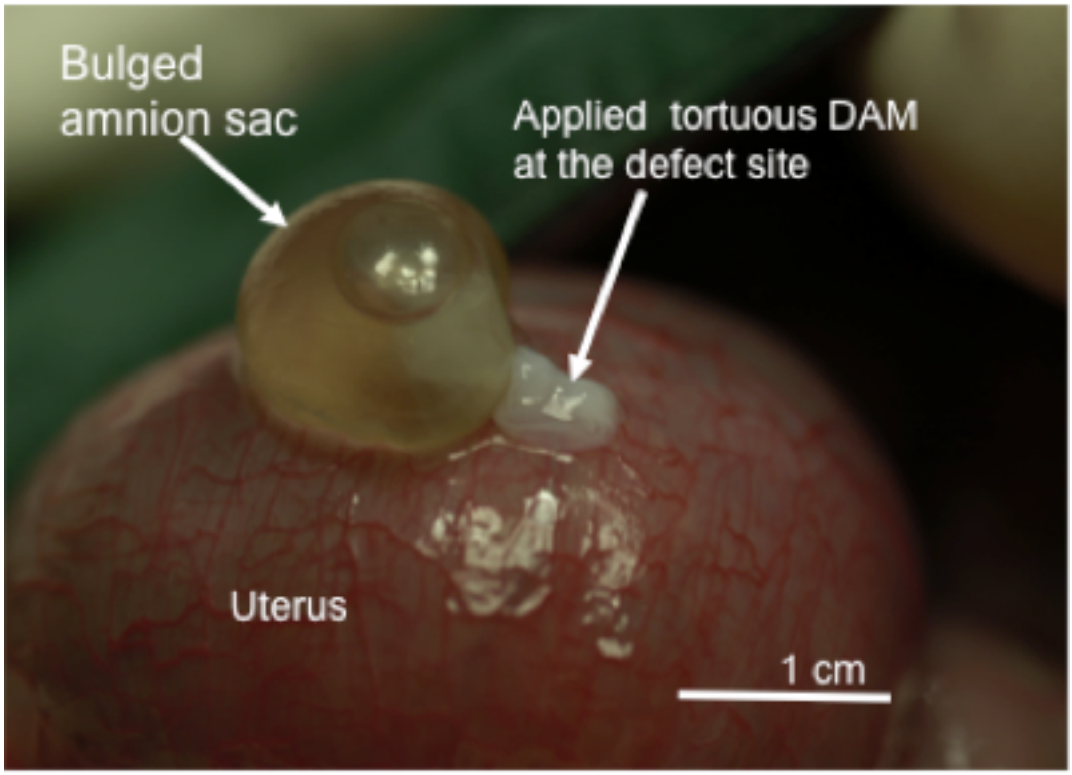

Figure 2.3: Decellularized term human amnion membrane plugs for closure of fetoscopic entry wounds in the exposed rabbit amniotic sac. The micrograph of the surgery site shows the dimension of a decellularized term human amnion membrane plug of (white lines) spanning through the fetal membranes into the bulged amniotic sac. Bar size: 1 cm. DAM, decellularized amnion membrane.

Although macroscopic inspection and the methylene blue test proved functional closure of punctured amniotic sacs, the histologic assessment of closure was problematic due to a difficulty in retrieving the fragile amniotic tissue with the bulky decellularized term human amnion membrane plug in intact form. We applied a new method, i.e. the staining of graft material with tattoo ink before implantation, to facilitate identification of the treatment site and engrafted material upon retrieval for histology. Ink-stained grafted decellularized term human amnion membrane could be

traced readily in hematoxylin eosin stained tissue sections (Figure 2.5B). Figure 2.5A shows a decellularized term human amnion membrane plug after explanation. Although the plugs tended to decoil during formalin fixation for histology, the piles of amnion layers as formed upon fetoscopic deployment were still apparent. Figure 2.5B shows a densely packed decellularized term human amnion membrane plug within the surrounding fibrin glue fixative. There were no signs of inflammation and no signs of anatomical healing.

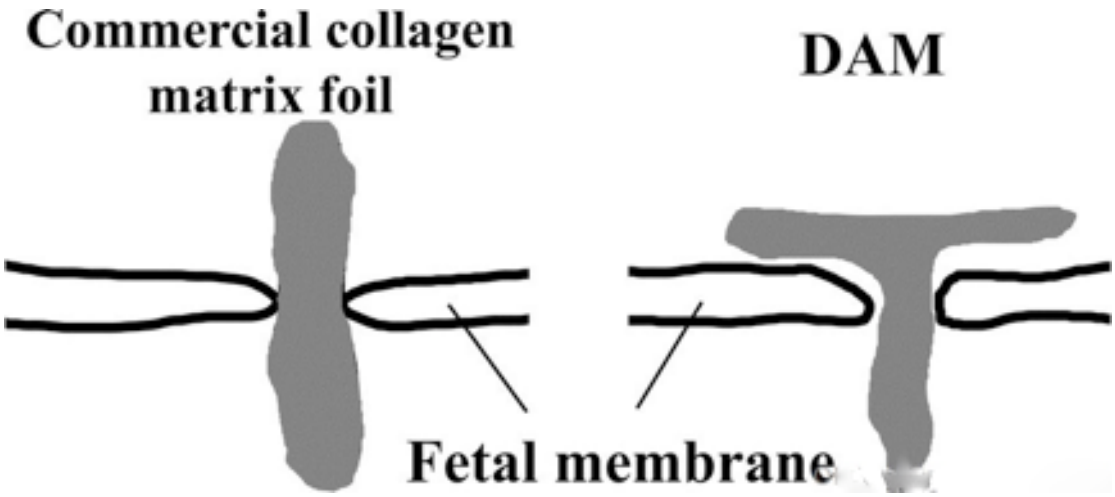

Figure 2.4: Sheets of the decellularized term human amnion membrane plug could be spread at the outer chorionic face of the fetal membrane to additionally anchor the plug. The resulting T-shaped decellularized term human amnion membrane plug compared with the T-shaped commercial collagen matrix foil plug is illustrated. DAM, decellularized amnion membrane

2.3 Materials and Methods

The study was performed between February and November 2006. Fetal membranes from six pregnancies were collected; this number was required for initial establishment of the protocol of decellularization of amnion membranes, and the final production of decellularized amnion membrane for direct use in the rabbit model. Written consent was obtained from all women. Mothers were 23 to 32 years old and gravida 1 or gravida 2. Mean gestational age was 37.3±2 weeks. The pregnancies were randomly selected after serologic negative testing for human immunodeficiency, hepatitis B and C viruses, *Streptococcus* infection, Rubella, and toxoplasmosis. The selected women had no history of diabetes, connective tissue disorders, or hypertension. The fetal membranes were collected from term placentas, 5 minutes

after elective cesarean delivery in the absence of labor, preterm rupture of fetal membranes, chorioamnionitis, and chromosomal abnormalities. Pieces of collected fetal membrane were approximately 150–200 cm^2. Amnion and chorion leave tissue were separated by blunt dissection(Okita et al., 1983), and the amnion was cut approximately 2 cm from the placental disc to avoid the "zone of altered morphology"(El Khwad et al., 2005; Osman, Young et al. 2006). Reference pieces of native amnion were collected and fixed in phosphate-buffered 4% paraformaldehyde solution. Cellular debris and blood were removed from the amnion samples by extensive washing in phosphate-buffered saline (PBS) containing 100 units/mL penicillin, 100 mcg/mL streptomycin. For decellularization, the amnion membranes were incubated in a decellularizing solution (PBS, pH7.4, 0.5% sodium deoxycholate, 0.02% ethylenediamine tetraacetic acid, and two protease inhibitor cocktail tablets (Roche Diagnostics GmbH, Mannheim, Germany) per 100 mL solution) with constant shaking for 1 hour at 4°C. Thereafter, the amnion membranes were incubated with 1.2 units/mL Dispase II (Gibco, BRL, Basel, Switzerland) in PBS for 45 minutes at 37°C, followed by gentle scraping of the membrane with cell scraper and washing with PBS to remove all cells from the surface. Finally, the amnion membranes were incubated with 2 mcg/mL DNAse and 0.2 mcg/mL of RNAse (Roche Diagnostics GmbH) for 3 hours at room temperature. The resulting decellularized term human amnion membrane sheets were washed three times in PBS/penicillin/streptomycin and kept in this buffer for storage in 50 mL centrifuge tubes until their surgical use. Small parts from each decellularized term human amnion membrane preparation were fixed in phosphate buffered 4% paraformaldehyde solution for histologic and electron microscopical assessment of decellularization. Before surgery, the decellularized term human amnion membrane sheets were transferred to 15-cm tissue culture plastic dishes (area 176.6 cm^2), spread onto the bottom of the dish, then cut into pieces of 1 cm x 1 cm using sterile microscissors and microforceps. The 1-cm^2 decellularized term human amnion membrane pieces were overlaid with PBS and antibiotics. For fetoscopic delivery, a single decellularized term human amnion membrane piece was carefully loaded into the needle with a pusher. Commercial collagen matrix foil is a biologic scaffold made from an equine collagen matrix (Resorba Wundversorgung GmbH & Co. KG).

Paraformaldehyde-fixed decellularized term human amnion membrane and control amnion membranes were embedded in paraffin. Staining was performed on deparaffinized sections with hematoxylin-eosin.

Decellularized term human amnion membrane and the control amnion membranes were fixed with 2.5% glutaraldehyde (Fluka, Bornem, Belgium) and washed with PBS. The specimens were dehydrated with graded series of ethanol followed by critical point drying. The specimens were mounted and gold sputtered to achieve surface conductivity during scanning electron microscopy.

Amnion epithelial and mesenchymal cells were isolated from term human amnion and cultured as described previously(Bilic, Ochsenbein-Kolble et al. 2004). In total, four amnion membranes were collected and used only for cell isolation during this study. Human umbilical vein endothelial cells were purchased from PromoCell (Heidelberg, Germany) and cultured in endothelial cell growth medium-2 (Clonetics, Baltimore, MD) additionally supplied with 20% fetal bovine serum. Dr. Manfred Welti, University Hospital Zurich, Switzerland, kindly provided human primary chondrocytes. Human fore- skin fibroblasts were purchased from Cascade Biologics (Mansfield, UK). Chondrocytes and human fore- skin fibroblasts were cultured in Dulbecco's Modified Eagle's Medium with 10% fetal bovine serum. For cell-seeding experiments, pieces of decellularized term human amnion membrane were chopped to fit the size of a well of a 12-well plate, placed into the well and equilibrated in cell culture medium. Each piece of decellularized term human amnion membrane was seeded with 10^5 cells. Comparative seeding experiments were performed on tissue culture plastic as control. Each experiment was performed in triplicate. To identify cell morphology as well as live and dead cells, 48-hour cultures on decellularized term human amnion membrane or tissue culture plastic were incubated for 10 minutes with a mix of calcein (which detects live cells; Sigma, St. Louis, MO) and of ethidium bromide homodimer (which detects dead cells; Sigma) at 1 μmol/L and 2 mcg/mL, respectively. Images of the fluorescently stained cultures were acquired with an Axiovert 200M microscope at the 10x magnification. The cultures were finally fixed in 4% paraformaldehyde and incubated with 4′, 6- Diamidin-2′-phenylindol-dihydrochlorid (Molecular Probes, Invitrogen, Basel, Switzerland) for 10 minutes to

stain the nuclei of all cells. Numbers of live and dead cells were determined from printed micrographs.

Eight time-dated pregnant New Zealand rabbits were housed 2 days before surgery. The housing was quiet, at room temperature and daylight. Average duration of pregnancy of the New Zealand White Rabbit is 31–32 days. Fetoscopic punctures in rabbit fetal membranes were created at midgestational day 23. Anesthesia and surgery were performed exactly as described in our previous work in this model. Interventions on the uterus and membranes were done with loupes (magnification 4) and microinstruments. Fetoscopy was done with a short, 1.2-mm, 10,000-pixel, 0° fiber endoscope (Karl Storz, Tuttlingen, Germany) housed within a 14-gauge needle. A midline abdominal incision was made to expose the pregnant uterus. The midline laparotomy was followed by a 2-mm to 3-mm hysterotomy with microinstruments on the antimesenteric side of the uterus. First, the gestational sacs were counted and numbered. Numbers of gestational sacs were nine to 12 per animal, two to 12 per cornu of the uterus bicornis. To minimize risk of abortion, gestational sacs immediately above the cervix were always excluded from treatment. Our long-term experience with this model has shown that gestational sacs closest to the cervix have the highest risk of abortion upon surgery, even when they did not get punctured. Experience tells that in the event of one abortion, all sacs in the rabbit will always abort and be lost. Every second amniotic sac was punctured, and unmanipulated sacs in between served as controls. The number of punctured sacs varied between two and four per animal. Punctured sacs were randomly assigned to one of the three study groups, i.e., treatment with decellularized term human amnion membrane (n=10) or commercial collagen matrix foil (n=10) or left open (n=7). These experimental group sizes compared those used by us others in this rabbit model(Papadopulos, Van Ballaer et al. 1998; Papadopulos, Klotz et al. 2006; Ochsenbein-Kolble, Jani et al. 2007). A 2-mm to 3-mm myometrial incision was created with microscissors as already described (Papadopulos, Van Ballaer et al. 1998; Deprest, Papadopulos et al. 1999), to separate the chorion and allow the amniotic membrane to bulge through the chorionic incision after gentle uterine pressure (Figure 2.3). The amniotic sac was then entered with the 14-gauge needle under view with loupes. Once in the amniotic cavity, the fetoscope was introduced into the needle to explore the amniotic cavity. During fetoscopy, the fetal body, extremities, face, and tail, as well as the placenta or the umbilical cord

were identified. The fetoscopy was limited to a maximum inspection time of 5 minutes with the use of up to 5 mL Ringer lactate amniodistention infusion at body temperature. Twenty-seven sacs were punctured and treated with decellularized term human amnion membrane (n=10) or commercial collagen matrix foil (n=10), or left without closure (n=7). Thirty-one sacs without puncture served as control. For surgical treatment, pieces of decellularized term human amnion membrane sheet stored in PBS were precut to 1 cmx1 cm, and then dyed with a biocompatible skin tattoo ink (Proposta Tattoo, SRT Testing & Inspection AG, Zurich, Switzerland) to facilitate identification at the time of retrieval of rabbit tissue. After withdrawal of the fetoscope from the needle, the decellularized human amnion membrane was loaded into the lumen, and the anion plug advanced exactly to the tip of the needlepoint by water pressure using a 1 ml syringe filled with Ringer lactate solution at body temperature. A similar technique was used for positioning precut commercial collagen matrix foil collagen foil with a maximal length of 1 cm (Papadopulos, Van Ballaer et al. 1998). Once in place, the collagen plug swells by absorbing surrounding fluid and locks itself in the access site. In the decellularized term human amnion membrane and commercial collagen matrix foil study groups, 0.3 mL fibrin sealant (Tissucol Duo-S 2 mL; Immuno, Baxter Deutschland GmbH, Unterschleissheim, Germany) was applied on the membrane defect area after application of decellularized term human amnion membrane or commercial collagen matrix foil plugs, and the myometrial layers were closed microsurgically. After repositioning the uterus, the abdomen was closed. Postoperative uterine relaxation was achieved by administering 4.5mg/kg medroxyprogesterone-acetate intramuscularly (Depo-Clinovir 150 mg, Pharmacia & Upjohn GmbH, Erlangen, Germany). No postsurgical inflammation was observed. The animals were then housed for 7 days under the same conditions as before surgery. At gestational day 30 the rabbit does were killed by pentobarbital injection at 60 mg/kg (Narcoren, Rhone-Merieux, LAupheim, Germany). The rabbit does died within approximately 1 minute. Second-look laparotomy was performed to assess amniotic integrity and fetal outcome characteristics using intraamniotic injection of 5–10 mL saline solution dyed with methylene blue. Fetal survival was accessed from fetal leg movement while the sacs were still connected to the uterus. Fetuses died from the barbiturate overdose, 15–25 minutes after the mother. Then, the amniotic sacs were opened and the dead fetuses delivered. Amniotic tissue from the plugged area was

collected for histologic evaluation. Further, skin color and quality of the fetuses were used as additional measures for their survival until death. Dead fetuses were dissected to assess wet fetal lung weight and to calculate the fetal lung-to-body weight ratio. Fetuses with beginning or advanced maceration were not further analyzed.

2.4 Discussion

From this study, we concluded that decellularized term human amnion membrane has the potential to be used as a surgical plug to restore the integrity of punctured fetal membranes. The surgical plugging method is not intended nor probably suitable for grafting of larger, undefined defects as produced upon spontaneous preterm PROM. Decellularized term human amnion membrane possesses several benefits for application in the clinic. It 1) possesses very good surgical handling characteristics, 2) is easy to manufacture, 3) is nonimmunogenic and biocompatible, and 4) is suitable for storage and transport for off-the-shelf use.

Decellularized term human amnion membrane represents the secreted product of amnion cells and consists of structural and functional proteins, such as collagen fibers, proteoglycans, and glycosaminoglycans arranged by residing amnion cells for the cells' needs. For decellularization, the starting tissue should be as thin as possible. Because the amnion layer of human fetal membranes is only 0.1 mm thin and lacks blood vessels, it is an ideal tissue to produce acellular ECM scaffold. We produced sheets of decellularized term human amnion membrane with a new, modified protocol that combines mechanical and enzymatic treatment with detergent extraction of

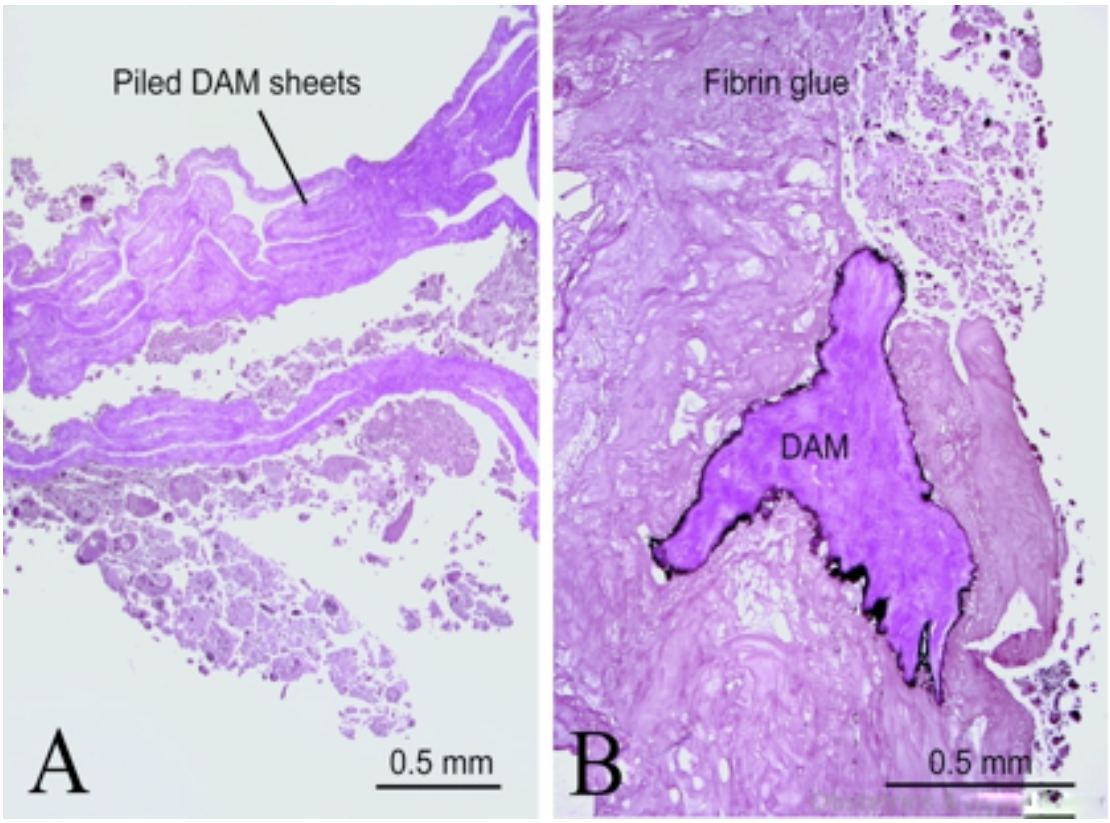

Figure 2.5: Hematoxylin-eosin stains of surgical decellularized term human amnion membrane plugs retrieved after 1 week. A. Piles of decellularized term human amnion membrane sheets, often coiled, formed the plug. B. Section through a piece of the decellularized term human amnion membrane plug surrounded by the fibrin glue fixative. The decellularized term human amnion membrane sheets appear highly compacted. The decellularized term human amnion membrane plugs were briefly soaked in black tattoo ink before surgery to facilitate identification of the material in treated tissue. The black ink lining identifies the borders of the decellularized term human amnion membrane plug. DAM, decellularized amnion membrane.

amnion tissue. The natural histoarchitecture of amnion ECM was preserved (Figure 2.1) and allowed different types of human cells, including amnion cells, to grow in contact with the material in vitro (Figure 2.2). There was no inflammatory reaction to the decellularized term human amnion membrane grafts in our rabbit model. Indeed, it is widely acknowledged that the method of decellularization renders allogeneic as well as xenogeneic tissue to become nonimmunogenic. Such decellularized term human amnion membranes may become useful as surgical wound dressing or vehicle

for cell transplantation in a broad range of tissue repair applications. Safety and off-the-shelf availability of decellularized term human amnion membrane will be clinically critical and important. At no point during the preparation of decellularized term human amnion membrane is amnion tissue in contact with serum products that are potential sources for viral pathogens. Strict serologic screening of the donor women before collection of fetal membrane, also performed in this study, is mandatory.

Our hypothesis about using surgical plugs of decellularized term human amnion membrane for closure of fetoscopic entry sites is from a descriptive study on a case series in eight rabbits. The sizes of experimental groups in the present study compared those used by others is low (Papadopulos, Van Ballaer et al. 1998; Papadopulos, Klotz et al. 2006; Ochsenbein-Kolble, Jani et al. 2007). For ethical as well as cost considerations, we kept number of animals low in our initial exploration of decellularized term human amnion membrane plugs minimal. Although both treatments with decellularized term human amnion membrane and commercial collagen matrix foil appeared to be working treatments, we could not substantiate our observations by statistics. In this surgical model, more than one sac is treated in the same rabbit, which makes nested analysis of variance necessary. A (meaningful) paired t test analysis could not be performed because of the small animal number, low number of sacs for evaluation (n=41; 19 of which punctured, see Table 2.1); plus the fact that four different treatment modalities were compared. Additionally, some animals had proportionally more sacs and received proportional more punctures (two to four) than others, leading to uneven distribution of treatments in rabbits. This study was set out with the assumption that a biologic decellularized term human amnion membrane scaffold may accomplish anatomic restoration of fetal membrane. Yet our experimental findings lead us to suggest that penetration of the compact decellularized term human amnion membrane plug by cells and its subsequent remodeling into a native fetal membrane tissue will be slow, or may not occur at all. First, the grafted decellularized term human amnion membrane plug (of size in the 1-cm range) is much thicker than the treated fetal membrane itself (0.2 mm) (Figure 2.3), and bulges far into the amniotic cavity. Remodeling of this massive plug into a thin sheet of native amnion membrane is unlikely, certainly at the 1-week scale of this experimental model. Second, histologic follow-up of fetoscopic entry wounds

indicated that spontaneous healing or remodeling capacity is low or absent in human amnion tissue (Gratacos, Sanin-Blair et al. 2006). We think that the decellularized term human amnion membrane plug's sealing function rests on presenting a physical barrier to amniotic fluid. The positive performance of human decellularized term human amnion membrane plugs is corroborated by positive results obtained with devitalized rabbit amnion grafts in the rabbit midgestational model, reported by Ochsenbein-Kolble and colleagues (Ochsenbein-Kolble, Jani et al. 2007). In their study, cell ingrowth into the grafted scaffold and abundant coverage with epithelial cells at its amniotic side was found, indicative of beginning anatomic healing. Whether grafted scaffold can mediate true anatomic healing needs confirmation in long-term studies.

The next steps of research should be directed to the question of whether decellularized term human amnion membrane plugs are applicable by percutaneous needle fetoscopy. The surgical sequence required in the midgestational rabbit model (uterine incision, separation of amnion and chorion, etc, see Methods section) does not mimic the fetoscopy in humans, which only involves percutaneous needle fetoscopy. Our previous experience revealed that the rabbit model is not suitable for this procedure. The number of gestational sacs in the abdomen of a rabbit doe can be 16 (or even more), each of which is 2–3 cm, and counting and numbering all amniotic sacs by ultrasound imaging, plus puncturing and closing of specific sacs was found not feasible. Further, insertion of the needle between the amnion and chorion, rather than into the amniotic cavity occasionally occurred. Together, percutaneous delivery of decellularized term human amnion membrane plugs to fetal membrane defects demands testing in larger animals.

The human situation will require the plug to last in the defect for several months. Stable integration and a low resorption rate that is in tune with material replacement by native tissue are areas of research for the future. Long-term follow-up is not possible in the rabbit model. Therefore, studies in nonhuman primates or sheep with gestations of 145–150 days or 150–165 days will become necessary to resolve whether durable sealing with amnion plugs can be achieved. We think that the dense nature of a decellularized term human amnion membrane plug could help prevent its rapid loss from the lesion by material resorption that would cause releakage of the

amniotic sac. Moreover, only long-term studies in sheep or primates may reveal the sealing mechanism at work, whether it results from true anatomic restoration of the fetal membrane, or physical plugging

Chapter 3

Injectible candidate sealants for fetal membrane repair: Bonding and toxicity in vitro

This part of my PhD thesis is a modified version of the publication:

Injectible candidate sealants for fetal membrane repair: Bonding and toxicity in vitro

Grozdana Bilic[1], Carrie Brubaker, Phillip B Messersmith[2, 3], Ajit S Mallik[1,6], Thomas M Quinn[4], Claudia Haller[1], Elisa Done[5], Leonardo Gucciardo[5], Steffen M Zeisberger[1], Roland Zimmermann[1], Jan Deprest[5], Andreas H Zisch[1,6],

[1]Department of Obstetrics & Gynecology, University Hospital Zurich

[2]Biomedical Engineering Department, Northwestern University, Evanston, Illinois, USA

[3]Material Science and Engineering Department, Northwestern University, Evanston, Illinois, USA

[4]Department of Chemical Engineering, McGill University, Montreal, Canada

[5]Department of Obstetrics & gynecology, university Hospital K.U. Leuven, Belgium
[6]Zurich Center for Integrative Human Physiology, Switzerland

3.1 Introduction

3.1.1 Outline of this work

Medical invasions into the amniotic cavity with needles or fetoscopes for diagnostic or therapeutic purposes, including mid-trimester genetic amniocentesis or fetal surgery, pose a risk for persisting leakage and iPPROM. Since such invasive procedures are performed in the second trimester of pregnancy, iPPROM usually occurs at an early gestational age, before the viability of the fetus. The incidence of iPPROM remains significant, with rates 20-77% (Taylor et al., 2002; Deprest et al., 2004; Picone et al., 2004). Hence, the morbidity rates associated with fetoscopic invasion procedures may overcome the benefits of the intervention.

Prophylactic plugging of fetoscopic punctures immediately after intervention has been considered to prevent subsequent rupture. The plug must be deployed under fetoscopic guidance into the defect before the fetoscope is finally retrieved. Various plugs such as sequential injection of platelets, fibrin glue, powdered collagen slurry and sponge materials have been applied directly to the puncture site to arrest the leakage of amniotic fluid following the endoscopic procedures (Reddy et al., 2001; Young et al., 2004; Liekens et al., 2008). These methods warrant further investigation as none of these glues and techniques has made into clinical practice. There is growing evidence that anatomic remodeling of the graft or glue material into membrane tissue will be incomplete or not occur, even at a longer duration. This has led us to consider synthetic polymer sealants that simply act as physical barriers to amniotic fluid without attempt for healing. To this aim, we tested 6 injectible surgical sealants, 4 commercial and 2 experimental formulations for their principal utility for membrane repair, focusing on bonding to fetal membrane tissue and acute cytotoxicity for fetal membrane tissue or cell isolates in vitro. Our screen of injectible was done on freshly collected fetal membranes and cultured amnion cells under ISO 10993-5 rules.

3.1.2 Bioglue and bioscaffolds in the closure of iPPROM

The major complications of invasive fetoscopic procedures are amniotic fluid leakage, separation of amnion and chorion, or even frank iatrogenic preterm premature rupture of the fetal membranes (iPPROM). The rates of iPPROM could vary between 6 to 45%(Liekens, Lewi et al. 2008) for fetoscopic interventions, but in a trial of fetal endoscopic tracheal occlusion for severe congenital diaphragmatic hernia the rate of iPPROM was as high as 100% (Harrison, Keller et al. 2003). These invasive procedures are performed, as early as in the second trimester of pregnancy, so the incidence of iPPROM is high in early pregnancy. Hence, the associated morbidity and mortality may compromise the expected benefits of the intervention. iPPROM is therefore a potentially serious complication for prenatal fetal surgery. Clinically, measures of plugging membranes after established rupture as well as of preventive plugging of fetoscopic access sites have been undertaken, as reviewed previously (Devlieger et al., 2006; Zisch and Zimmermann 2008). For closure after obvious iatrogenic rupture, intra-amniotic injection at the puncture site of maternal platelets mixed with fibrin cryoprecipitate ('amniopatch') has evolved as promising route to seal (Quintero 2001; Quintero 2003). However, the sudden activation of a large number of platelets in the amniopatch was accounted for otherwise unexplained fetal demise in some cases (Quintero 2003). But increasing efforts have been concentrated on taking prophylactic measures prior to rupture rather than therapy after established or symptomatic rupture of the membranes. Several preventive plugging methods such as dry collagen and gelatin plugs or liquid blood-derived sealants have already been clinically investigated (Young, Roman et al. 2004; Chang et al., 2006). Preliminary experience supports this prophylactic intervention for prevention of iPPROM. A study report on a 27 patient cohort found a 4.2% rate of postoperative PPROM upon gelatin plug (Gelfoam) insertion upon port retrieval in endoscopic fetal surgery (Chang, Tracy et al. 2006). In another small clinical study, sequential injection of platelets, fibrin glue and powdered collagen slurry directly to the puncture site successfully prevented amniotic fluid loss after endoscopic procedure (Young, Roman et al. 2004). Still, the positive outcomes with these methods await to be reproduced in different centers. Of note, collagen fleece plugs (Lyostypt) are now routinely used for prophylactic plugging of iatrogenic membrane defects following fetoscopic

endoluminal tracheal occlusion for in utero therapy of congenital diaphragmatic hernia in one center, in Leuven, Belgium.

Other prophylactic plugging techniques such as bioscaffold-type plugs manufactured directly from decellularized amnion tissues have been so far only evaluated in animal models (Mallik et al., 2007; Ochsenbein-Kolble, Jani et al. 2007)Further, also laser welding, pre-emptive placement of synthetic surgical sealants before fetoscopic access, direct injection into amniotic fluid of fibrinogen/thrombin- based tissue sealant, and sealing with platelet-rich plasma were evaluated in laboratory settings (Louis-Sylvestre et al., 1998; Reddy, Shah et al. 2001; Petratos et al., 2002; Cortes et al., 2005). An emerging notion is that spontaneous healing appears slow, if not absent in human fetal membranes. Histological follow-up of fetoscopic puncture defects in membranes of human patients several months after the procedure showed that the defects did not close by growth of new tissue(Gratacos, Sanin-Blair et al. 2006). The amnion layer contains few cells and does not contain blood vessels, which makes healing response in this layer highly unlikely. Trials in rabbits of prophylactic plugging of membrane defects with decellularized amnion scaffolds showed effective sealing without detectable signs of biological repair after a 1-week period (Mallik, Fichter et al. 2007), which is the maximum achievable duration in this experimental model. Recent studies in the midgestational rabbit observed signs of early healing of membrane defects upon addition of platelets or amniotic fluid cells to collagen plugs (Papadopulos, Klotz et al. 2006; Liekens, Lewi et al. 2008); it is unclear whether this effect could assume relevant degrees of long-term healing. The criteria for a prophylactic plug material may be to present an immediate, non-toxic and ideally, durable physical barrier to amniotic fluid, and not necessarily induction of biological healing. With this strategy in mind, we examined five liquid synthetic sealants, namely two types of cyanoacrylate glues and three poly (ethylene glycol-based) hydrogel-type polymers, for their principal aptitude for fetal membrane repair. Repair of defective tissue in moist/wet conditions or even underwater presents a particular challenge. In the present study, we addressed adhesion to moist, intact fetal membranes. Alkyl-cyanoacrylate glues were chosen on the basis of their well-known strong bonding to tissue, and their use as tissue adhesives in surgical and traumatic wound repair(Papadopulos, Klotz et al. 2006). Our choice of three synthetic poly (ethylene glycol) (PEG)-based hydrogel sealants, photopolymerizable gel, mussel-

mimetic adhesive and commercial SprayGel was based on data showing their interfacial bonding to various tissues, and the possibility to deliver them in minimally invasive liquid form for gelation in situ (West and Hubbell 1996; Johns et al., 2003; Burke et al., 2007). Two types of PEG-based hydrogels under present study, SprayGel and photopolymerized PEG, were already used clinically. SprayGel has been clinically used as bioabsorbable anti-adhesion barrier in patients undergoing myomectomy (Mettler et al., 2004). A clinically approved formulation of photopolymerized PEG hydrogel sealant, FocalSeal-L sealant, proved successful for closure of pulmonary air leaks in the lung occuring at cardiac operations(Gillinov and Lytle 2001). For the experimental mussel-mimetic adhesive hydrogel formulation of the present study, no clinical data exist yet. Here we estimated applicability of these synthetic polymers as sealants on fetal membranes based on their bonding to fetal membranes and toxicity in vitro, using the biosurgical Tissucol fibrin glue sealant as internal reference.

3.2 Results

3.2.1 Contact-mediated effect of sealants for membrane morphology

Histology in Figure 3.1 illustrates the effect of treatment for overall membrane morphology for the six bioadhesives under test. Fibrin glue and cPEG adhesive formed a continuous layer tightly bound to tissue (Figure 3.1B, arrow heads). The normal membrane morphology appeared maintained, with the amnion epithelial layer intact. SprayGel and pPEG exhibited partial or no binding to tissue, respectively. In the case of pPEG, we found the hydrogel layer sloughed into the culture medium shortly after immersion of the membranes in culture medium. Binding of Dermabond and Histoacryl to fetal membranes resulted in disruption of the amnion layer and change of overall membrane morphology, which was more pronounced for Dermabond. The effects of 50µl treatment volumes were very similar.

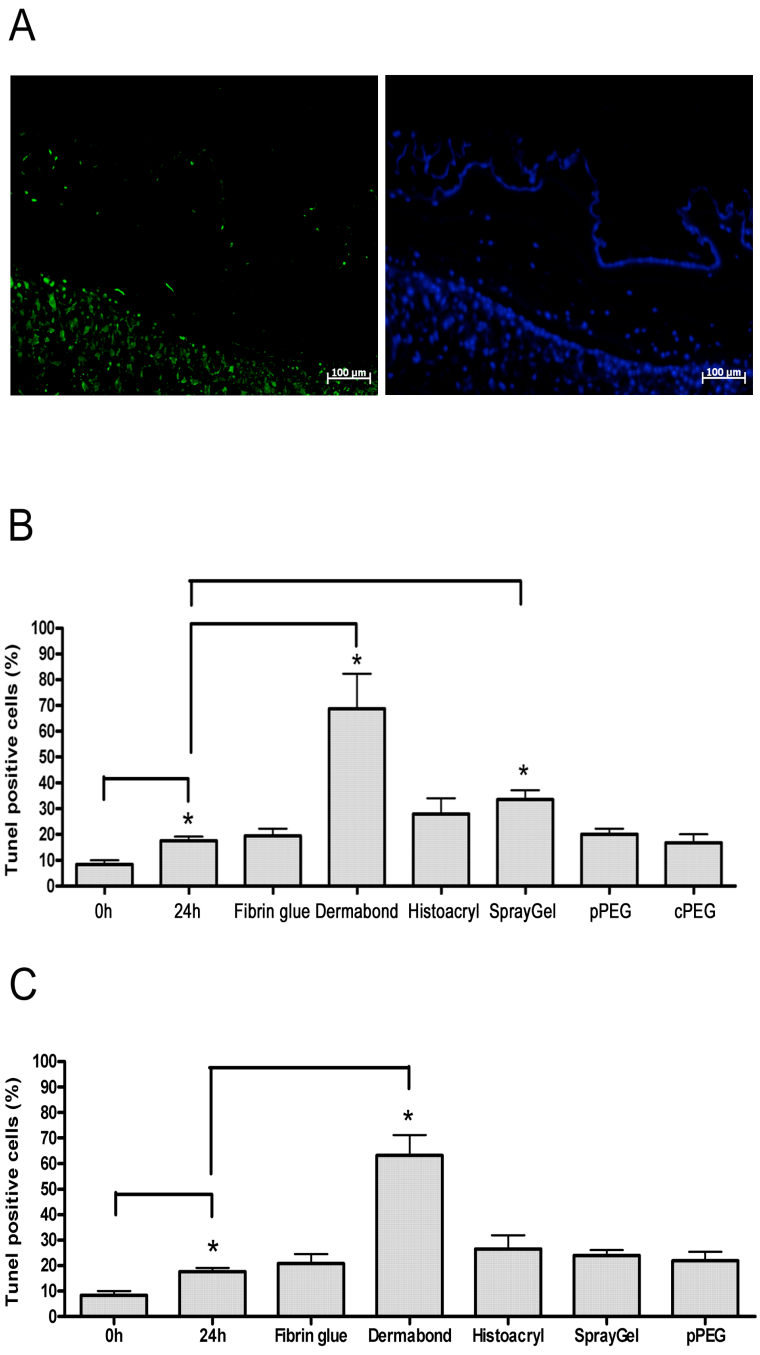

Figure 3.1: Direct contact-mediated cytotoxic effects of sealants for fetal membranes. (A) Fluorescence micrographs of apoptotic cells (green) and total cells (DAPI). The example shows a section of a membrane treated with Dermabond. (B) Apoptosis rates in membranes treated with 200µl sealant volumes. (C) Apoptosis rates in membranes treated with 50µl sealant volumes. Values are mean ± SEM. * indicates $p < 0.05$

3.2.2 Direct contact-induced apoptosis

We estimated acute toxic effects of sealants by measuring apoptosis in fetal membranes after 24h of direct contact with sealants. Figure. 3.2A depicts fluorescence micrographs of apoptotic cells (TUNEL) and all cell nuclei in tissue (DAPI) in fetal membranes treated with Dermabond. Figure 3.2B gives the apoptosis rates for the 200µl test series. In untreated reference membranes, the apoptosis rate increased to 17±2% during the 24h incubation. Treatment with fibrin glue, cPEG adhesive, and pPEG did not enhance apoptosis over control. Dermabond and SprayGel treatment significantly ($p < 0.05$) enhanced apoptosis by 3.9-fold to 69±13 % and by 1.9-fold to 34±3% over the control, respectively. Histoacryl treatment produced a 1.6- fold increase of apoptosis rate to 28±6%, which was not statistically significant over control. The outcome in the 50µl test series was similar, except that at lower dose, the apoptosis rate by SprayGel was not significant over control (Figure 3.2C).

3.2.3 Elution toxicity of sealants for primary cultures of amnion cells

To test the toxicity of the compounds released from the sealants, we investigated cell lysis, cell detachment and change of cell shape in hAECs and hAMCs that were grown in extracts of sealants in culture medium. None of the cultures, except those grown in extracts of Dermabond, appeared affected by toxic compounds after 24 hours and 72 hours. There was no difference between extracts prepared from sealant alone, or from sealants applied to membranes. hAMSCs were not affected in any condition as estimated by cell size and cell number. Only in the condition of hAECs grown in Dermabond, we observed modest, insignificant reduction of cell size and number. Cell sizes of hAECs cultured in Dermabond extracts were 1138±166 µm2 (n=193 cells) versus 1423±196 µm2 (n=168 cells); cell numbers in the Dermabond condition were lower (323±31 cells/optical field) compared to control cultures (424±47 cells/optical field). TUNEL staining of hAEC and hAMC cultures did not show any induction of apoptosis, and live/dead staining with calcein and ethidium bromide showed that practically all cells in culture were alive. Overall, extracts of sealants behaved non-toxic for amnion primary cultures.

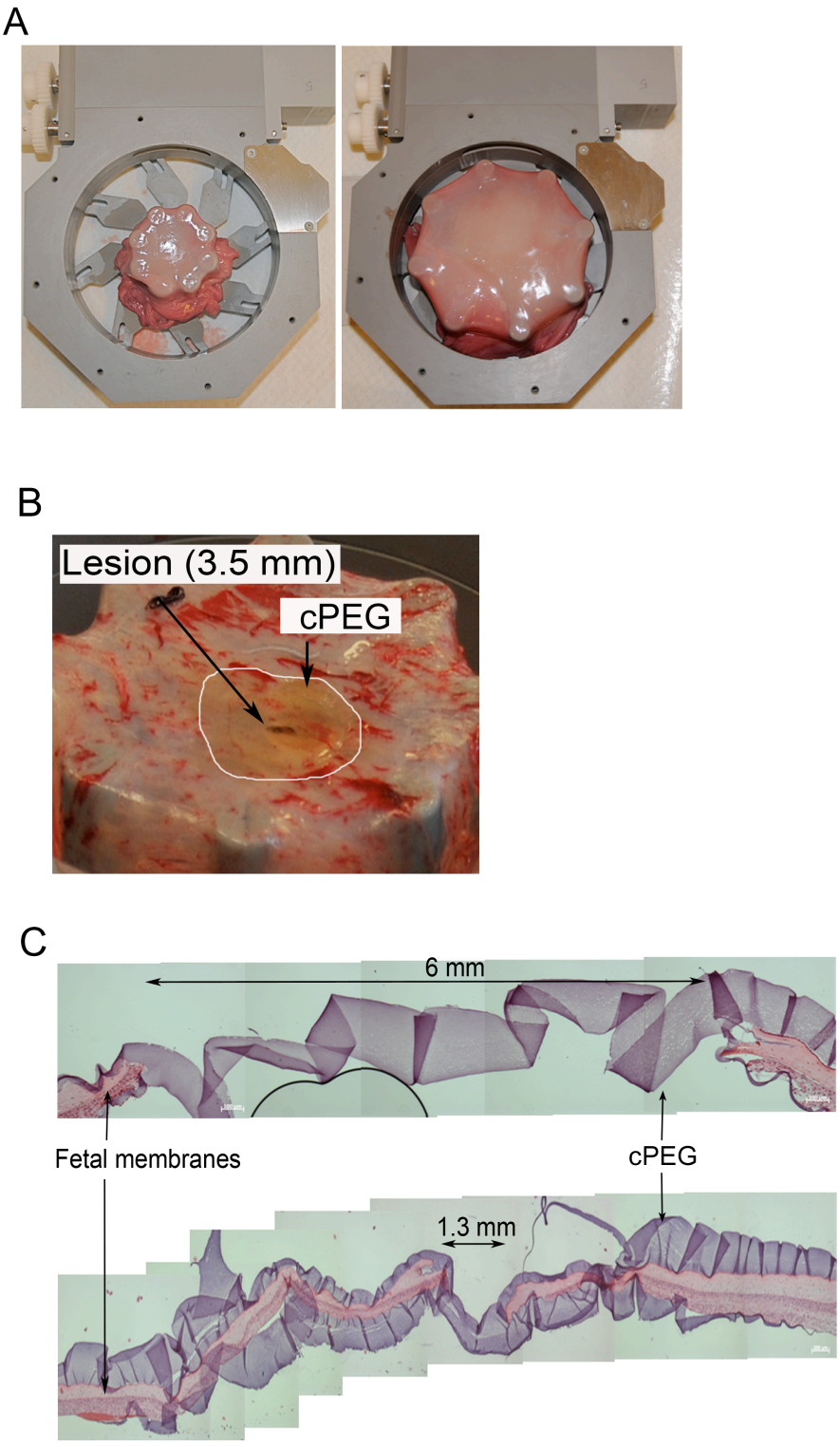

Figure 3.2: Ex vivo sealing of fetal membrane defects with mussel-mimetic adhesive. (A) Fetal membranes mounted in a computerized radial stretch device before and after stretch. (B) Through-thickness puncture wounds (arrow) were created on fresh fetal membranes with a Ø 3.5mm trocar. Approximately 0.5 mL of adhesive was applied over the defect. The white line marks the area of sealant. (C) Hematoxylin/eosin

stained cross-section of a trocar puncture treated with cPEG adhesive. The hydrogel appears as ribbon-like structure that bridges the puncture edges. The bottom image shows a cross-section of the same lesion at a narrow location.

3.2.4 Sealing of punctured lesions in vitro

Our stratification revealed that cPEG adhesive and Tissucol fibrin glue both show strong bonding to fetal membranes and behave non-toxic, which are two basic prerequisites for prospective candidates towards the iPPROM repair. cPEG adhesive is a new formulation that has never been tested before for sealing of membrane defects. We tested 0.5 mL cPEG adhesive for closure of Ø 3.5mm trocar puncture wounds in fetal membranes mounted in a biomechanical test device (Figure 3.3). Successful closure was achieved in all three test cases. Application of cPEG tissue adhesive over the defect resulted in an immediate leak-proof membrane seal that remained functional upon further radial stretch of the membranes. Figure 3.3C shows representative histologic images from two locations of a puncture lesion sealed with cPEG tissue adhesive. Histology confirmed that the cPEG tissue adhesive connected the wound edges over a distance of approximately 6 mm, which was the maximum diameter in such lesions. cPEG tissue adhesive was found adhered to both the amnion side, (which is the surface of application in these experiments), and also to the chorionic side of the membranes, thus, sealant apparently passed through the lesion and spread underneath the membranes in this current set up.

3.3 Material and Methods

3.3.1 Membrane collection and amnion cell isolation

A total of 15 fetal membranes were collected with written patient consent from elective caesarean sections. Mean gestational age was 38 ±1 weeks in the absence of labor, preterm rupture of membranes, chorioamnionitis, or chromosomal abnormalities. Fetal membrane pieces of 150-200 cm^2 were collected. The fetal membranes were cut approximately 2 cm from the placental disc to avoid the 'zone of altered morphology' overlying the cervix that is considered to be a naturally

predefined breaking site of the membranes (Mallik, Fichter et al. 2007). Human amnion epithelial (hAEC) and amnion mesenchymal cells (hAMC) were isolated and cultured as described earlier (Portmann-Lanz, Ochsenbein-Kolble et al. 2007).

3.3.2 Sealants

Alkyl-cyanoacrylate glue sealants: Dermabond (Ethicon Inc., Norderstedt, Germany) and Histoacryl (B. Braun GmbH, Tuttlingen, Germany) are 2-octyl cyanoacrylate monomer and n-butyl-2-cyanoacrylate monomer, respectively. These formulations possess syrup-like viscosity. These glue act through anionic polymerization of hydroxyl groups from the minute amounts of moisture normally present on actual surfaces that are glued, including biological surfaces. Cyanoacrylate glues are known to be extremely adhesive to tissue (Leggat et al., 2007; Liekens, Lewi et al. 2008). Water act as a catalyst to accelerate this polymerization. The polymerization occurs within minutes after application to tissue. The resulting resin is water resistant. Both Dermabond and Histoacryl are marketed as topical skin adhesives to hold skin edges of wounds from surgical incisions. As specified by the manufacturer of Dermabond, it is not for application on wet wounds.

Hydrogel sealants:

SprayGel (Confluent Surgical, Inc., Waltham, MA) is a sprayable anti-adhesion barrier polymer that consists of two synthetic liquid precursors that when mixed together, rapidly cross-link to form a solid absorbable hydrogel in situ. The first precursor is a modified polyethylene glycol (PEG) with terminal electrophilic esters groups while the other precursor solution contains PEG that has nucleophilic amine groups (Cortes, Wagner et al. 2005). SprayGel is marketed outside the US for use in abdominal and pelvic surgical procedures. It has also been tried clinically to reduce formation of adhesion following ovarian surgery (Johns, Ferland et al. 2003). SprayGel was deposited at the fetal membranes through the air pump-assisted SprayGel Laparoscopic Sprayer. The gel is formulated to stay adherent on the site of application for approximately five days, thereafter it is absorbed by gradual hydrolysis.

Photopolymerized PEG hydrogel sealant (pPEG) was formed via in situ interfacial photopolymerization of PEG diacrylate precursor of average molecular weight 700 Da

(Sigma) according to a previously described gelation protocol (Devlieger, Millar et al. 2006)[20]. Fetal membranes were flushed with a tissue adsorbing photoinitiator eosin Y (1mM in 10mM 4-(2- hydroxyethyl) piperazine-1-ethanesulfonic acid, pH 7.4, 0.15M sodium chloride; (HEPES- buffered saline). Then solution containing 10% PEG diacrylate and the co-catalysts triethanolamine (13.2 µL/mL) and 1-vinyl-2-pyrrolidine (3.5µL/mL) in HEPES-buffered saline was applied to the membranes and photopolymerized by irradiation at 480-520 nm and 75mW/cm^2 for 1 min from a portable Cermax xenon fiber optic light source, CXE300 (ILC Technology Inc., USA).

The mussel-mimetic tissue sealant is a catechol-functionalized poly (ethylene glycol) (cPEG) whose molecules crosslink into a hydrogel by way of oxidation after addition of sodium periodate (Lee, Dalsin et al. 2002). The composition and synthesis of cPEG is described in reference (Lee, Lee et al. 2007) . For gelation, equal volumes of the polymer precursor solution (300 mg/mL in phosphate-buffered saline (PBS)) and the cross-linking solution (12 mg/mL sodium periodate in water) were mixed using a dual syringe applicator device equipped with a blending connector with mixer (FibriJet; Micromedics, Inc., St. Paul, MN). Hydrogels prepared from cPEG polymer and its derivatives are expected to possess the ability to secure very strong adhesion to almost any surface, even under wet conditions. The presence of catechol in cPEG sealant was inspired by the wet adhesive properties conferred by the catechol side chain of 3,4-dihydroxyphenylalanine (DOPA) amino acid, which is found in high concentrations in the foot proteins of marine or freshwater mussels (Lee et al., 2006; Lee, Lee et al. 2007). Tissucol Duo S fibrin glue (Baxter AG, Volketwil, Switzerland) is a biological two-component adhesive that forms by mixing of human plasma cryoprecipitate solution with thrombin solution. The chemical and physical polymerization of the main component of fibrin glue sealant, fibrinogen, mimics the last step of the natural blood clot formation; Fibrin glue is clinically widely applied as hemostatic surgical sealant or adjunct to suture (West and Hubbell 1996).

3.3.3 Toxicity tests

Toxicity of sealants for fetal membrane cells was evaluated using direct contact and elution tests, as per International Organization for Standardization (ISO) 10993-5 guidelines.

3.4.3-1 Direct contact cytotoxicity:

Direct contact studies were performed with term fetal membranes obtained from three cases. The amniotic layer was chosen for sealant application (Figure 3.1A) because this layer was proposed to be the strength-bearing layer of fetal membranes and major determinant for PPROM.31 2x1cm patches of freshly harvested fetal membranes were placed into wells of 6- well plates with amnion layer up. The sealants were applied at 50µl and 200µl volumes except cPEG adhesive, which were only tested at 200µl volume because of limited material. Membranes covered with sealant were covered with 3 mL culture medium (Ham's F- 12/DMEM supplemented with 10% FBS, 100 U/ml penicillin, and 100 µg/ml streptomycin) and cultured for 24h at 37°C. Controls were untreated membranes that were immediately processed for histology (control '0') or cultured for 24h (control '24'). After 24h, the treated membranes were fixed in 4% formaline, embedded in paraffin and sectioned for histology. Deparaffinized sections were either stained with hematoxylin-eosin (H/E), or stained for apoptotic cells using TUNEL technology (Terminal deoxynucleotidyl transferase dUTP nick end labeling; In Situ Cell Death Detection Kit, Fluorescein (Roche Diagnostics GmbH, Mannheim, Germany). For total cell counts, all cell nuclei were counterstained with 4',6-diamidin-2'-phenylindol-dihydrochlorid (DAPI; Sigma, Buchs, Switzerland). The histologic images were taken with a Zeiss Axiovert 200M fluorescent microscope (Carl Zeiss, Goettingen, Germany) equipped with a Zeiss AxioCam MRc digital camera and analysed with AxioVision Rel. 4.5 software (Carl Zeiss). Apoptotic and total cell counts were acquired from fluorescence micrographs using automated image analysis software ImageJ 1.34s (National Institute of Health, Bethesda, ML). One tissue section per case was analysed, taking four optical fields per section for analysis.

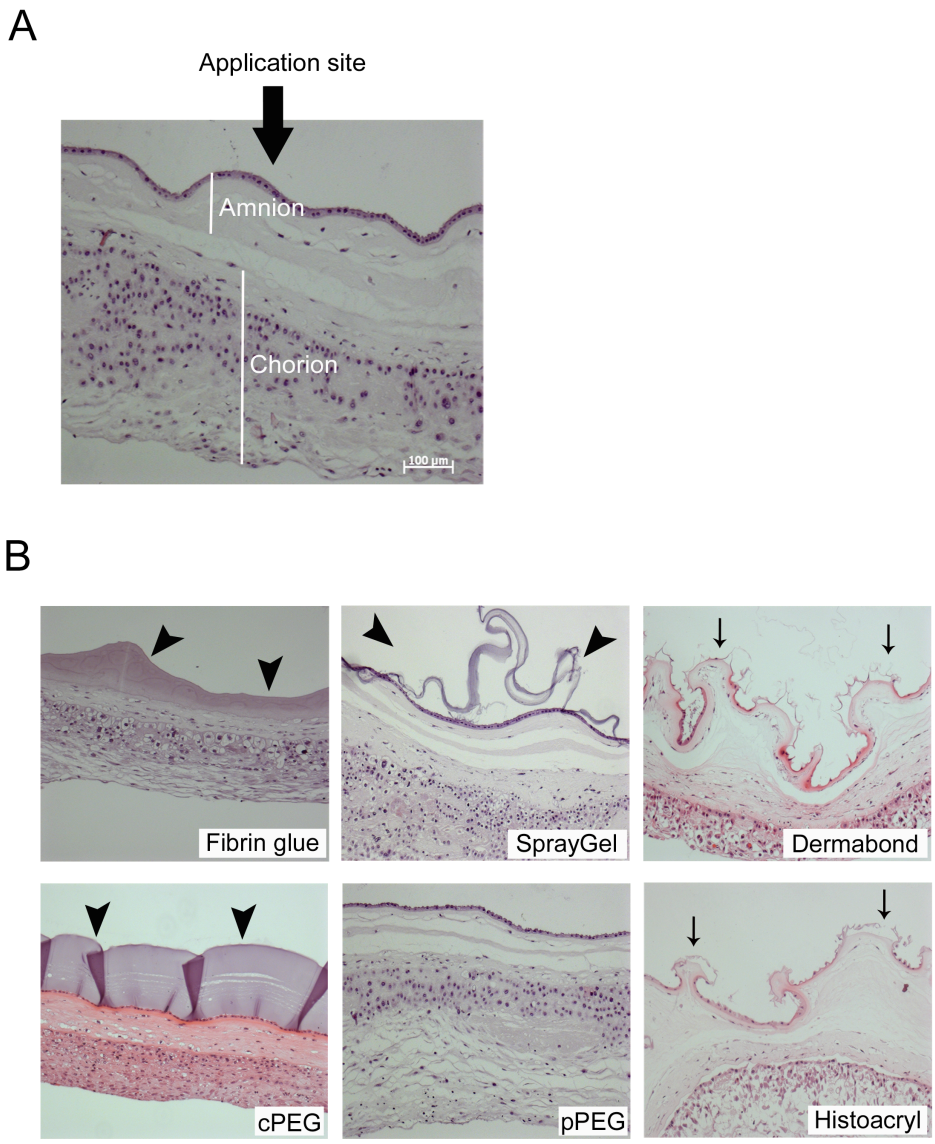

Figure 3.3: Histologic assessment of bonding properties and effect for membrane morphology of bioadhesives. (A) Sealants were applied on the amniotic site of fetal membranes. (B) Images of hematoxylin/eosin-stained cross-sections of fetal membranes that were incubated with sealants for 24h. Fat arrows mark the hydrogels; thin arrows mark the damage to the amnion layer by Dermabond and Histoacryl. Bar size: 100 µm

3.3.3-2 Elution toxicity:

To test potential toxicity of soluble compounds released from the sealants for cultured amnion cells, two types of extractions were performed: First, extracts from sealant alone. For that, 0.2 mL of glue/hydrogel were incubated for 24 hour in 3 mL Ham's-F12/DMEM/FCS culture medium. Second, extracts from sealants applied to membranes. The second method was to resolve whether treatment of membranes could result in production of cytokines by hAECs and hAMCs that add to induction of apoptosis. For that 0.2 mL glue /hydrogel sealant were applied to 2 x 1 cm pieces of fetal membranes and incubated for 24h in 3 mL Ham's- F12/DMEM/FCS culture medium. The extracts were collected and stored at -80°C until use for culture. Amnion cells from four human cases were subjected for assay of toxicity, and for each sealant the extraction test was evaluated in triplicate. $2x10^4$ hAECs or hAMSCs were seeded per well of 48 well plates and cultured in Ham's/F12/DMEM/FCs standard medium near to confluence. Then medium was removed, and cells overlaid with 0.4 mL of extracts from either sealant alone, or extract from membranes + sealant. Extracts from untreated membrane samples from the same patients in standard culture medium served as controls. The cells were cultured for 72 hours. Cell morphology was assessed microscopically, and degree of cell detachment and lysis was judged qualitatively. Following evaluations were performed:

(i) For total cell count, hAECs and hAMSCs were stained with DAPI (ii) Apoptotic cells were detected with in situ Cell Death Detection Kit (Roche Diagnostics GmbH). Total cell counts and apoptotic cell counts were acquired from fluorescence fluorescence micrographs using automated image analysis software ImageJ 1.34s (National Institute of Health, Bethesda, ML). (iii) Areas of individual cells were measured using LeicaQ Win Image Analysis software (Leica Imaging System Ltd, Cambridge, UK). (iv) Live/dead cell staining was performed. For that, amnion cell cultures were incubated for 3 min with a mix of calcein to detect live cells and ethidiumbromide homodimer to detect dead cells at 1μM and 2μg/ml, respectively. All experiments were performed in triplicates and four optical fields were analysed for each sample.

3.3.4 Sealing of fetal membranes lesion in vitro

Sealing performance of cPEG adhesive was tested on trocar punctures through fresh fetal membranes. For that, wet fetal membranes were flat-mounted with the amnion side up on a commercial motorized mechanical stretch device named 'The Cellerator' (Cytomec GmbH, Switzerland; http://www.cytomec.com/) that we further adapted for use in fetal membrane studies (Figure 3.3A). The Cellerator device permits expansion of fetal membranes expansion in a quasi-isotropic fashion, with points of attachment distributed in a near-circular pattern around the mounted membrane. While mounted in this device, membranes were continually kept moist with PBS. Puncture lesions were created with a three-side pointed Ø 3.5mm trocar (Richard Wolf GmbH, Knittlingen, Germany), and approximately 0.5 mL cPEG adhesive was applied over the membrane defect. Two minutes after treatment, membranes were further stretched by about 30% of their original area. To demonstrate leak-proof sealing, the stretched membranes, still mounted in the device, were overlaid for 10 min with 0.3 L water. After the leak-proof test, the area of the treated membrane defect was excised and processed for standard histology. Histologic sealing was estimated microscopically from hematoxylin/eosin stained sections by the ability of the sealant to form a continuous bridge between the wound edges.

3.3.5 Statistical analysis

Data are shown as mean ± SEM. Two-tailed unpaired t test was performed using GraphPad Prism version 4.00 for Windows (GraphPad Software, San Diego, CA, USA). Significance level was set at $p< 0.05$.

3.4 Discussion

Three commercial and two experimental synthetic sealants were tested along with Tissucol fibrin glue for applicability on fresh, moist human fetal membranes, using interfacial bonding and cytotoxicity after a 24h direct contact duration in vitro for performance assessment. Four of the five synthetic sealants failed to meet the combined requirements of membrane bonding and non-toxicity, which excludes them for this type of repair. Our screen identifies one synthetic hydrogel, cPEG tissue adhesive, that exhibits bonding to membranes and non-toxic characteristics that favorably compare to fibrin glue. cPEG adhesive demonstrated repair capacity for 3.5

mm trocar punctures, accomplishing immediate leak-proof sealing, which may warrant further evaluation in vivo.

Membrane bonding properties of the six bioadhesives under this study demonstrated large variability. Cyanoacrylate-based glues seem inappropriate for application on fetal membranes. The observation of their strong bonding to fetal membrane tissue was accompanied by obvious damage to the amnion epithelial layer and disruption of membrane structure, especially the amnion layer. Amniotic integrity is considered more important than chorionic integrity because the amnion is thought to have greater tensile strength.31 In addition, Dermabond, but not Histoacryl, exhibited significant cytotoxicity. Two of the PEG- based hydrogel polymers, photopolymerizable PEG hydrogel and SprayGel, failed to bond to fetal membranes sufficiently. Photopolymerized PEG-diacrylate hydrogels were previously used to create thin intravascular barriers to block thrombus deposition after balloon-induced arterial injuries in animal models, and firm adhesion of the PEG-diacrylate hydrogel to arterial walls was reported (Hill-West et al., 1994; West and Hubbell 1996). Although the pPEG and SprayGel hydrogels could be polymerized on fetal membranes, they sloughed off from the membranes quickly after the immersion of the membranes in culture medium. Neither the hydrogel itself nor the one-minute laser irradiation required for hydrogel curing produced adverse effects for membrane integrity. In the case of SprayGel, the resulting polymer layer was discontinuous, weakly bonded to membranes, and cytotoxic.

cPEG adhesive, on the other hand, displayed membrane bonding and compatibility comparable to that of Tissucol fibrin glue. cPEG adhesive is a two-component, self-cross linking polymer with the remarkable property to form strong and durable bonds to many surfaces even in wet environment. Creation of cPEG adhesive has been inspired by the composition of liquid adhesives secreted by marine mussels, which allow these organisms to firmly anchor themselves to any surface. The wet adherence of native mussel adhesive proteins rests on the unusual amino acid residue 3,4 dihydroxyphenylalanine (DOPA) that is present in high concentrations in the foot proteins of mussels (Waite 1999; Lee et al., 2007; Lee et al., 2007). Work in the group of one of the authors (P.B.M.) and other laboratories has demonstrated that the wet adherence ability of mussel foot proteins can be conferred onto synthetic polymers by

way of incorporating DOPA and DOPA analogues (Deming 1999; Yamada et al., 2000; Lee et al., 2002; Burke, Ritter-Jones et al. 2007). Indeed, previous work has demonstrated that DOPA- functionalized PEG precursors cross-link via sodium periodate-mediated oxidation to form adhesive hydrogels with high rigidity (Lee, Dalsin et al. 2002). In the present study, the cPEG polymer contains a simplified mimic of DOPA in the form of a reactive catechol group, generating a new variation of the adhesive that can be used under the same preparative conditions. This formulation possesses both appealing and potentially problematic characteristics for use as fetal membrane sealant. Properties that we consider favorable are fast gelation (under a minute); very slow hydrolysis over several months, allowing for durable sealing; and excellent tissue adhesion. Recent analysis revealed that bonds formed by a mussel-mimetic adhesive between porcine dermal tissues were several times stronger than those formed by fibrin glue (Burke, Ritter-Jones et al. 2007). Possible disadvantages of the present formulation are the use of the strong oxidizing reagent sodium periodate as trigger of polymerization, which is known to be strongly irritating. However, a rapid chemical reaction ensues upon contact of periodate with pPEG, which ultimately gives rise to chemical crosslinking of the polymer but also results in reduction of periodate to less harmful oxidative species (Burke, Ritter-Jones et al. 2007). Our estimates of direct contact cytoxicity were obtained after 24h, which is the minimal contact duration for assessment according to the ISO 10993-5 test guidelines. Additional studies with extended contact between fetal membranes and cPEG sealant in organ culture in vitro37 and in animal models will be necessary to establish long-term safety for membrane sealing. Issues of in vivo irritation and inflammatory tissue response to cPEG adhesive are currently addressed in another study involving the use of cPEG for transplantation of mouse islets. While the results of that study in mice, like the in vitro data reported herein, reveal favorable biocompatibility, ultimately the full effects of cPEG on uterine contractions and fetal survival and integrity will require further evaluation in the pregnant rabbit model. Of further note, the present study was performed with membranes from the third trimester of pregnancy, while operative fetoscopy is usually performed in the second trimester. Membranes of earlier gestation could exhibit different reactivity to sealants and further testing on such membranes will be necessary.

In summary, this study points to a new synthetic hydrogel formulation, mussel-mimetic sealant, and the biological Tissucol fibrin glue with appealing properties for membrane sealing. Still, we are aware that such data in vitro are limited in their ability to predict success in the in vivo situation.

Chapter 4

Relation between uniaxial mechanical properties and microstructure of human fetal membranes

This part of my PhD thesis is a modified version of the publication:

Relation between mechanical properties and microstructure of human fetal membranes: An attempt towards quantitative analysis

Mahmood Jabareen[1*], Ajit Sankar Mallik[2*, 3], Grozdana Bilic[2], Andreas hugo Zisch[2, 3], Edoardo Mazza[1, 4]

[1]Department of Mechanical and Processing Engineering, ETH Zurich, Switzerland

[2]Department of Obstetrics, University Hospital Zurich, Switzerland

[3]Zurich Center of Integrative Human Physiology

[4]Swiss Federal laboratory for Materials Testing and Research (EMPA), Switzerland

[*]Both authors contributed equally

4.1 Introduction

4.1.1 Outline of this work

Understanding the relationship between fetal membrane micro constituents and its deformation and rupture properties is essential for developing strategies for prevention of iPPROM. Several studies have addressed the biomechanical properties of fetal membranes, but no information exists so far on quantitative correlations between membrane microstructure constituents (elastin, collagen) and the mechanical parameters characterizing the deformation behaviour of fetal membrane. In this study, we designed to measure the baseline behaviour of fetal membranes in a uniaxial set up, in order to determine constitutive model parameters, and to examine their relation to collagen, elastin and thickness of the fetal membranes.

4.1.2 Biomechanics of Fetal membranes

In the normal arrangement of fetal membranes, thin avascular amnion layer is passively attached to the thicker, chorion layer. The extracellular matrix (ECM) component is largely made of collagen, predominantly types III, and I in the compact layer of amnion and throughout chorion. The collagens undergo constant turnover throughout pregnancy to accommodate the increasing volume and tension as gestation progresses (Kanayama et al., 1985) . Results from laboratory tests suggest that the amnion is a remarkably resilient tissue material (Oxlund et al., 1990; Oyen et al., 2006). Its mechanical behavior is typical of nonlinear viscoelastic materials, and depends on deformation history (Oyen, Cook et al. 2004). Gestational aging, inflammation and labor decrease fetal membrane strength and elasticity (Oyen, Cook et al. 2004; Calvin and Oyen 2007). The ECM components collagens and elastin are of particular interest due to their well-known mechanical function in connective tissues. Determinations of total collagen content from hydroxyprolene measurements showed that collagen content of amnion is around twice that of chorion, some 33–52% versus 12– 15% (Halaburt et al., 1989; Hampson et al., 1997; MacDermott and Landon 2000; Meinert et al., 2001). Biochemical studies of human fetal membranes indicated that decreased collagen content, altered collagen structure, and increased collagenolytic activity associate with premature rupture (Fortunato et al., 1997). Till

the last decade, efforts to identify elastin in human fetal membranes had been unsuccessful (Verbeek et al., 1967; Aplin and Campbell 1985). Only recent studies (Hieber et al., 1997) confirmed the existence of tropoelastin mRNA in amnion, chorion and deciduas of human samples. Quantitative studies of elastin content in human fetal membranes produced hugely diverging results: Hieber et al. (Hieber, Corcino et al. 1997) estimated the amount of elastin in whole fetal membranes as 0.08% of fat free dry weight, whereas Wilshaw et al. (Wilshaw et al., 2006) measured that elastin constitutes ca. 36% of total weight of fresh amnion. This discrepancy points to an obvious challenge of quantitative determination of elastin in tissues.

Most data on fetal membranes mechanical behavior have come from three types of mechanical testing: (1) uniaxial tensile testing; (2) biaxial inflation burst testing; (3) biaxial puncture testing (Calvin and Oyen 2007). Here we used a uniaxial test setup to characterize the mechanical properties of nine intact human fetal membranes. A limitation of previous studies of physical parameters of fetal membranes has been the lack of information on membrane thickness as well as the lack of information on biochemical correlates for the sample under test. In light of these former mechanical studies, the present study is distinguished by its attempt to correlate stress–strain response with microstructural parameters (total soluble collagen, soluble elastin, amnion thickness, chorion thickness) for each fetal membranes sample. We here introduce a new histologic protocol for exact determination of amnion and chorion thickness. Methods of nonlinear continuum mechanics were applied for the analysis of the stress–strain curves. The data were analyzed towards a quantitative evaluation of the relationship between mechanical behavior and tissue's micro- structure.

4.2 Results

4.2.1 Thickness measurement

As stated by (Calvin and Oyen 2007), the importance of a precise measurement of membranes' thickness for a biomechanical evaluation of fetal membranes cannot be overemphasized. Table 2 summarizes the thicknesses of the nine tested membranes as determined from histologic sections. Average thickness of the amnion and chorion layers was 111 ± 78 μm, and 431 ± 113 μm, respectively. There was no correlation between chorion and amnion thickness. The here introduced non-contact, optical method for thickness measurement was chosen over earlier trials using a conventional

micrometer. In fact, the perception of pressing and the amount of membrane squeezing in the latter was user-subjective and generated non- related variable thickness values. In addition, the present protocol with separation of amnion and chorion enables a distinct evaluation of the thickness of each layer. Our measurements found the thicknesses of amnion and chorion considerably larger (about twice) than previously reported in literature (Oxlund, Helmig et al. 1990; Helmig et al., 1993; Prèvost 2004), whereas the relative values of amnion with respect to chorion (with the thickness of amnion approximately one quarter of that of chorion) are in line with previous findings.

4.2.2 Elastin content

The method for elastin determination applied in the present work provides estimates of the oxalic acid-soluble elastin component in fetal membranes. Table 4.2 lists the elastin content of the tested membranes, ranging between 1.1 and 3% of wet weight, with an average of 2.1%. The variability of the measured elastin content among the donors was pronounced, with an overall standard deviation in the range of 30% of the mean value. No correlation was found between elastin content and amnion or chorion thickness.

Table 4.1: Microstructural data, layer thickness, elastin, collagen

Membrane #	Amnion [μm]	Chorion [μm]	Chorioamnion (Average)	Elastin [% ww]	Collagen [% dw]
I	305 ± 41	325 ± 47	630	2.10	12.98
II	105 ± 5	420 ± 6	525	3.03	5.47
III	125 ± 16	600 ± 20	725	1.67	11.63
IV	95 ± 7	431 ± 8	526	2.74	5.54
V	120 ± 6	458 ± 36	578	1.83	14.82
VI	87 ± 10	590 ± 11	677	1.20	6.46
VII	43 ± 11	310 ± 8	353	2.43	8.12
VIII	78 ± 15	460 ± 38	538	1.13	21.51
IX	46 ± 3	287 ± 27	332	2.94	7.91

The present data are significantly higher than the values reported earlier in reference (Hieber, Corcino et al. 1997), giving some 0.08% in fat free dry weight amnion, and much lower than in reference (Wilshaw, Kearney et al. 2006), which found some 36% in fresh human amnion. This discrepancy between the studies points to the well appreciated difficulty to measure elastin content in tissue with biochemical methods.

Morphometric analysis of histologic sections of fetal membranes could be an alternative method to estimate elastin content. We performed Van Giesson staining for collagen (pink to red) and elastin (blue-black) on sections of all donor membranes (see Figure 4.2). However, this stain showed inadequate to detect elastin against the 'background' of strong collagen staining in amnion and chorion. Together, the biochemical elastin data provide an indication of relative elastin density in each membrane, but the absolute numbers of elastin content could be different than the values reported in Table 4.2.

The dry weight amount of the elastin content may be estimated based on the water content of the membrane, which could be as high as 80%, according to references (Halaburt, Uldbjerg et al. 1989; Prèvost 2004). This leads to an average value of approximately 10% dry weight equivalent elastin content for the present data.

4.2.3. Soluble collagen content

Soluble, non-denatured collagen content of whole fetal membranes, amnion and chorion, was determined colorimetrically with the Sircol^{TM} assay, using pooled extracts of salt-soluble collagens (1M NaCl) and acid/pepsin-soluble collagens (0.5M acetic acid + pepsin). The total soluble collagen content measured for fetal membranes averaged 10.5% of dry weight. Table 4.2 summarizes the values for each sample of fetal membranes. The overall variability among the donors was in the range of 50% of the corresponding mean value, thus considerably larger than the scatter of elastin. Measurement of total collagen content was repeated three times for each sample with high reproducibility. The present values of total soluble collagen content are considerably lower than total collagen contents previously evaluated by the method of hydroxyproline determination (Halaburt, Uldbjerg et al. 1989; Meinert, Eriksen et al. 2001; Prèvost 2004); this is expected, as the latter method captures all collagen in tissue. Determination of total collagen content, and the quantification of different collagen types in fetal membranes for correlation with mechanical behavior will become subject of future investigations. As shown in Figure 4.1, there is a pronounced correlation with an inverse proportionality between soluble collagen and elastin content. One single membrane appeared far from the observed distribution (membrane number VI, indicated with a square in the Figure 4.1). The data point

corresponding to this membrane was not considered for the determination of the trend line in Figure 4.3.

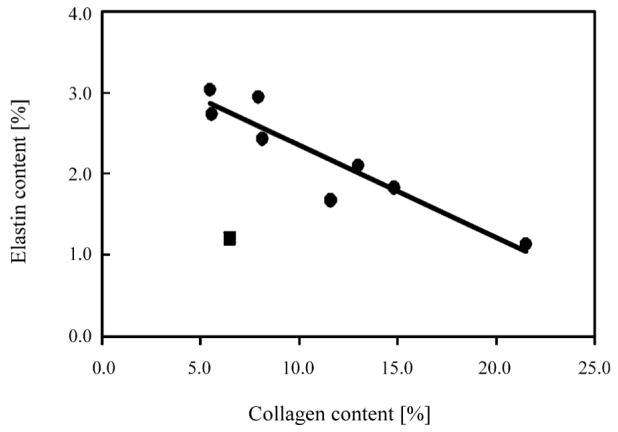

Figure 4.1: Correlation between measured elastin and collagen content (square: membrane VI)

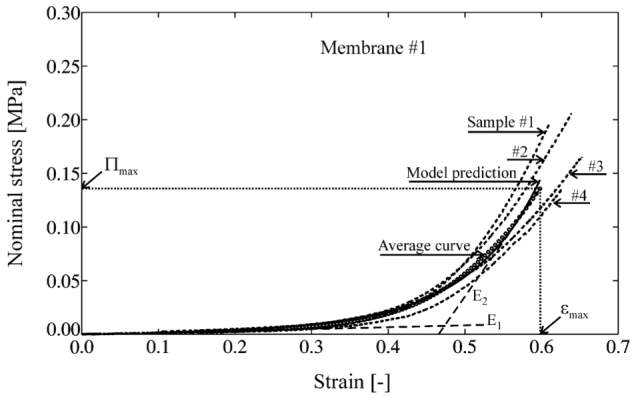

Figure 4.2: Stress–strain curves of four samples (membrane I), and the corresponding average curve. The scalar parameters characterizing the average curve are indicated

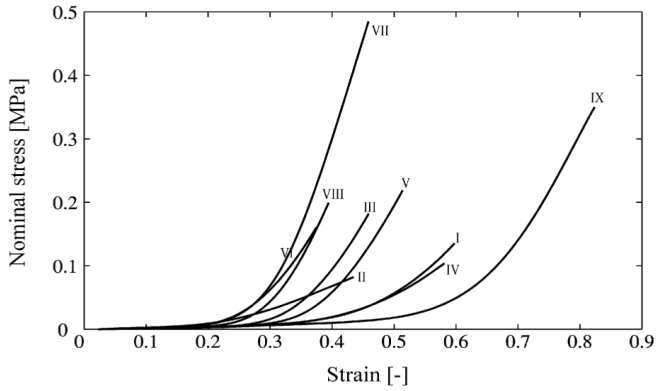

Figure 4.3: Stress–strain mean curves of all membranes.

4.2.3 Mechanical behavior

Table 4.3 gives the results of fitting the experimental data to the Rubin–Bodner equation. Regression analysis revealed high coefficient of determination R^2 for each measured curve. R^2 ranges between 0.829 and 0.992, with a mean value of 0.940. Prior the strain to rupture tests, a precondition phase was applied with 5 cycles of loading and unloading between 0 and 20% of nominal strain. It was found that the hysteresis loops shift vertically downward along the stress axis, and the difference between two consecutive cycles decreases with increasing the number of cycles.

Table 4.2: Mechanical parameters from the stress–strain curves: low-strain elastic modulus, E_1, high-strain elastic modulus, E_2, maximum strain, ϵ_{max}, maximum stress, $\prod_{max}$, and the parameters μ_0, q/μ_0 of the Rubin–Bodner equation.

Membrane #	E_1 [10^{-2} MPa]	E_2 [MPa]	ε_{max} [%]	Π_{max} [MPa]	μ_0 [10^{-3} MPa]	q/q_0 [MPa^{-1}]
I	1.62 ± 0.53	1.05 ± 0.24	63.2 ± 1.8	0.176 ± 0.032	2.44 ± 0.91	689.10
II	2.54 ± 0.61	0.42 ± 0.08	43.7 ± 4.1	0.083 ± 0.002	2.55 ± 1.24	633.89
III	1.17 ± 0.20	1.70 ± 0.28	48.1 ± 1.4	0.222 ± 0.037	0.92 ± 0.19	1965.03
IV	1.78 ± 0.95	0.66 ± 0.08	58.3 ± 1.7	0.106 ± 0.002	2.84 ± 1.96	584.18
V	1.48 ± 0.63	1.91 ± 0.42	54.5 ± 4.5	0.277 ± 0.061	1.44 ± 0.60	1213.48
VI	1.39 ± 0.28	1.74 ± 0.10	42.0 ± 4.0	0.239 ± 0.078	0.85 ± 0.23	2141.44
VII	2.31 ± 0.49	3.61 ± 1.45	50.6 ± 8.9	0.646 ± 0.151	1.65 ± 0.31	1040.44
VIII	1.39 ± 0.21	2.30 ± 0.53	42.6 ± 2.2	0.283 ± 0.101	0.85 ± 0.15	2141.78
IX	2.06 ± 0.13	1.94 ± 0.44	83.8 ± 4.2	0.382 ± 0.031	4.25 ± 0.39	363.61

The maximum stress in the 5th cycle was typically of the 80% of the corresponding value in the first cycle. Figure 4.2 shows the nominal stress (force per unit undeformed area) vs. the nominal strain curves for the four samples of membrane I, as well as the corresponding average (mean) stress–strain curve, and the prediction of the constitutive model. The average stress–strain curves of each of the nine membranes are plotted in Figure 4.3. It can be seen that the variability among different membranes is considerably larger than the scatter observed in measurements on samples from the same membrane. The curves are characterized by a low initial stiffness, with a nearly linear stress–strain relation. At larger strains considerable stiffening occurs, leading to a strongly nonlinear mechanical response. This behavior might be characterized using the low-strain elastic modulus, E_1, and the high-strain elastic modulus, E_2 (see Figure 4.2). Further characteristic parameters are the maximum nominal stress and strain denoted by $\prod_{max}$ and ϵ_{max}, respectively. The values of all four parameters are given in Table 4.3.

Table 4.3: Correlation coefficients between mechanical parameters and microstructural data.

	E_1	q/μ_0	E_2	ε_{max}	Π_{max}
Amnion thickness	−0.271	−0.142	−0.447	0.079	−0.452
Chorion thickness	−0.671	0.789	−0.178	−0.664	−0.407
Elastin content	0.827	−0.926	−0.314	0.544	−0.027
Collagen content	−0.548	0.485	0.301	−0.172	0.081

A quantitative comparison of these parameters with the corresponding values previously reported in literature (Oxlund, Helmig et al. 1990; Helmig, Oxlund et al. 1993) is impaired by the influence of specific characteristics of the experimental protocol, such as: (i) the strain rate (material's viscoelastic behavior leads to higher stiffness for higher speed of elongation in tensile tests); (ii) the number of cycles (and the corresponding strain range) prior to the effective testing (related to the loading history dependence of the mechanical response, ''preconditioning''); (iii) the clamping procedure, with ''gentle'' clamping leading to possible slippage (and thus influencing the actual value of elongation), and tied clamping leading to membrane damage and thus early failure; (iv) fracture originating at the clamping points: this phenomenon not only affects the values of maximum stress and strain, but also impairs the evaluation of the large strain deformation response (e.g. the parameter E_2); (v) the geometry of the membrane samples, with low aspect ratio of long to short side leading to apparent stiffer response, due to biaxial stress state at the clamped boundaries; (vi) the initially very low stiffness, which introduces an uncertainty related to the definition of a force threshold value at the beginning of the tensile test (in our case: 0.01N), and thus influences the horizontal position of the stress–strain curve; (vii) the environmental conditions, with dehydration affecting samples tested in air, and a possible influence of samples temperature; (viii) the protocol for sample collection, conservation and preparation; and finally (ix) the procedure for data analysis (determination of geometry, in particular thickness values, extraction of mean curves).

Derivation of constitutive models and direct comparison of mechanical parameters obtained in different laboratories will require the influence of all above effects to be quantified and corresponding ''standard'' experimental configurations and analysis

procedures to be defined. In the present study we applied the same protocol to all membranes. In this way, differences in the mechanical parameters can be considered as representative of differences in the mechanical behavior of the membranes, and thus be used for the analysis of correlation with the histological observations.

Failure at the end of the tensile experiments almost invariably occurred within the neighborhood of the clamping point and was thus due to local stress concentrations. For this reason, the measured values of maximum stress or maximum strain within the gage section do not correspond to the critical values of stress or elongation that locally induced failure in the membrane. These local values cannot be quantified. It is however interesting to note that the measured maximum values of strain in the present uniaxial experiments largely exceeds the corresponding values of membrane physiological deformation at term: in reference (Millar et al., 2000) a mean area stretch of 1.7, corresponding to principal strains of about 30%, was measured, whereas the lowest value of maximum strain in Table 4.3 is 42%. The value of E_2 is also affected by this uncontrolled influence of local effects, since its value is determined from the 10% last part of the curve, measured from the point of rupture. For these reasons, correlation with histological parameters is expected only for the mechanical data unaffected by local effects (leading to failure at the clamping points), i.e. the parameters E_1 and q/μ_0.

4.2.4 Correlation between mechanical and structural parameters

Correlation coefficients were calculated between microstructural data (soluble elastin and collagen, layer thickness) and mechanical parameters, see Table 4.4. The large strain elastic modulus E2 does not correlate with elastin or collagen content. The same applies for $\prod_{max}$, ϵ_{max}. As per previous explanations, these mechanical data are affected by uncontrolled (and non-systematic) local effects at the clamping points, so that no correlation was expected.

There is a high correlation between elastin content and the parameters E_1 and q/μ_0 (see Table 4.4 and Figure 4.4). A direct proportionality is observed between elastin and small strain elastic modulus E_1, whereas the coefficient q/μ_0 decreases with increasing elastin content. The latter coefficient is in the argument of the exponential

function of Eq. (2), and thus represents a measure of the degree of stiffening at larger strains.

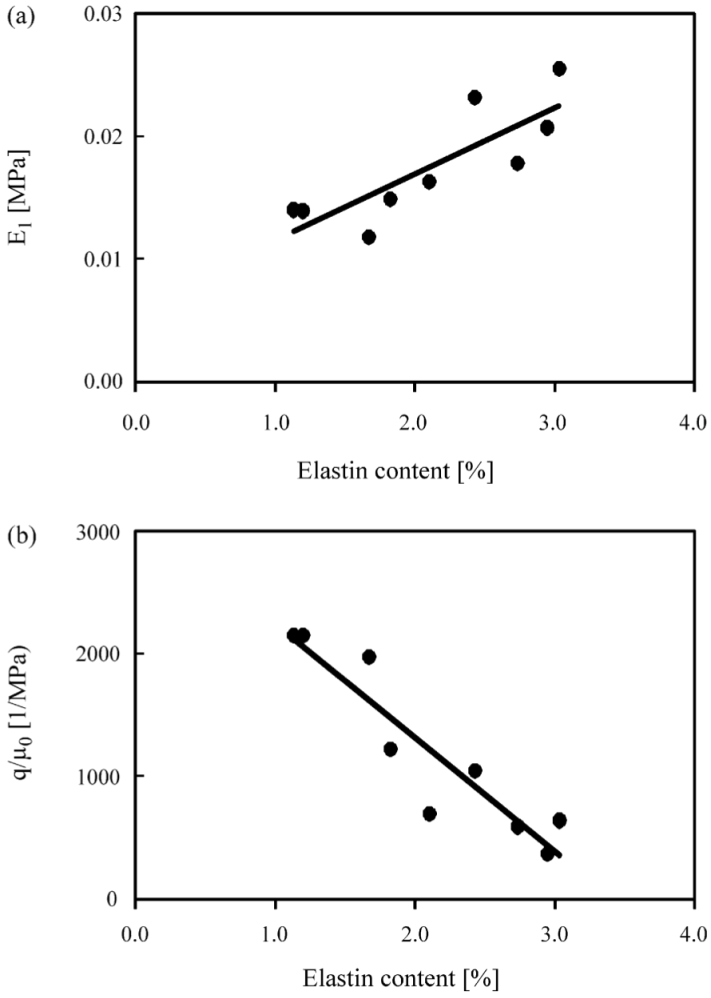

Figure 4.4: Correlation between the elastin content and (a) the low strain elastic modulus E_1; (b) the ratio q/μ_0.

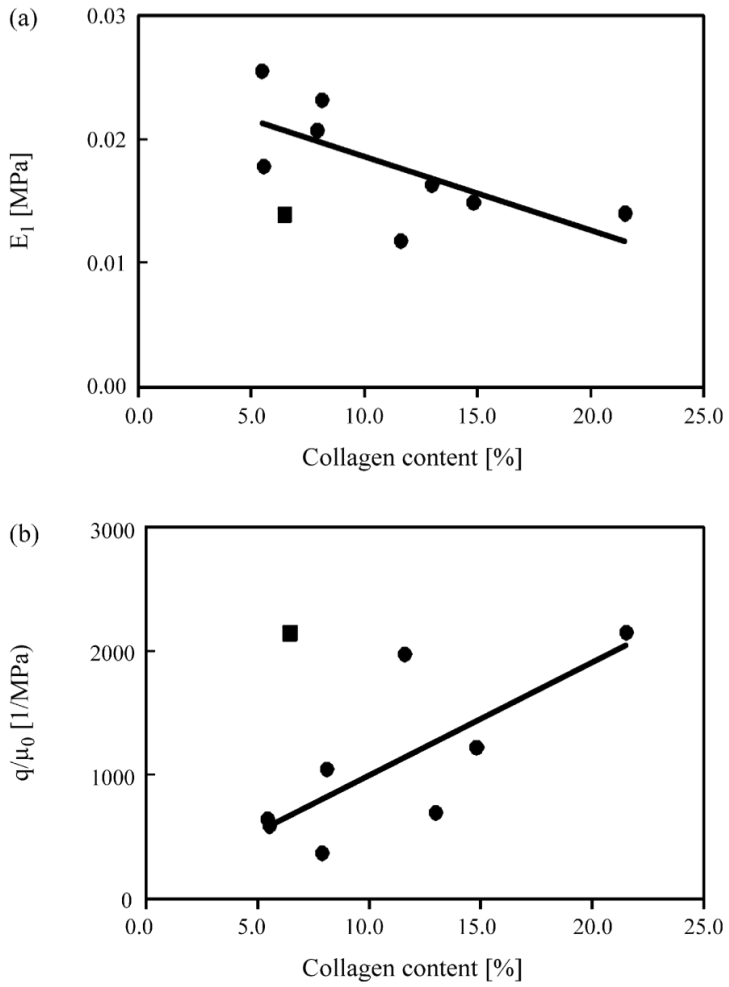

Figure 4.5: Correlation between the collagen content and (a) the low strain elastic modulus E_1; (b) the ratio q/μ_0 (square: membrane VI).

A (weaker) correlation is found also between the collagen content and E1 and q/μ_0 (see Figure 4.5). Here the proportionality is opposite as compared to elastin: direct proportionality between q/ m0 and collagen and inverse for E_1.

These observations are in line with expectations. In fact, contribution of collagen fibers to mechanical resistance is expected at larger strains, when fibers are reoriented and straightened through bending and twisting in the direction of loading, from an initially ‘‘crimped’’ state. Their stiffness at high strain thus dominates as compared with the more compliant elastin contribution. Bearing in mind the limitations due to the low number of membranes, the correlations observed in the present study might thus lead to the following interpretation: the initial stiffness (E_1) of the membrane

increases with larger elastin content, whereas larger amount of collagen leads to stronger stiffening at larger elongations (q/μ_0). On the other hand, the respective inverse proportionalities of elastin to q/μ_0 and collagen to E_1 might be attributed to the inverse proportionality observed between elastin and collagen content (Figure 4.1).

It might be speculated that a membrane with larger amount of elastin and less collagen behaves as an ‘‘elastic’’ layer, which resists small deformations with a gradually increasing force, but allows for large extensibility, without ‘‘locking’’ behavior. On the other hand, a membrane with more collagen and less elastin provides low resistance to deformation for small strains, but builds a rapidly increasing resistance with larger deformation and tends to limit the possible elongation (locking). In line with this hypothesis, it is observed that the stress–strain curve of membrane II differs from all other membranes in Figure 4.3. This membrane corresponds to the ‘‘early’’ delivery (31 weeks, in place of 37–38 of all other membranes), presents the highest value of elastin, the lowest value of soluble collagen, the highest value of E_1 and a low value of q/μ_0.

4.3 Materials and Methods

4.3.1 Sample collection

Fetal membranes from nine pregnancies were collected. The Ethical Committee of the District of Zurich that operates under federal legislation approved the protocol (study Stv22/2006). Table 4.1 lists the obstetrical parameters. The pregnancies were randomly selected after serologic negative testing for human immunodeficiency, hepatitis B and C viruses, Streptococcus infection, Rubella and Toxoplasmosis. The selected women had no history of diabetes, connective tissue disorders or hypertension. The fetal membranes were collected immediately after elective cesarean sections in the absence of labor, chorioamnionitis, premature rupture or chromosomal abnormalities. Pieces of collected fetal membranes were approximately 150–200 mm^2. The fetal membranes were cut approximately 2 cm from the placental disc to avoid the ‘‘zone of altered morphology’’ (Osman, Young et al. 2006). Membranes were stored in physiological saline at 4°C until the samples were prepared and tested at the same day of delivery.

4.3.2 Sample preparation for mechanical testing

Fetal membranes were spread out and sandwiched between two layers of paper. A section of approximately 70 mm x 80 mm was mounted on a custom-built chopping frame designed to generate samples with size of 15 mm x 60 mm. The samples were obtained by careful incision along the borders f the grooves on the chopping frame using a surgical scalpel.

4.3.3 Uniaxial tensile test

Experiments were performed on a standard Zwick 1456 universal uniaxial test machine (Zwick Inc., Ulm, Germany). Samples were carefully fixed outside the test setup on two aluminum clamps, with an initial gage length of 40 mm. The clamps were coated with sandpaper in order to prevent slippage of the fetal membrane sample. It should be noted that this technique might cause local damage of the tissue at the grips site. Immediately after clamping, the samples were introduced into a custom built bio-chamber with temperature regulation (37°C) to simulate ‘‘in vivo’’ conditions. During the whole duration of uniaxial testing the samples remained entirely immersed in the physiological saline. The tensile force was measured with a 50 N load cell. A xy-bench was installed on the load cell to precisely align the sample along the machine’s axis. Tests were carried out under displacement-controlled conditions, with an elongation rate of 0.5% nominal strain per second. In order to obtain a ‘‘preconditioned’’ (YC 1993) state, the samples were subjected to five cycles of loading and unloading between 0 and 20% of nominal strain. Thereafter, the samples underwent uniaxial loading till rupture. Four samples were tested for each membrane.

4.3.4. Analysis of stress–strain curves

Fetal membrane tissue undergoes finite deformation and exhibits strong nonlinearity in the force–elongation relation, with typical exponential stiffening at higher loads. Therefore, the mechanical behavior of the fetal membrane must be analyzed-

Table 4.4:

Membrane #	Age [year]	GA [week + day]	Birth weight [kg]
I	31	38 + 3	3.85
II	41	31 + 2	1.73
III	30	38 + 1	3.10
IV	31	37 + 5	3.34
V	40	38 + 5	3.37
VI	39	38 + 3	3.32
VII	37	38 + 6	3.10
VIII	37	38 + 6	3.60
IX	36	38 + 2	3.50

within the realm of nonlinear continuum mechanics. In the present work the material response was evaluated using the constitutive model proposed by Rubin and Bodner (M. B. Rubin 2002). This model was originally developed for rationalizing the response observed in uniaxial experiments on excised samples of face tissue. It is capable of describing time and history dependence of the mechanical response of (anisotropic) biological tissue. No information on tissue anisotropy can be derived from our experimental observations neither on time dependent dissipative behavior, since all experiments were performed at constant (low) strain rate. For this reason, only the isotropic elastic part of the Rubin–Bodner equations was used for the present analysis. The model is characterized by the specific (per unit mass) strain energy function, Ψ, given by

$$\rho_0 \Psi = \frac{\mu_0}{2q}\left[e^{qg} - 1\right] \quad \textbf{Equation 4.1}$$

Where ρ_0 is the mass density in the reference configuration, q, μ_0 are material parameters. The function $g= 2m_1[J-1-\ln(j) + m_2(\varphi_1-3)]$ is specified in an additive form and contains the dependence on the kinematics variables J and φ_1. A detailed description of this model can be found in reference (M. B. Rubin 2002).

Four material parameters characterize the mechanical response according to this model, i.e. μ_0, q, m_1 and m_2, with $m_1\mu_0$ corresponding to the small strain bulk modulus, while $m_2\mu_0$ is the small strain shear modulus. According to the common assumption of incompressible behavior of biological tissues, volume preservation was considered in the present analysis, leading J = 1 in the above equations. It should be noted however, that from the available observations volume reduction due to fluid ‘‘exudation’’ at large strains couldn’t be excluded. The parameter m2 was determined

from the slope of the stress–strain curves (i.e. m_2 μ_0 = E1/3, with E1 as the small strain elastic modulus obtained from the experimental data). The two parameters (m0, q) were determined from fitting the whole stress–strain curve. Fitting was carried out with respect to the ‘‘preconditioned’’ final loading cycle, assuming a uniaxial stress state over the whole gage length. Specifically, the axial nominal stress, $\prod_{xx}$ (axial force per unit undeformed area), can be derived from the corresponding expression of Cauchy's stress tensor, and reads

$$\Pi_{xx}^{an} \frac{E_1}{3} \exp^{((qE1/3\mu 0)(\alpha 1-3))} \left((\varepsilon_{xx}+1) - \frac{1}{(\varepsilon_{xx}+1)^2} \right), \qquad \textbf{Equation 4.2}$$

$$\phi_1 = \left(\varepsilon_{xx}+1\right)^2 + \frac{2}{\left(\varepsilon_{xx}+1\right)}$$

with ϵ_{xx} being the axial nominal strain. The best fit value of (μ_0, q) was obtained by means of the Nelder-Mead simplex method (MATLAB), using the following objective function:

$$f = \sum_{i=1}^{n} \left(\Pi_{xx,i}^{an} - \Pi_{xx,i}^{\exp} \right)^2 \qquad \textbf{Equation 4.3}$$

Where, $\Pi_{xx,i}^{\exp}$ is the measured nominal stress component at the ith data point of each test.

The stress–strain curves are sometimes associated with a bilinear behavior (YC 1993)[73], characterized through two scalar quantities: the low-strain elastic modulus, E_1, and the high-strain elastic modulus, E_2. These values were calculated here from the initial and final 10% of the stress–strain curves of each membrane

4.3.5. Histology and thickness measurement

Thickness of the fetal membranes was measured after histological preparation. The stepwise sample preparation is described below:

1. Blunt dissection to separate amnion from chorion (Figure 4.6)

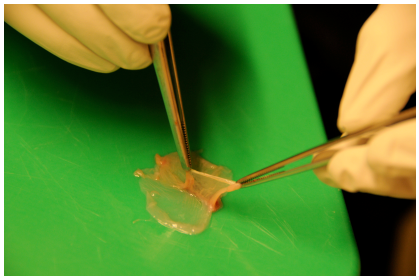

Figure 4.6: Amnion and chorion layers are separated from one another.

2. A small piece of filter paper is inserted between the amnion and chorion layer (Figure 4.7)

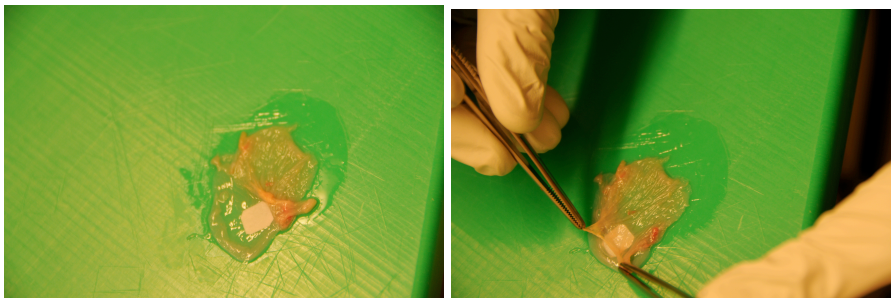

Figure 4.7: While placing the filter paper care is taken not to injure or stretch the layers

3. The fetal membrane sample along with the filter paper in between them is placed in the histological tissue cassette for paraffin embedding and further processing for hematoxylin and eosin staining (H&E stain) (Figure 4.8).

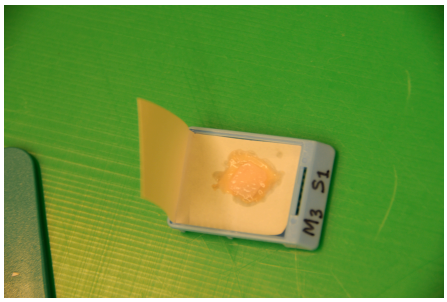

Figure 4.8: Fetal membrane sandwich with filter paper in between, ready for paraffin embedding

The paraffin sections were cut into slices of 4 µm in a microtome and stained for H&E. The measurement of the thickness was performed optically, using a Zeiss Axiovert 200 M microscope (with AxioVision Rel 4.5 software). Figure 4.9 gives an example. The amnion was identified by the epithelial cell monolayer. Following capture of the single microscopic field, the end-to-end thickness of each of amnion and chorion was measured by a scale bar perpendicular to the longitudinal axis of the membrane in the histological section. An average value of thickness of each layer was calculated out of six measurements along the histological section of the membrane. For qualitative visualization of the elastin and the collagen, the histological sections were stained with Van Giesson stain. An example of the Van Giesson stain is shown in Figure 4.10.

4.3.6. Biochemical assays

Insoluble elastin was extracted from the fetal membranes as soluble cross-linked polypeptide elastin fragments called alpha- elastin by the method of hot oxalic acid extraction. Briefly, a small piece of the fetal membrane was freeze-dried with liquid nitrogen in a small porcelain mortar, and then powdered with a pestle. 350 mg of the powdered tissue was transferred into an eppendorf tube, mixed with 0.75 ml of 0.25M oxalic acid, and then boiled in a water bath for 1 h. The supernatant was collected by centrifugation, and sediment was submitted to a second and third extraction under the same conditions. 0.2 ml of each of the three extracts were pooled, and then subjected to elastin assay. Soluble elastin content in the oxalic extracts was determined colorimetrically with the Fastin^{TM} elastin assay kit method (Pawlicka et al., 1999)

based on the fastin dyereagent:5,10,15,20-tetraphenyl-21,23-pophrinesulfonate (http://www.biocolor.co.uk/fastin.html; Biocolor Ltd., Newtonabbey, Northern Ireland; Product no. F2000) following the manufacturer's instructions. Absorbance was measured at 540nm. Human alpha elastin provided in the Fastin^{TM} elastin assay kit was used as standard. Final values were expressed as µg of elastin per wet weight. For preparation and determination of total soluble collagen, we followed the protocol of Hampson et al (Hampson, Liu et al. 1997) with some modifications. Briefly, 50 mg of dried (speed vacuum) fetal membrane sample was incubated in 25 ml of 1 M NaCl, 20 mM EDTA and cocktail protease inhibitors (Roche Diagnostics GmbH, Mannhein, Germany; 1Roche cocktail tablet/50 ml). The following steps were performed at 4 8C. Collagens were precipitated by addition of solid sodium chloride to a concentration of 4 M to the above solution with constant stirring for 24h. Following centrifugation at 10,000 g for 30 min, the pellet was resuspended in equal volume (25 ml) of 0.5 M acetic acid at pH 3 with 1mg/ml pepsin and stirred for 24 h. The insoluble material was removed by centrifugation at 10,000g for 30 min and 2M NaCl was added to the supernatant for salt precipitation, and stirred for 24 h. The above solution was centrifuged at 10000g for 30 min and this time the supernatant was discarded. The pellet was resuspended in 0.5M acetic acid at pH 3 and stored at -20°C till the final collagen assay. The total volume of collagen extract was 8 ml. The soluble collagen was determined colorimetrically using the Sircol^{TM} assay kit (http:// www.biocolor.co.uk/sircol.html), measuring the absorbance of the test samples and supplied standards at 540 nm in a 96-well micro titer plate. The Sircol dye reagent contains Sirius red which is an anionic dye with sulphonic acid side chain groups; these groups react with the side chain groups of the basic amino acids present in collagen. The specific affinity of the dye for collagen, under assay condition is due to the elongated dye molecules becoming aligned parallel to the long, rigid structure of native collagens that have intact triple helix organization. This assay does not permit to discriminate between different collagens types. The total collagen was expressed as mg of collagen per dry weight of the membranes.

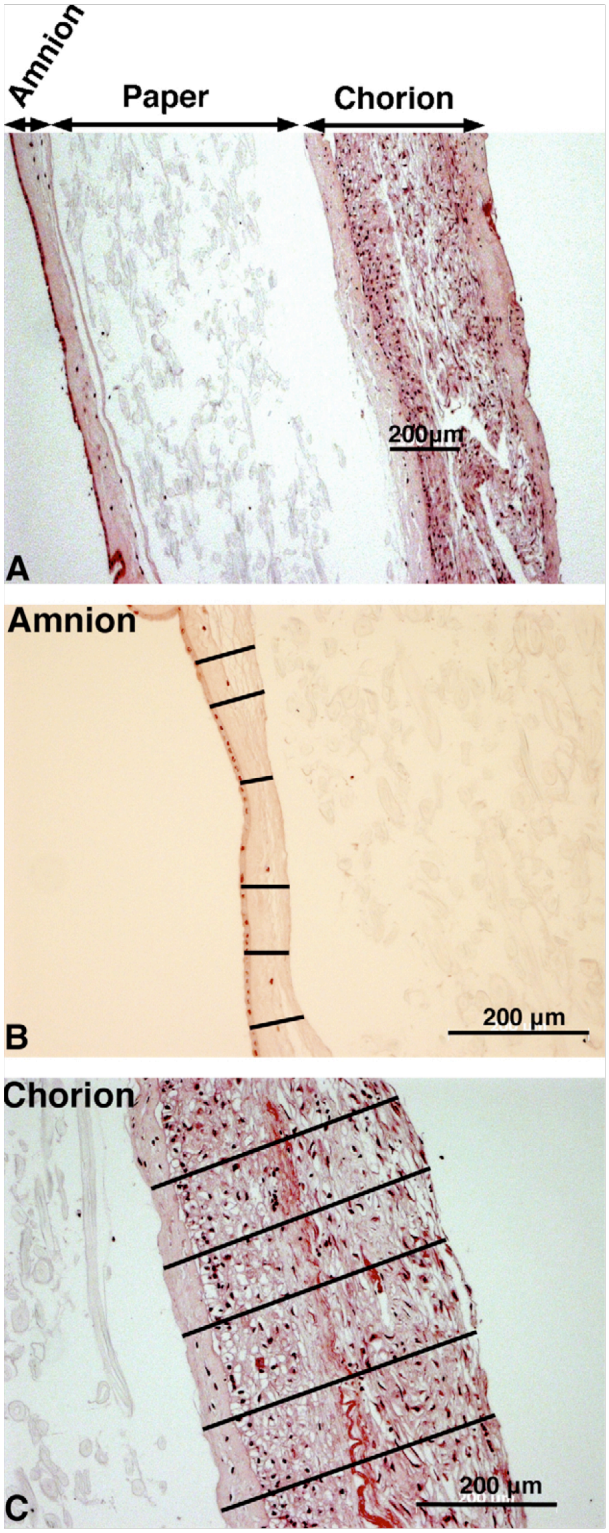

Figure 4.9: Optical method for thickness measurement: (A) view of the whole histological section, with amnion, paper, and chorion layers; higher magnification view of (B) amnion (C) chorion.

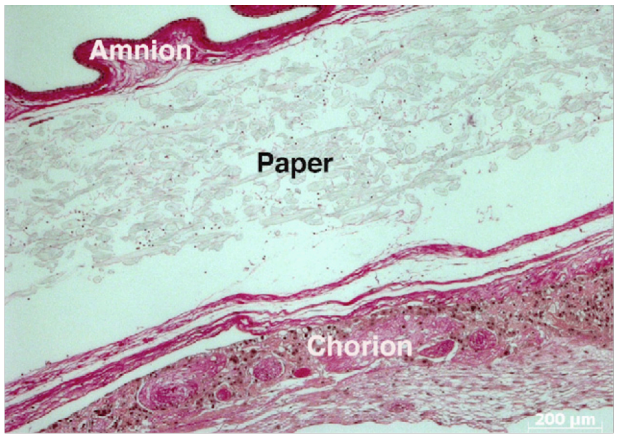

Figure 4.10: Van Giesson staining of fetal membrane sections. Collagen: Pink to red; Elastin: Blue black; Nucleus: Black-brown.

4.3.7. Statistics

Data of amnion and chorion thickness as well as all mechanical parameters are shown as mean ± standard deviation. Note that the assumption of a normal distribution underlying this characterization using mean value and standard deviation might be not completely appropriate for the present measurements with significant variability. Correlation coefficients were calculated using the built in function of MATLAB.

4.4. Discussion

This study represents a first attempt towards a quantitative analysis of the relationship between membranes microstructure and nonlinear deformation behavior. We now have established a straightforward histologic method that permits objective determination of thickness of amnion and chorion. Further, biochemical analysis of collagen and elastin was performed on each tissue sample subjected to mechanical experiment, in order to correlate the measured mechanical response with tissue's microstructure. It was found that soluble elastin and soluble collagen content are inversely proportional. The uniaxial tests showed highly nonlinear behavior of the nominal stress vs. strain curves. Correlations were found between biochemical data and mechanical parameters: there is clearly a direct proportionality between small strain elastic modulus and elastin content; a (less pronounced) direct correlation was

observed between collagen content and the parameter governing the increase in stiffness at larger strains in the nonlinear mechanical model. We are well aware that the biochemical data on elastin and collagen are affected by uncertainties related to the great difficulty to quantify collagen and elastin in tissue. Of note, the values of collagen content in this study only reflect the soluble portion of collagen in tissue, and not total collagen. Efforts to establish reliable quantitative methodology for determination of different collagen types are underway in our laboratory. In parallel we are developing a novel technique for biomechanical testing of fetal membranes. The setup is based on the idea of inflating a flat membrane and is therefore called ‘‘inflation device’’. Specifically, a piece of membrane is clamped in a rig and fluid pressure is applied on one side, perpendicular to the plane of the membrane. The inflation experiment produces a biaxial state of stress, which more closely represents physiological loading conditions as compared to conventional uniaxial tensile experiments. Ultimately, biochemical and mechanical data should allow to gather new insights into the nature and sequence of membrane failure, and to develop strategies for preventative intervention to avoid membranes rupture.

Chapter 5

Biaxial mechanical properties in relation to microcomponents of human fetal membranes

Manuscript in preparation

5.1 Introduction

5.1.1 Outline of this work

Understanding the mechanical behaviour of fetal membranes with or without rupture is a necessary foundation for the development of a sealing method to prevent rupture from puncture. In my earlier work (Jabareen et al., 2009), the mechanical base line behaviour of fetal membranes was correlated with the elastin and collagen contents in a uniaxial platform. However, in physiology, fetal membranes behave in a biaxial state to inflate along the course of pregnancy till rupture. It is essential to evaluate the biomechanical parameters of the fetal membrane in a biaxial stress state, so that it can be more closely compared with physiological loading conditions as compared to conventional uniaxial tensile experiments. With the insight gained from my earlier uniaxial study (Jabareen, Mallik et al. 2009), I participated in the development of a novel biomechanical set up in collaboration with Prof. Eduardo Mazza's laboratory at the Institute of Mechanical Systems, ETH Zurich for the biaxial stretching and inflation of the fetal membranes. Similar to the earlier uniaxial study, in this current study, I correlated the biaxial mechanical read out parameters with the total elastin, collagen and thickness of fetal membranes.

5.1.2 Experimental biomechanics of fetal membranes

Biomechanical evaluation of physical characteristics of fetal membranes is not straightforward. The mechanical test geometries used so far in experimental set up fall in three categories: (i) uniaxial tensile tests (rupture strength (Oxlund, Helmig et al. 1990)), non-linear force-elongation characteristics and viscoelastic responses (Oyen, Cook et al. 2004), (ii)"burst" testing that provides information on biaxial strength (Lavery et al., 1982) and (iii) punch testing, a simplified biaxial strength assessment (Oyen, Calvin et al. 2006; Calvin and Oyen 2007). These existing mechanical test set-ups fail in providing a tight control of local boundary conditions at the location of membrane rupture, so that the quantitative evaluation and comparison of different experimental results is impaired. Therefore, the challenge is to develop a biomechanical test device that permits to mimic physiological loading conditions of fetal membranes ex vivo, in order to measure mechanical behaviour of native, wounded and repaired fetal membranes. We earlier developed a computerized device for defined circumferential stretch in fetal membranes, which failed in the actual

experiment since the thin fetal membranes got damaged when clamped for their fixation and slipping of fetal membranes over the grips. These difficulties have been overcome by a new design of this dynamic membrane testing set up in which the fetal membrane is mounted on a fluid-filled pressure vessel and inflated by fluid pressure forming a "bubble". Control of fluid pressure and temperature in this set up, enables reproducing physiological loading conditions as well as increased loading till the membrane ruptures. The pressure and displacement data is monitored and collected constantly in this computerized device and this allows isolation of material parameters of the fetal membrane with a method known as "inverse problem". The basic principle of this "inverse problem" is to replicate the experiment on a computer simulation and iteratively adapt the mathematical description of the material until simulation and experiment come to match.

In my earlier study (Jabareen, Mallik et al. 2009), 9 fetal membranes were subjected to standard uniaxial material test machine to determine the constitutive model parameters for the fetal membranes. These uniaxial tests showed highly nonlinear behaviour of the true stress (Cauchy stress) vs. stretch curves. From the complimentary analysis of the microcomponents, it was found that there is a good correlation between one of the material parameters of the Rubin-Bodner model and the elastin content. These initial uniaxial tests revealed a relatively low variability of measurements on samples from the same membrane but an unexpected large variation between donors

In the present study, we acquired the mechanical properties for a "close to physiological" loading condition as opposed to conventional uniaxial study. As this study was conducted in a biaxial set up, the rupture properties (strength, maximum stretch) we obtained were not biased by local stress concentrations at clamping points or force application tools. This study allowed us to establish a correlation between elastin content, collagen content and thickness of the fetal membranes with the mechanical properties based on non-linear continuum theory.

5.2 Results

5.2.1 Thickness measurement

There exists an inherent relationship between rupture strength and thickness of fetal membranes. Earlier studies involving uniaxial tests and burst inflation, showed a decrease in fracture strength as thickness of the fetal membrane increased while other variables were kept constant (Calvin and Oyen 2007). Therefore the accurate and precise measurement of thickness of each individual sample of fetal membrane undergoing the mechanical testing can't be overemphasized.

Here we are using a non-contact optical method for the thickness measurement. This rules out the introduction of subjective error if measured by using a contact method such as pressing the fetal membrane between the spindle and anvil of a conventional micrometer. This present protocol allows the separation of amnion and chorion, hence distinct evaluation of thickness of each layer in the same setting. Table 5.1 summarizes the thickness of 14 tested membranes from the corresponding histological sections.

Table 5.1: Microstructural data: thickness of amnion, chorion, elastin and collagen

	Amnion (µm)	Chorion (µm)	Chorioamnion (Average; µm)	Elastin (% dry wt)	Collagen (% dry wt)
M1	43.93±11.5	435.86±70.58	480	16.8	14.8
M2	149.52±217.07	375.01±175.44	525	18.95	21.9
M3	55.1±28.67	203.01±84.6	258	16.59	25.6
M4	57.28±36.29	372.01±106.92	429	17.8	16.1
M5	75.43±45.89	476.46±212.24	552	17	21.7
M6	138.2±69.11	618.7±77.6	757	16.9	9.8
M7	34.55±6.09	473.5±63.56	508	16.9	18.5
M8	86.13±29.64	458.86±141.15	545	15.6	16.9
M10	70.18±43.88	459.18±123.1	529	18	17.3

M11	48.73±35.82	364.6±70.84	413	16.21	17.1
M12	76.37±49.89	487.71±86.95	564	17.36	15.1
M13	93.54±28.52	639.75±156.58	733	21.43	12.6
M14	117.93±40.05	490.41±110.67	608	15.75	18
M17	83.14±31.63	461.59±161.78	545	17.02	19.5

The average thicknesses of amnion and chorion layers were 81 ± 33 μm and 448 ± 103 μm respectively. These findings are in line with the normal measurements of thickness as chorion contributes to 80% thickness of fetal membranes. Our measurements show variations and consistent with the earlier published range for thickness of amnion between 100 to 500μm (Wilshaw, Kearney et al. 2006) . The scatter for the thickness measurement is depicted in Figure 5.9.

5.2.2 Elastin Content

The applied method to measure elastin content of fetal membrane in this study, estimates the fraction of elastin, which is soluble in oxalic acid. Table 5.1 lists the elastin content of all the membranes tested and it ranges from 15.6% to 21% of dry weight, with an average of 17%. This is expected in terms of our earlier studies in which we measured the elastin amount in wet weight (Jabareen, Mallik et al. 2009). Our observations stand with a higher range of elastin content reported earlier by (Hieber, Corcino et al. 1997) as 0.08% of elastin in fat free dry weight of amnion and lower than the findings by (Wilshaw, Kearney et al. 2006) i.e. 36% in fresh human amnion. Such discrepancy between various studies, points to the well-appreciated difficulty to estimate elastin by a unified chemical assay method in tissue samples specifically in fetal tissues. Morphometric analysis is semi quantitative and is often obscured by excess “background” in the tissue section by native collagen. We therefore have to assume that the current protocol for elastin determination is only estimation and the absolute density of elastin could be different. The inter and intra membrane variations of elastin amount is shown in Figure 5.9

5.2.3 Collagen Content

Collagen content of the whole membrane was determined by acid hydrolysis method (6N HCl), detecting the end product hydroxyproline in a colorimetric assay. Each measurement was repeated 3 times for each sample. The total collagen measured for the fetal membranes averaged 17.4% of dry weight. Table 5.1 summarizes the values for each of the fetal membranes tested. Figure 5.10 shows the variation of collagen content in % of dry weight between the samples. The present value of collagen content falls within the range of earlier reports that followed similar hydroxyproline method (Halaburt, Uldbjerg et al. 1989; Meinert, Eriksen et al. 2001)

5.2.4 Correlations

Various correlations were attempted between biomechanical, biological and microstructural data. The two biological parameters i.e. mother's BMI (Basal Metabolic Rate) and weight of the newborn at birth were included to check any relationship with the mechanical parameters. Correlation coefficients were calculated between various parameters are presented in the Table 5.2.

5.2.4.1 Collagen vs Load Parameters

Collagen being the major matrix component, contributes to the loading pattern of fetal membranes during physiology and also in the process of labor. The initial correlations that were investigated were the collagen amount vs. the critical pressure. No definite pattern of association between collagen content and the critical pressure was obtained (Figure 5.11). Such a finding would be expected, as the typical resistance of collagen fibers to the applied critical pressure not only depends on the absolute amount of collagen but also is a phenomenon of arrangement and orientation of the individual fibers. This particular reason led us to find a weaker correlation between the collagen content and the small strain elastic modulus in our earlier uniaxial study (Jabareen, Mallik et al. 2009). We further decided to investigate the biomechanical correlation with a more material specific approach, correlating the membrane tension with the collagen amount. The result presented in Figure 5.12, shows a tendency but still no obvious pattern of correlation

Table 5.2: Correlation coefficients between mechanical parameters and biological data

Coefficient of Correlation	Collagen Content	Elastin Content	Mother's BMI	Baby Weight
Critical Pressure	**0.2444**	**0.23928**	**-0.31697**	**-0.21023**
Critical Displacement	**0.22363**	**0.26722**	**-0.026409**	**-0.37512**
Critical Membrane Tension	**0.53351**	**0.39719**	**-0.19456**	**-0.14588**
Critical Stress	**0.78184**	**-0.014548**	**-0.18949**	**-0.035483**
Inflation Stiffness for Small Strain Regime	**0.43416**	**0.41253**	**0.050576**	**0.023694**
Inflation Stiffness for High Strain Regime	**0.52721**	**0.35245**	**0.057705**	**0.0013612**

5.2.4.2 Elastin vs Load Parameters

The interplay between elastin and collagen makes the fetal membrane behave as an "elastic layer" that resists small deformations but larger extensions of the membrane are allowed with gradual increment of applied force. Following the similar strategy as total collagen, a possible correlation between total elastin content and load parameters was sought. As shown in Figures 5.13 and 5.14, no pattern of correlation was observed.

5.2.4.3 Mother's BMI, Birth weight vs Mechanical parameters

In the same line as collagen and elastin content, when mother's BMI and birth weight of the newborn were compared with mechanical parameters, no trend in the correlation was found as shown in the calculated correlation coefficients in Table 5.2.

5.3. Materials & Methods

5.3.1 Sample collection

Fetal membranes from 14 pregnancies were collected immediately after elective cesarean sections. The Ethical Committee of the Canton Zurich that operates under federal legislation approved the protocol (study Stv22/2006). All these pregnancies were randomly chosen after thorough serological screening that was negative for HIV (Human Immuno Deficiency Virus), HBV (Hepatitis B Virus), HCV (Hepatitis C Virus), infections with streptococcus, Rubella and Toxoplasmosis. The selected pregnancies had no history of hypertension, diabetes mellitus or connective tissue disorders. These unlaboured elective cesarean sections were without chorioamnionitis, premature rupture of fetal membrane or any chromosomal abnormalities of the fetus. The collected membranes were approximately of size 15−20cm^2, and were always stored in physiological saline at 4C until the samples were prepared and tested at the same day of delivery.

5.3.2 Sample preparation for inflation testing

The intact fetal membranes were spread on a non-adherent soft plastic sheet with the chorion side of the membrane facing upwards (Figure 5.1). Sand paper rings were prepared with inner and outer diameters of 50mm and 70mm, respectively. A commercial cyanoacrylate based glue was applied on the outer margin of the smooth surface of these pre-cut sand paper rings. This glued sand paper ring was gently applied onto a chosen area of the spread fetal membrane devoid of any visible defects like holes, distortions, tearing or separation of the components of membrane. Depending on the available area, devoid of any obvious flaw mentioned above, numbers of such glued sand paper rings were placed on the chorion side of the membrane such that the rough surface of the

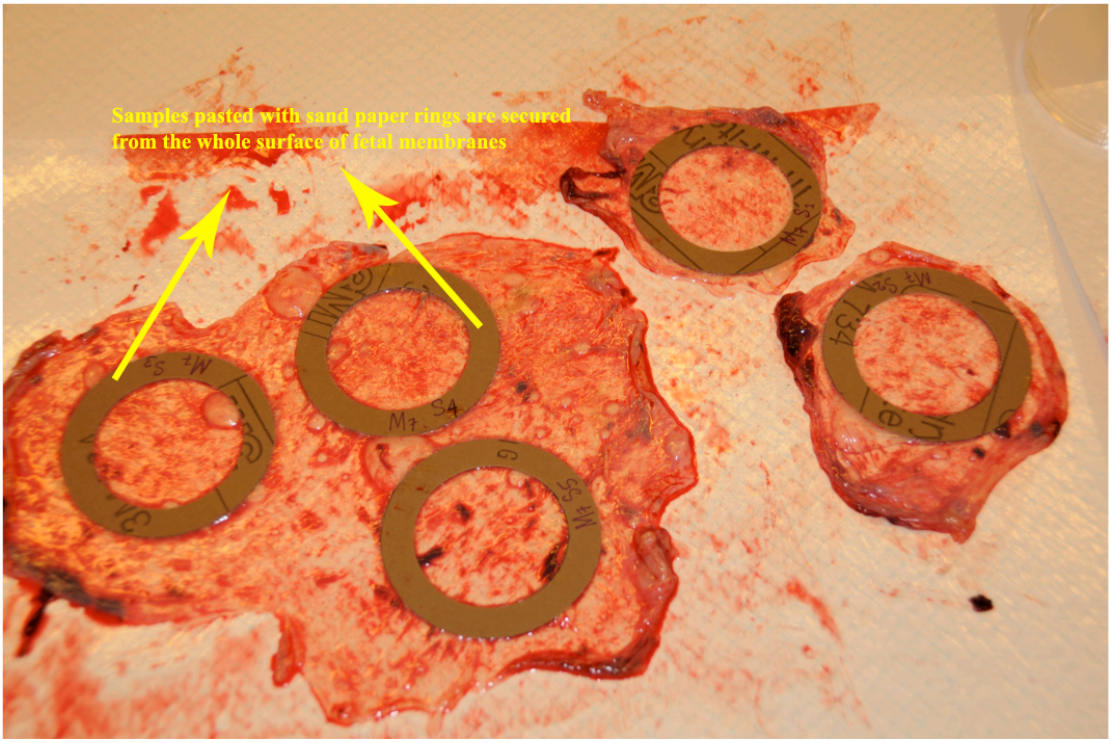

Figure 5.1: Sample preparations by choosing sections on the spread fetal membrane and applying glued sand paper rings of desired dimensions. The portion of the fetal membrane outside the sand paper rings are chosen to have random samples for thickness, elastin and collagen measurements

sand paper ring came in contact with the chorion layer. The fetal membrane glued on the chorion side was made up side down with much care, such that, the attached sand paper rings stay on the surface and the amnion surface faces up. Again glued sand paper rings were carefully superimposed onto the membrane so that each ring exactly apposed and aligned to the area of the sand paper ring applied on the chorion surface in the earlier step. This created areas of fetal membranes sandwiched between the rough surfaces of the two sand paper rings of same dimensions. These sandwiched areas of the fetal membranes were cut with a sharp scissor along the outer margin of the ring. The pieces of fetal membranes were stored in NaCl solution at room temperature till further mounting. Generally, four to eight sandwiched pieces were prepared for later testing.

5.3.3 Biaxial inflation device

5.3.3.1 Experimental Setup

A custom-built inflation platform was designed which can inflate membrane-like tissue under the pressure of liquid. The core structure of this platform is a metallic cylinder with a connected peristaltic pump (Watson-Marlow, type: 314VBM, 0-360rpm, ~0-100 ml/min) that supplies physiological saline according to a given pressure history. The pump flow rate to reach this given pressure history is controlled over a desktop computer through a custom-made program using the PID (= Proportional–Integral–Derivative) control strategy. The inner diameter of the cylinder is 50mm and the outer diameter is 70mm. When filled with physiological saline up to the upper rim, the cylinder along the fluid surface allows soft membranous structures like silicon membranes, fetal membranes to stay flat. Subsequent fluid supply induces an upward semi globular deformation of the soft flat structure, provided this structure is clamped along the upper rim of this metallic cylinder (Figure 5.2). A clamping ring sits on the upper surface of the cylinder to keep the mounted soft tissue or structure in its flat form before application of any form of pressure. This clamping ring is secured with six screws distributed uniformly along the perimeter. The metal cylinder is connected to a pressure sensor, which detects the hydrostatical pressure inside the closed unit vessel-membrane with an acquisition rate of 6.66 Hz.

Other parts of this system are:

1. A CCD camera (PointGrey, type: DragonFly2, resolution: 480x640) pixels) with a telecentric objective (Computar, type: TEC-M55, used with a reductor TEC-M55-75), which takes the pictures of the deformed membrane from the side. The images are taken isochronically with pressure recordings. The camera is fixed at a distance of 1 m in such a way that the rim of the cylinder corresponds to the lower part of the field of view. As any image-based measurement is done in pixel unit, one needs to convert these measurements in engineering units using a so-called calibration factor. The calibration factor is obtained by comparing the pixel-size of accurate spheres (DIN 5401) placed on the cylinder with its known dimension. The displacement history of the apex of the mounted fetal membrane i.e. d (t) is extracted from the acquired pictures in an off line post-processing step.

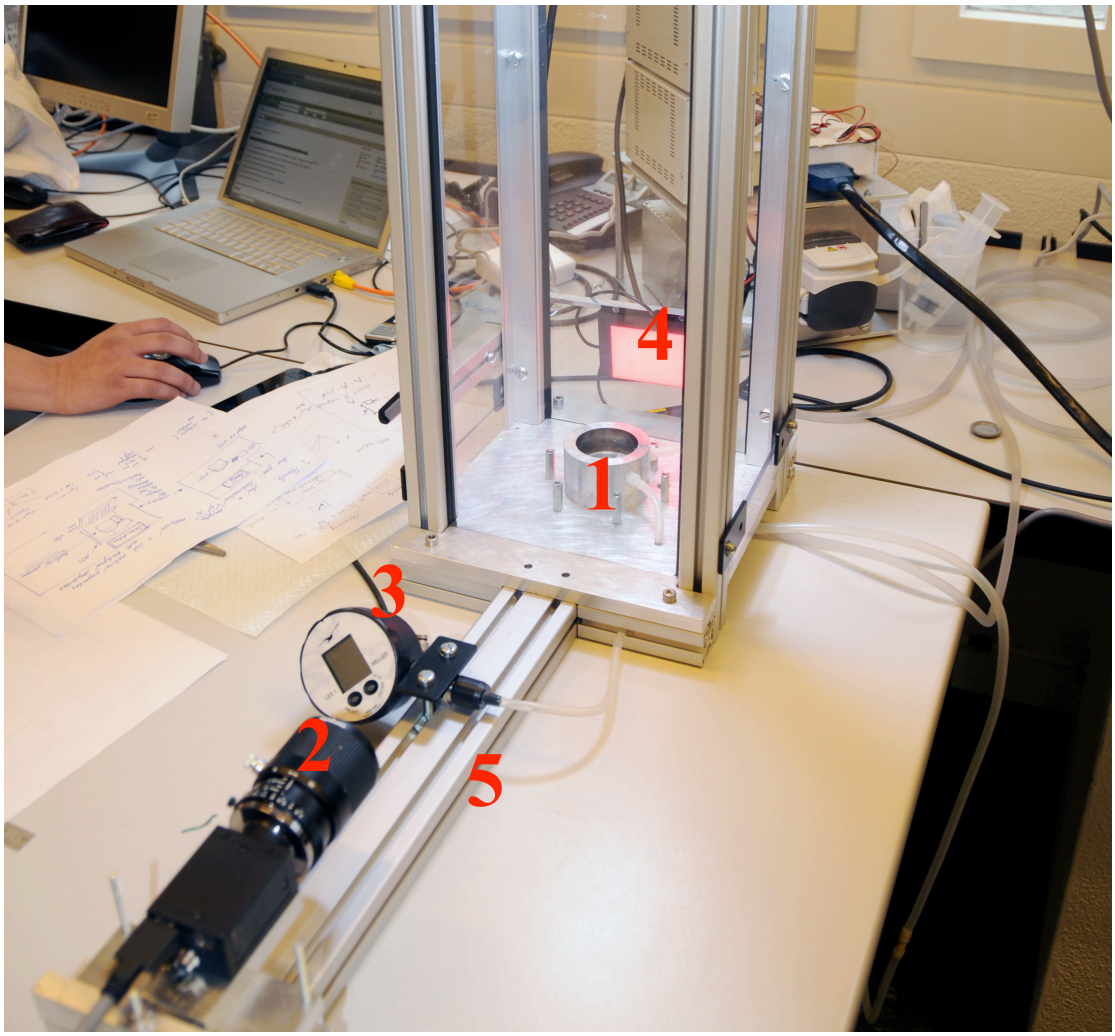

Figure 5.2: The biaxial inflation setup with various parts described inset; 1: Cylinder onto which fetal membrane is mounted, 2- CCD camera that captures pictures, 3- Pressure sensor, 4- LED screen on which image falls, 5- Rail to adjust the focus of CCD camera.

2. Pictures of the deformed membrane are captured on a LED screen placed behind the observed deforming membrane. This enhances the contrast between the deforming membrane and the background.

3. A connector block ensures the transfer of the signals from the computer that governs all the experimental parameters to the different instruments (Pump, pressure sensor).

The user interface enabling the experiment control was written with Lab View (LABVIEW 8.2) platform. Through this LABVIEW program, the user can for instance specify the desired pressure history and the acquisition rate. For all the experiments presented here the acquisition rate was set to 6.66 Hz and the used pressure history is presented on Figure 5.4.

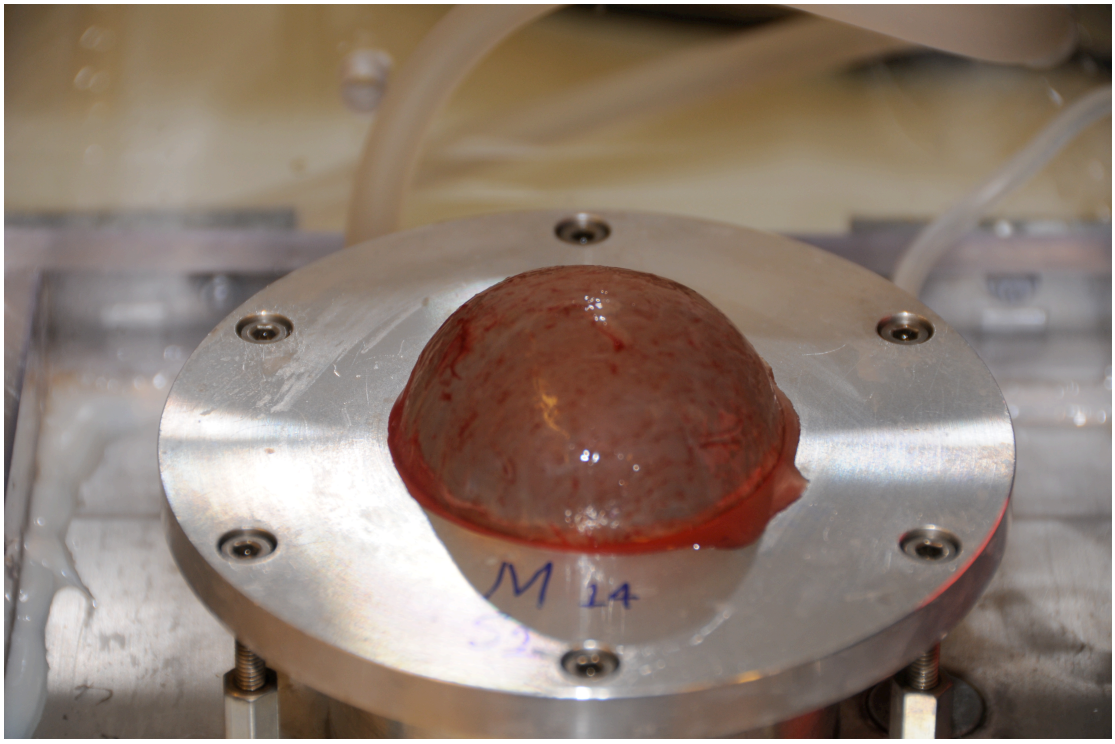

Figure 5.3: Inflated human fetal membranes on the biaxial setup

The final read outs parameters of the experiments are

a) Actual pressure course *p(t)*

b) Displacement history of the membrane at the apex *d(t)*

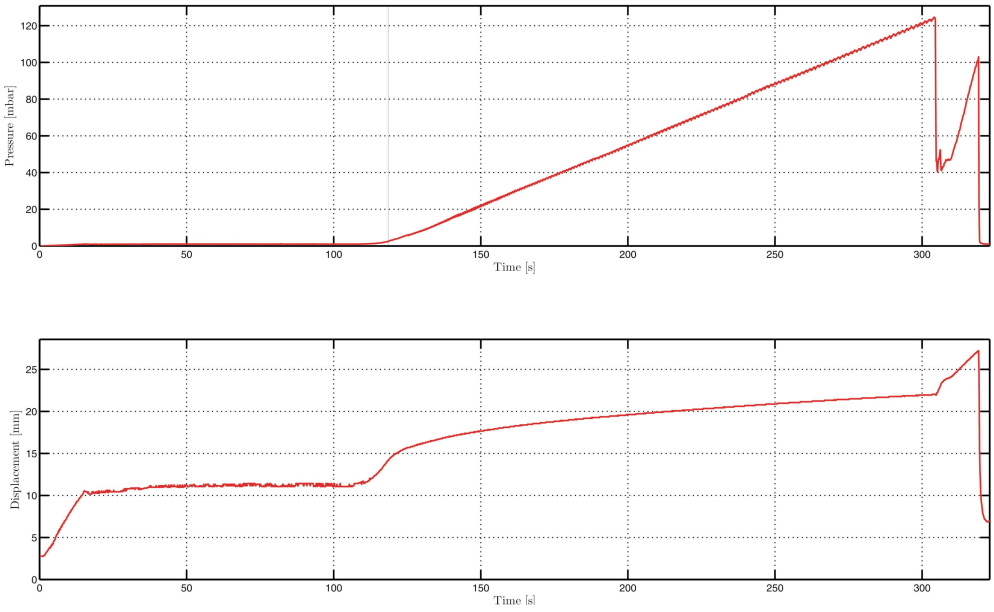

Figure 5.4: Pressure and displacement history for a prototype acquisition against inflation of a fetal membrane sample

5.3.3.2 Normalization Process

The sandwiched membranes were placed on the cylinder in a stress free state, the so-called "slack state" which was characterized by the presence of wrinkles. As the number and size of the wrinkles were not the same for each sample, the need for a normalization process was evident. This normalization was based on the localization of the time point where the membrane starts to bear load, the so-called "wrinkle free state". As opposed to the "slacked state" the "wrinkle free state" marks the beginning of stretching. This normalization process will now be presented:

The pressure measured with the pressure sensor has two components. The hydrostatic pressure exerted by the fluid inside the bubble and the resistance force exerted by the membrane on the liquid.

The hydrostatic pressure of the liquid can be mathematically described with the Bernouilli equation:

$$p_{hydro}(t) = \rho \cdot g \cdot d(t)$$

where ρ is the density of the fluid

g is the acceleration due to gravity

$d(t)$ is the height of the water column under the bubble, which correspond to the displacement history of the apex.

Since the membrane is not bearing load until reaching the "wrinkle free state", we can localize this state, where the measured pressure deviates from the theoretically derived baseline pressure $p_{hydro}(t)$ (Figure 5.5)

5.3.3.3 Inflation Stiffness Curves

The gathered pressure and displacement histories can then be combined to produce the "Inflation Stiffness Curves" that give information about the mechanical behavior of the fetal membrane.

The displacement values of the Wrinkle-free state are displayed on the x-axis and the corresponding pressure values displayed on the y-axis (Figure 5.5).

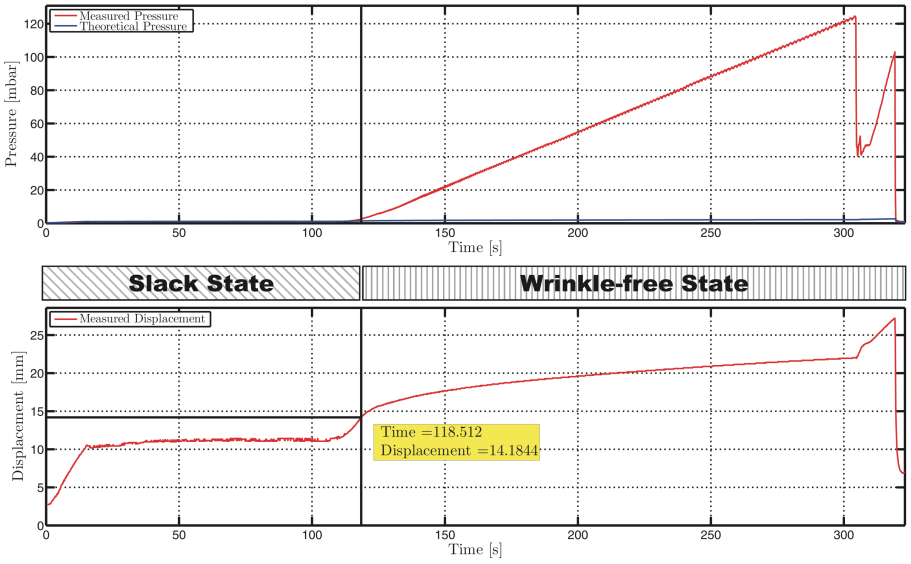

Figure 5.5: The slack state is seen in the initial part of the displacement-time curve shaded in tilted lines; the wrinkle –free state is marked by rise of pressure in vertical parallel lines.

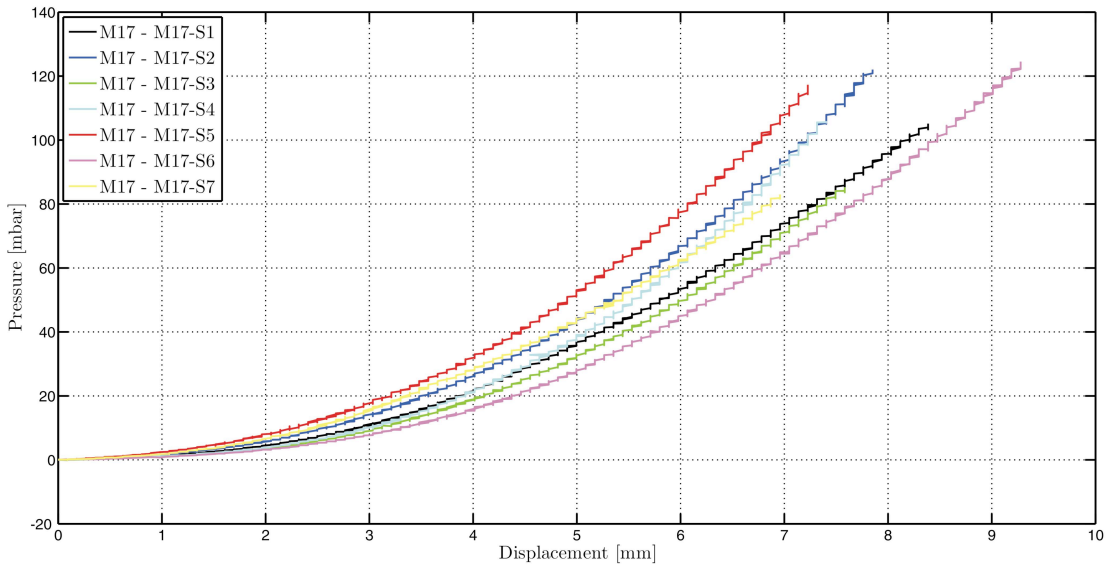

Figure 5.6: Pressure-Displacement curve of wrinkle-free state of the membrane upon inflation.

5.3.4 Parameter description

5.3.4.1 Critical Mechanical parameters

These parameters describe the mechanical status and magnitude before the rupture of fetal membranes in the experiment. The critical parameters are sample specific.

a) Critical Pressure:

Critical pressure denotes the magnitude of pressure in mbar at which the piece of mounted fetal membrane ruptures for the given cylinder size upon inflation. This is a measure to describe the ability of the particular sample to withstand the applied load in the current experimental set up (Figure 5.6)

b) Critical Displacement

Critical displacement defines the displacement in mm, at the end of the inflation at which the membrane ruptures for the given inflation cylinder size. This parameter describes the ability of the membrane to withstand a given deformation in the present experimental setup.

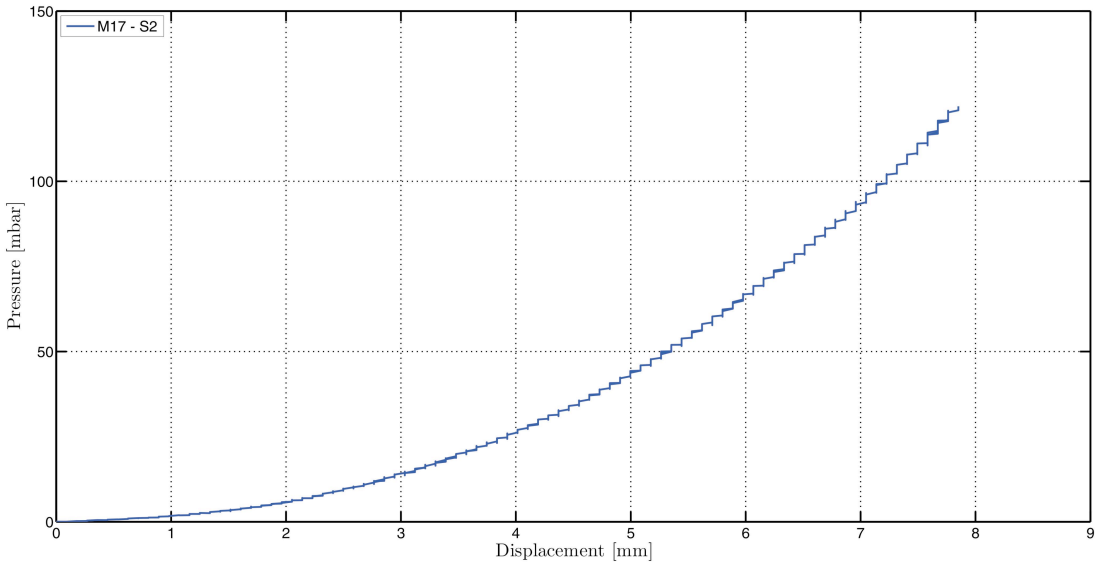

Figure 5.7: Pressure- Displacement curve

c) Critical Membrane Tension

This defines line load (force over length unit) that the membrane can bear before it ruptures; measured in N/mm. Critical Membrane Tension has the advantage over the critical pressure as the former is independent of specifications of the experiment and can be compared with values obtained for different cylinder size. This parameter describes the ability of the membrane to withstand a given load.

d) Critical Stress

This denotes the load (force per unit area) that the membrane can bear before it ruptures; measured in N/mm^2. It has the advantage over Critical Membrane Tension as the variability of the thickness of the membrane is taken into account.

e) Inflation Stiffness for Low Strain Regime

This denotes the amount of pressure required to move the apex of the deforming membrane by 1 mm. It is measured in mbar/mm. It is the average slope of the Displacement-Pressure-Curve taken for the initial 10% of the curve. This parameter describes the stiffness of the membrane at a low strain regime

f) Inflation Stiffness for High Strain Regime

This denotes the parameter exactly like Inflation stiffness for low strain regime but in the terminal 10% of the curve.

5.3.4.2 Theoretical description of Mechanical parameters

The equation formulated by Pierre Simon Laplace, which defines the relation between the hydrostatic pressures inside spherical shaped elastic membrane and the tension occurring in the membrane itself.

$$2 \cdot \pi \cdot R(t) \cdot T(t) = p(t) \cdot \pi \cdot R(t)^2$$ Equation 5.1

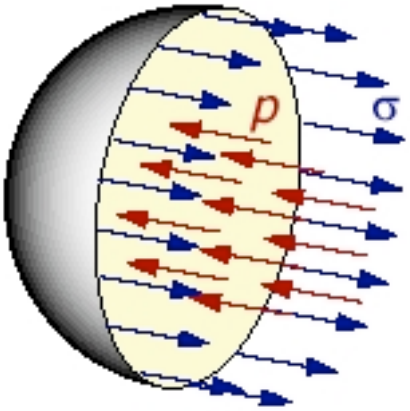

Figure 5.8: Schematic representation of a sphere to describe the relationship between hydrostatic pressure (p) and stress (σ) as per Laplace relationship

Where, R = Radius of curvature of the spherical membrane

T = Membrane Tension

p = hydrostatic pressure inside the vessel

With this formula, one can easily get the approximation of the membrane tension:

$$T(t) = \frac{p(t) \cdot R(t)}{2}$$ Equation 1.2

The tension being the product of the stress by the thickness, Equation 5.2 can be rewritten as

$$T(t) = \sigma(t) \cdot t(t) = \frac{p(t) \cdot R(t)}{2}$$ Equation 5.3

with σ = Stress in the membrane

t = Thickness of the membrane

Taking the thickness of the membrane as constant, the approximated stress that the membrane has to bear shortly before burst can be expressed as:

$$\sigma_{approx}(t_{burst}) = \frac{p(t_{burst}) \cdot R(t_{burst})}{2 \cdot t_0}$$ Equation 5.4

The pressure value at this time can be read out of the pressure course.

Through a numerical procedure, using both contour identification algorithms and fitting methods, the position and radius of a circle can be optimized to match the curvature of the portion of the membrane near the apex for the last image registered before burst.

5.3.4.3 Biological Parameters

a) Elastin estimation

Insoluble elastin was extracted from the fetal membranes as soluble cross-linked polypeptides by oxidation with oxalic acid. Briefly, 100mg of lyophilized fetal membrane tissue was weighed for this assay. Each sample of 100mg was boiled in a dry oven, at 100°C with 2ml of 0.25M oxalic acid for 1 hour. Then samples were spun down at 3000 rpm at 22°C for 10 mins. The extraction of the membrane pellets following boiling with oxalic acid was repeated twice and all the extracts were pooled. The content of soluble elastin in the oxalic acid extract was determined colorimetrically following the manufacture's instruction in the Fastin elastin assay kit (http://www.biocolor.co.uk; Biocolor Ltd., Newtonabbey, Northern Ireland) based on the fastin dye reagent 5, 10, 15, 20 tetraphenyl-21,23-porphyrine sulfonate.

Absorbance was measured at 540 nm in an ELISA reader. Human alpha elastin, supplied with the kit was used as standard. Final values were expressed as µg of elastin per dry weight of the membrane sample.

b) Collagen estimation

For the estimation of total collagen, we followed the modified acid hydrolysis method using 6N Hydrochloric acid (HCl) to determine the hydroxyproline as described by C.A Edwards and W.D O'Brien (Edwards and O'Brien 1980). Briefly, lyophilized fetal membrane tissue was weighed for each sample. Each sample was subjected to a long hydrolysis with Hydrochloric acid (10mg lyophilized sample/1ml of 6N HCl) for 20 hours at 120°C in a dry oven. In this step, the tissue collagen gets converted to hydroxyproline. To 50µl of this solution, 450 µl of Chloramine T (Sigma Aldrich) was added and kept for 25 mins at room temperature. Chloramine T converts the hydroxyprolene to pyrrole-2-carboxylic acid, which was reacted with 4-dimethylaminobenzaldehyde prepared in propan-2-ol and perchloric acid for 20 mins at 60°C. This reaction produced a red coloration proportional to the amount of hydroxyprolene and it was measured at 540nm absorbance using a 96 well plate in a microplate reader. An aqueous solution of trans-4-hydroxypriline (Sigma Aldrich) was used as standard.

c) Thickness measurement

In this study, we measured the thickness of each tissue sample, subjected to inflation by an already described histological method (Jabareen, Mallik et al. 2009). After the inflation test, a small piece of the tissue was resected. A small piece of filter paper was inserted between the layers of amnion and chorion while they were separated by blunt dissection by a forceps. Much care was taken not to distort, harm both layers of the fetal membrane while separating them. This membrane sandwich with the filter paper was put in a histology cassette and fixed in 4% buffered formalin later to be embedded in paraffin. The paraffin sections were cut vertically into slices, such that each section consisted of both layers of the fetal membranes and the filter paper in between them. Following hematoxylin and eosin (H&E) staining, the microsections were observed under a Zeiss Axiovert 200M microscope.

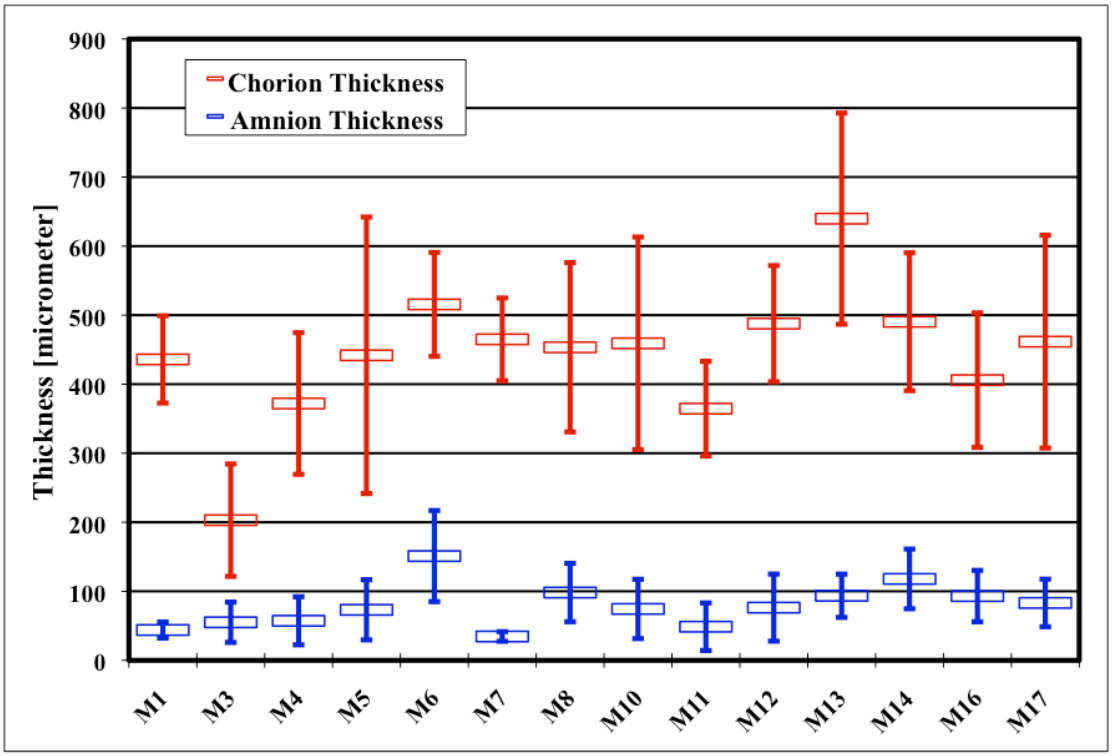

Figure 5.9: Scatter in the thickness of each membrane sample for chorion and amnion

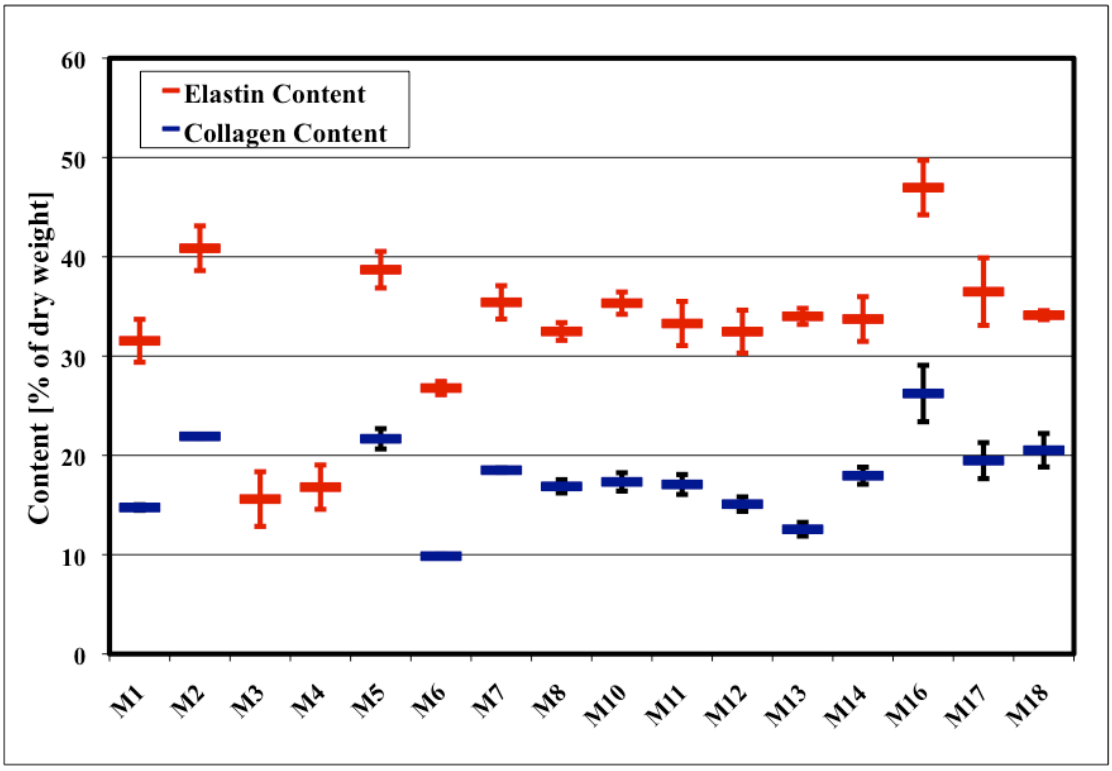

Figure 5.10: Scatter in the collagen and elastin content of all membranes tested.

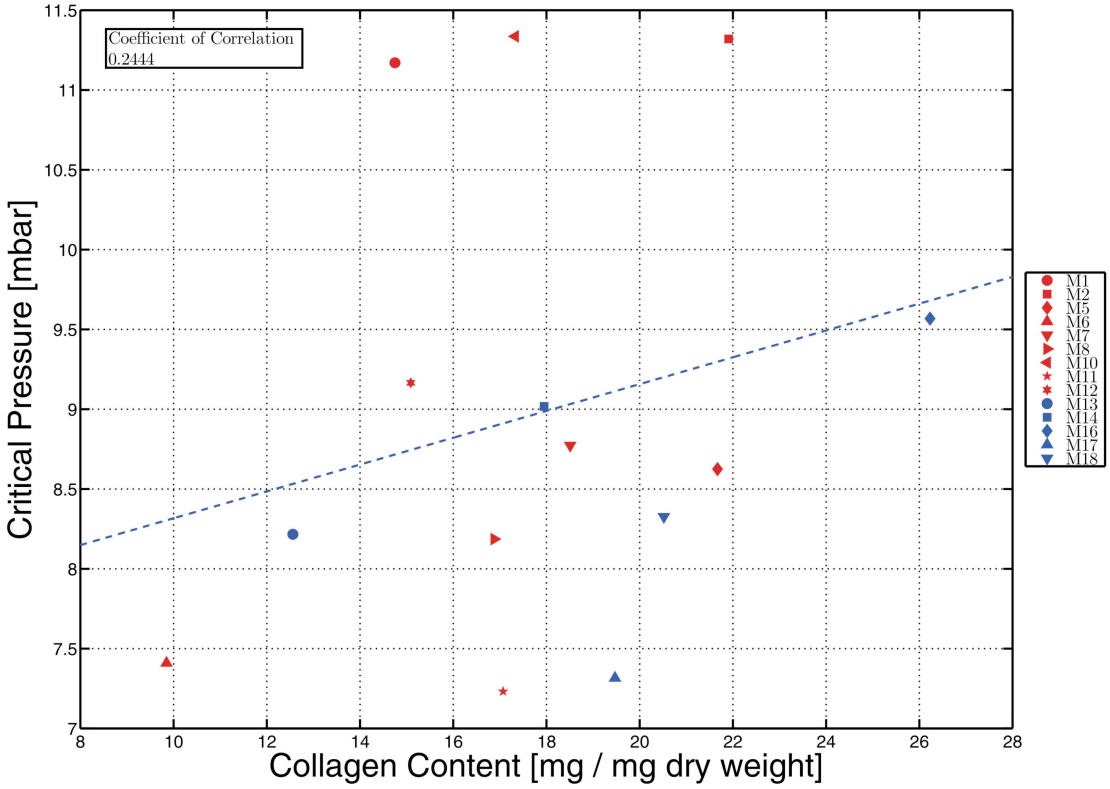

Figure 5.11: Correlation between Collagen content and Critical pressure

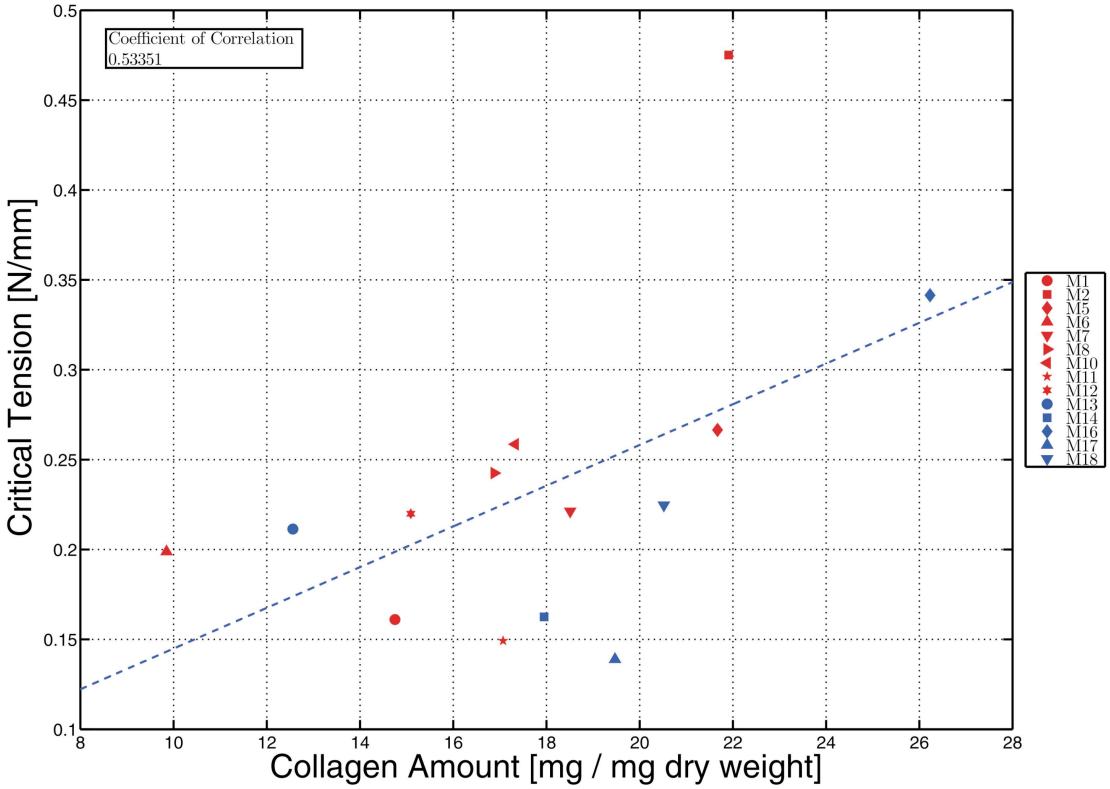

Figure 5.12: Correlation between Collagen content and Critical tension

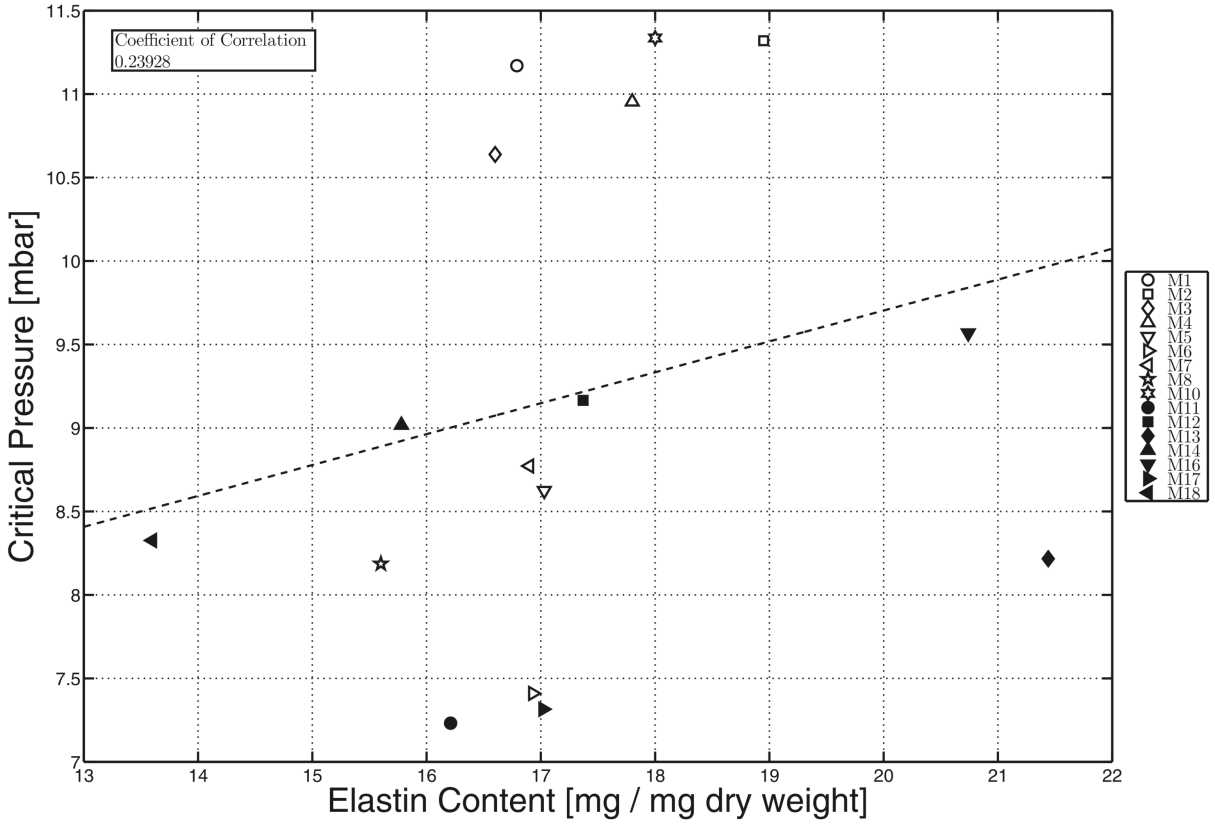

Figure 5.13: Correlation between Elastin content and Critical pressure

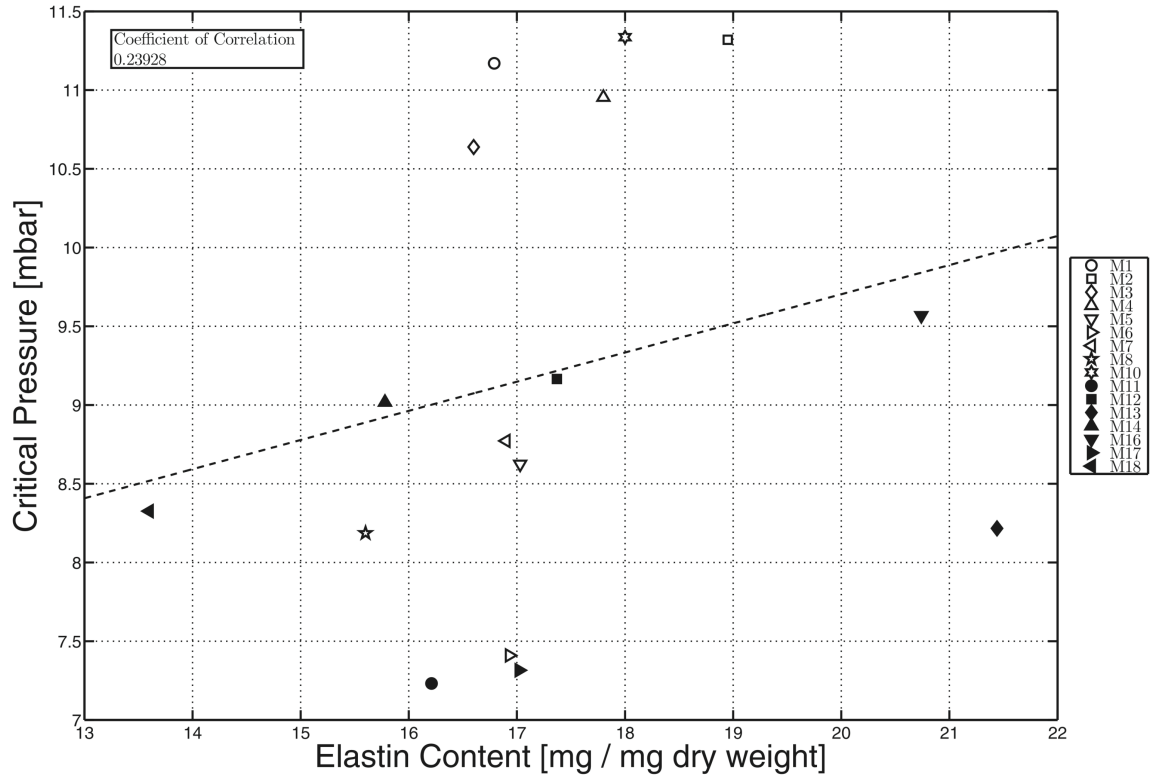

Figure 5.14: Correlation between Elastin content and Critical Pressure

5.4 Discussion

This study describes numerical techniques and optimization algorithms to establish a correlation between the mechanical parameters under biaxial condition and the thickness, microstructure components of fetal membranes. Our initial data point to low or absent correlation between mechanical parameters and microcomponents. The reasons can be summarized as

1. Fetal membranes are highly inhomogeneous across their surfaces in terms of thickness and microstructural contents. So when we compare mechanical parameters, which are sample specific to biological parameters, which are membrane specific, a pattern of error may be introduced. This condition has forced us to average the sample specific values to at least reach a comparable state. In the ideal case, for each sample of fetal membrane, which is inflated biomechanically, the corresponding elastin, collagen and thickness should be estimated. The major reason not to perform such one to one comparison is that the amount of tissue per sample is not sufficient to estimate both collagen and elastin.

2. In some samples, the rupture upon inflation was observed close to the border of clamping and we did not include such samples in our study. This event reduces the absolute sample size for a given fetal membrane and does not provide a statistically significant sample size, hence weakening the association at final correlation.

As in the study based on uniaxial experiments, one of the goals of the current inflation experiment was to characterize the material through solving the “inverse problem”. The “inverse problem” solving consists of finding an appropriate material model and of optimizing its material parameters so that the simulated experiment matches the reality.

For the uniaxial case the solution of the inverse problem could be found using an analytical model without FEM (Finite Element Modelling) model. Given the complexity of the load and the kinematics of the inflation experiment, the solution of the inverse problem can only be achieved with the use of a FEM.

At the present point, all commonly used FEM have been investigated as candidates to describe the fetal membrane tissue. None of them were satisfying our expectations.

Based on our first experiences, the development of such a model will represent a big challenge in itself and be even more complex if the model is expected to fit to both uniaxial and biaxial loadings.

REFERENCES

The Mathworks: *Matlab Documnetation,* version 7.0.4.

Aplin J D and Campbell S (1985) An immunofluorescence study of extracellular matrix associated with cytotrophoblast of the chorion laeve. Placenta 6(6): 469-79.

Bilic G, Hall H, Bittermann A G, Zammeretti P, Burkhart T, Ochsenbein-Kolble N and Zimmermann R (2005) Human preterm amnion cells cultured in 3-dimensional collagen I and fibrin matrices for tissue engineering purposes. Am J Obstet Gynecol 193(5): 1724-32.

Bilic G, Ochsenbein-Kolble N, Hall H, Huch R and Zimmermann R (2004) In vitro lesion repair by human amnion epithelial and mesenchymal cells. Am J Obstet Gynecol 190(1): 87-92.

Bryant-Greenwood G D and Millar L K (2000) Human fetal membranes: their preterm premature rupture. Biol Reprod 63(6): 1575-9.

Burke S A, Ritter-Jones M, Lee B P and Messersmith P B (2007) Thermal gelation and tissue adhesion of biomimetic hydrogels. Biomed Mater 2(4): 203-10.

Calvin S E and Oyen M L (2007) Microstructure and mechanics of the chorioamnion membrane with an emphasis on fracture properties. Ann N Y Acad Sci 1101: 166-85.

Chang J, Tracy T F, Jr., Carr S R, Sorrells D L, Jr. and Luks F I (2006) Port insertion and removal techniques to minimize premature rupture of the membranes in endoscopic fetal surgery. J Pediatr Surg 41(5): 905-9.

Cortes R A, Wagner A J, Lee H, Clifton M S, Grethel E, Yang S H, Ball R and Harrison M R (2005) Pre-emptive placement of a presealant for amniotic access. Am J Obstet Gynecol 193(3 Pt 2): 1197-203.

Deming T J (1999) Mussel byssus and biomolecular materials. Curr Opin Chem Biol 3(1): 100-5.

Deprest J, Gratacos E and Nicolaides K H (2004) Fetoscopic tracheal occlusion (FETO) for severe congenital diaphragmatic hernia: evolution of a technique and preliminary results. Ultrasound Obstet Gynecol 24(2): 121-6.

Deprest J A, Papadopulos N A, Decaluw H, Yamamoto H, Lerut T E and Gratacos E (1999) Closure techniques for fetoscopic access sites in the rabbit at mid-gestation. Hum Reprod 14(7): 1730-4.

Devlieger R, Millar L K, Bryant-Greenwood G, Lewi L and Deprest J A (2006) Fetal membrane healing after spontaneous and iatrogenic membrane rupture: A review of current evidence. Am J Obstet Gynecol.

Duff P (1996) Premature rupture of the membranes in term patients. Semin Perinatol 20(5): 401-8.

Edwards C A and O'Brien W D, Jr. (1980) Modified assay for determination of hydroxyproline in a tissue hydrolyzate. Clin Chim Acta 104(2): 161-7.

El Khwad M, Stetzer B, Moore R M, Kumar D, Mercer B, Arikat S, Redline R W, Mansour J M and Moore J J (2005) Term human fetal membranes have a weak zone overlying the lower uterine pole and cervix before onset of labor. Biol Reprod 72(3): 720-6.

Falk S J, Campbell L J, Lee-Parritz A, Cohen A P, Ecker J, Wilkins-Haug L and Lieberman E (2004) Expectant management in spontaneous preterm premature rupture of membranes between 14 and 24 weeks' gestation. J Perinatol 24(10): 611-6.

Fortunato S J, Menon R and Lombardi S J (1997) Collagenolytic enzymes (gelatinases) and their inhibitors in human amniochorionic membrane. Am J Obstet Gynecol 177(4): 731-41.

Fowler S F, Sydorak R M, Albanese C T, Farmer D L, Harrison M R and Lee H (2002) Fetal endoscopic surgery: lessons learned and trends reviewed. J Pediatr Surg 37(12): 1700-2.

Gilbert T W, Sellaro T L and Badylak S F (2006) Decellularization of tissues and organs. Biomaterials 27(19): 3675-83.

Gillinov A M and Lytle B W (2001) A novel synthetic sealant to treat air leaks at cardiac reoperation. J Card Surg 16(3): 255-7.

Goldenberg R L, Culhane J F, Iams J D and Romero R (2008) Epidemiology and causes of preterm birth. Lancet 371(9606): 75-84.

Graham R L, Gilstrap L C, 3rd, Hauth J C, Kodack-Garza S and Conaster D G (1982) Conservative management of patients with premature rupture of fetal membranes. Obstet Gynecol 59(5): 607-10.

Gratacos E, Sanin-Blair J, Lewi L, Toran N, Verbist G, Cabero L and Deprest J (2006) A histological study of fetoscopic membrane defects to document membrane healing. Placenta 27(4-5): 452-6.

Halaburt J T, Uldbjerg N, Helmig R and Ohlsson K (1989) The concentration of collagen and the collagenolytic activity in the amnion and the chorion. Eur J Obstet Gynecol Reprod Biol 31(1): 75-82.

Hampson V, Liu D, Billett E and Kirk S (1997) Amniotic membrane collagen content and type distribution in women with preterm premature rupture of the membranes in pregnancy. Br J Obstet Gynaecol 104(9): 1087-91.

Harrison M R, Keller R L, Hawgood S B, Kitterman J A, Sandberg P L, Farmer D L, Lee H, Filly R A, Farrell J A and Albanese C T (2003) A randomized trial of fetal endoscopic tracheal occlusion for severe fetal congenital diaphragmatic hernia. N Engl J Med 349(20): 1916-24.

Helmig R, Oxlund H, Petersen L K and Uldbjerg N (1993) Different biomechanical properties of human fetal membranes obtained before and after delivery. Eur J Obstet Gynecol Reprod Biol 48(3): 183-9.

Hieber A D, Corcino D, Motosue J, Sandberg L B, Roos P J, Yu S Y, Csiszar K, Kagan H M, Boyd C D and Bryant-Greenwood G D (1997) Detection of elastin in the human fetal membranes: proposed molecular basis for elasticity. Placenta 18(4): 301-12.

Hill-West J L, Chowdhury S M, Slepian M J and Hubbell J A (1994) Inhibition of thrombosis and intimal thickening by in situ photopolymerization of thin hydrogel barriers. Proc Natl Acad Sci U S A 91(13): 5967-71.

Imseis H M and Iams J D (1996) Glucocorticoid use in patients with preterm premature rupture of the fetal membranes. Semin Perinatol 20(5): 439-50.

Jabareen M, Mallik A S, Bilic G, Zisch A H and Mazza E (2009) Relation between mechanical properties and microstructure of human fetal membranes: an attempt towards a quantitative analysis. Eur J Obstet Gynecol Reprod Biol 144 Suppl 1: S134-41.

Johns D A, Ferland R and Dunn R (2003) Initial feasibility study of a sprayable hydrogel adhesion barrier system in patients undergoing laparoscopic ovarian surgery. J Am Assoc Gynecol Laparosc 10(3): 334-8.

Kanayama N, Terao T, Kawashima Y, Horiuchi K and Fujimoto D (1985) Collagen types in normal and prematurely ruptured amniotic membranes. Am J Obstet Gynecol 153(8): 899-903.

Lavery J P, Miller C E and Knight R D (1982) The effect of labor on the rheologic response of chorioamniotic membranes. Obstet Gynecol 60(1): 87-92.

Lee B P, Dalsin J L and Messersmith P B (2002) Synthesis and gelation of DOPA-modified poly(ethylene glycol) hydrogels. Biomacromolecules 3(5): 1038-47.

Lee H, Dellatore S M, Miller W M and Messersmith P B (2007) Mussel-inspired surface chemistry for multifunctional coatings. Science 318(5849): 426-30.

Lee H, Lee B P and Messersmith P B (2007) A reversible wet/dry adhesive inspired by mussels and geckos. Nature 448(7151): 338-41.

Lee H, Scherer N F and Messersmith P B (2006) Single-molecule mechanics of mussel adhesion. Proc Natl Acad Sci U S A 103(35): 12999-3003.

Leggat P A, Smith D R and Kedjarune U (2007) Surgical applications of cyanoacrylate adhesives: a review of toxicity. ANZ J Surg 77(4): 209-13.

Liekens D, Lewi L, Jani J, Heyns L, Poliard E, Verbist G, Ochsenbein-Kolble N, Hoylaerts M and Deprest J (2008) Enrichment of collagen plugs with platelets and amniotic fluid cells increases cell proliferation in sealed iatrogenic membrane defects in the foetal rabbit model. Prenat Diagn 28(6): 503-7.

Lockwood C J, Costigan K, Ghidini A, Wein R, Chien D, Brown B L, Alvarez M and Cetrulo C L (1993) Double-blind; placebo-controlled trial of piperacillin prophylaxis in preterm membrane rupture. Am J Obstet Gynecol 169(4): 970-6.

Louis-Sylvestre C, Rand J H, Gordon R E, Salafia C M and Berkowitz R L (1998) In vitro studies of the interactions between platelets and amniotic membranes: a potential treatment for preterm premature rupture of the membranes. Am J Obstet Gynecol 178(2): 287-93.

Luks F I, Deprest J A, Peers K H, Steegers E A and van Der Wildt B (1999) Gelatin sponge plug to seal fetoscopy port sites: technique in ovine and primate models. Am J Obstet Gynecol 181(4): 995-6.

M. B. Rubin S R B (2002) A three-dimensional nonlinear model for dissipative response of soft tissue
. International Journal of Solids and Structures 39(19): 5081-5099

MacDermott R I and Landon C R (2000) The hydroxyproline content of amnion and prelabour rupture of the membranes. Eur J Obstet Gynecol Reprod Biol 92(2): 217-21.

Mallik A S, Fichter M A, Rieder S, Bilic G, Stergioula S, Henke J, Schneider K T, Kurmanavicius J, Biemer E, Zimmermann R, Zisch A H and Papadopulos N A (2007) Fetoscopic closure of punctured fetal membranes with acellular human amnion plugs in a rabbit model. Obstet Gynecol 110(5): 1121-9.

Meinert M, Eriksen G V, Petersen A C, Helmig R B, Laurent C, Uldbjerg N and Malmstrom A (2001) Proteoglycans and hyaluronan in human fetal membranes. Am J Obstet Gynecol 184(4): 679-85.

Mettler L, Audebert A, Lehmann-Willenbrock E, Schive-Peterhansl K and Jacobs V R (2004) A randomized, prospective, controlled, multicenter clinical trial of a sprayable, site-specific adhesion barrier system in patients undergoing myomectomy. Fertil Steril 82(2): 398-404.

Michels B (1950) [Observations on 2320 births with premature rupture of the amnion at term.]. Zentralbl Gynakol 72(10): 597-609.

Millar L K, Stollberg J, DeBuque L and Bryant-Greenwood G (2000) Fetal membrane distention: determination of the intrauterine surface area and distention of the fetal membranes preterm and at term. Am J Obstet Gynecol 182(1 Pt 1): 128-34.

Nelson L H, Anderson R L, O'Shea T M and Swain M (1994) Expectant management of preterm premature rupture of the membranes. Am J Obstet Gynecol 171(2): 350-6; discussion 356-8.

O'Brien J M, Barton J R and Milligan D A (2002) An aggressive interventional protocol for early midtrimester premature rupture of the membranes using gelatin sponge for cervical plugging. Am J Obstet Gynecol 187(5): 1143-6.

O'Brien J M, Milligan D A and Barton J R (2002) Gelatin sponge embolization. a method for the management of iatrogenic preterm premature rupture of the membranes. Fetal Diagn Ther 17(1): 8-10.

Ochsenbein-Kolble N, Jani J, Lewi L, Verbist G, Vercruysse L, Portmann-Lanz B, Marquardt K, Zimmermann R and Deprest J (2007) Enhancing sealing of fetal membrane defects using tissue engineered native amniotic scaffolds in the rabbit model. Am J Obstet Gynecol 196(3): 263 e1-7.

Okita J R, Sagawa N, Casey M L and Snyder J M (1983) A comparison of human amnion tissue and amnion cells in primary culture by morphological and biochemical criteria. In Vitro 19(2): 117-26.

Osman I, Young A, Jordan F, Greer I A and Norman J E (2006) Leukocyte density and proinflammatory mediator expression in regional human fetal membranes and decidua before and during labor at term. J Soc Gynecol Investig 13(2): 97-103.

Oxlund H, Helmig R, Halaburt J T and Uldbjerg N (1990) Biomechanical analysis of human chorioamniotic membranes. Eur J Obstet Gynecol Reprod Biol 34(3): 247-55.

Oyen M L, Calvin S E and Landers D V (2006) Premature rupture of the fetal membranes: is the amnion the major determinant? Am J Obstet Gynecol 195(2): 510-5.

Oyen M L, Cook R F and Calvin S E (2004) Mechanical failure of human fetal membrane tissues. J Mater Sci Mater Med 15(6): 651-8.

Papadopulos N A, Dumitrascu I, Ordonez J L, Decaluwe H, Lerut T E, Barki G and Deprest J A (1999) Fetoscopy in the pregnant rabbit at midgestation. Fetal Diagn Ther 14(2): 118-21.

Papadopulos N A, Klotz S, Raith A, Foehn M, Schillinger U, Henke J, Kovacs L, Horch R E and Biemer E (2006) Amnion cells engineering: a new perspective in fetal membrane healing after intrauterine surgery? Fetal Diagn Ther 21(6): 494-500.

Papadopulos N A, Van Ballaer P P, Ordonez J L, Laermans I J, Vandenberghe K, Lerut T E and Deprest J A (1998) Fetal membrane closure techniques after hysteroamniotomy in the midgestational rabbit model. Am J Obstet Gynecol 178(5): 938-42.

Pawlicka E, Bankowski E and Jaworski S (1999) Elastin of the umbilical cord arteries and its alterations in EPH gestosis (preeclampsia). Biol Neonate 75(2): 91-6.

Petratos P B, Baergen R N, Bleustein C B, Felsen D and Poppas D P (2002) Ex vivo evaluation of human fetal membrane closure. Lasers Surg Med 30(1): 48-53.

Picone O, Benachi A, Mandelbrot L, Ruano R, Dumez Y and Dommergues M (2004) Thoracoamniotic shunting for fetal pleural effusions with hydrops. Am J Obstet Gynecol 191(6): 2047-50.

Portmann-Lanz C B, Ochsenbein-Kolble N, Marquardt K, Luthi U, Zisch A and Zimmermann R (2007) Manufacture of a cell-free amnion matrix scaffold that supports amnion cell outgrowth in vitro. Placenta 28(1): 6-13.

Prèvost T P (2004). Biomechanics of the Human Chorioamnion. Department of Material Science and Engineering, Massachutts Institute of Technology. **Masters Thesis:** 115.

Quintero R A (2001) New horizons in the treatment of preterm premature rupture of membranes. Clin Perinatol 28(4): 861-75.

Quintero R A (2003) Treatment of previable premature ruptured membranes. Clin Perinatol 30(3): 573-89.

Quintero R A, Morales W J, Allen M, Bornick P W, Arroyo J and LeParc G (1999) Treatment of iatrogenic previable premature rupture of membranes with intra-amniotic injection of platelets and cryoprecipitate (amniopatch): preliminary experience. Am J Obstet Gynecol 181(3): 744-9.

Quintero R A, Morales W J, Bornick P W, Allen M and Garabelis N (2002) Surgical treatment of spontaneous rupture of membranes: the amniograft--first experience. Am J Obstet Gynecol 186(1): 155-7.

Reddy U M, Shah S S, Nemiroff R L, Ballas S K, Hyslop T, Chen J, Wapner R J and Sciscione A C (2001) In vitro sealing of punctured fetal membranes: potential treatment for midtrimester premature rupture of membranes. Am J Obstet Gynecol 185(5): 1090-3.

Sciscione A C, Manley J S, Pollock M, Maas B, Shlossman P A, Mulla W, Lankiewicz M and Colmorgen G H (2001) Intracervical fibrin sealants: a potential treatment for early preterm premature rupture of the membranes. Am J Obstet Gynecol 184(3): 368-73.

Seldinger S I (1953) Catheter replacement of the needle in percutaneous arteriography; a new technique. Acta radiol 39(5): 368-76.

Sener T, Ozalp S, Hassa H, Yalcin O T and Polay S (1997) Maternal blood clot patch therapy: a model for postamniocentesis amniorrhea. Am J Obstet Gynecol 177(6): 1535-6.

Taylor M J, Shalev E, Tanawattanacharoen S, Jolly M, Kumar S, Weiner E, Cox P M and Fisk N M (2002) Ultrasound-guided umbilical cord occlusion using bipolar diathermy for Stage III/IV twin-twin transfusion syndrome. Prenat Diagn 22(1): 70-6.

Thomas I T and Smith D W (1974) Oligohydramnios, cause of the nonrenal features of Potter's syndrome, including pulmonary hypoplasia. J Pediatr 84(6): 811-5.

Verbeek J H, Robertson E M and Haust M D (1967) Basement membranes (amniotic, trophoblastic, capillary) and adjacent tissue in term placenta. An electron microscopic study. Am J Obstet Gynecol 99(8): 1136-46.

Ville Y, Khalil A, Homphray T and Moscoso G (1997) Diagnostic embryoscopy and fetoscopy in the first trimester of pregnancy. Prenat Diagn 17(13): 1237-46.

Waite J H (1999) Reverse engineering of bioadhesion in marine mussels. Ann N Y Acad Sci 875: 301-9.

West J L and Hubbell J A (1996) Separation of the arterial wall from blood contact using hydrogel barriers reduces intimal thickening after balloon injury in the rat: the roles of medial and luminal factors in arterial healing. Proc Natl Acad Sci U S A 93(23): 13188-93.

Wilshaw S P, Kearney J N, Fisher J and Ingham E (2006) Production of an acellular amniotic membrane matrix for use in tissue engineering. Tissue Eng 12(8): 2117-29.

Yamada K, Chen T, Kumar G, Vesnovsky O, Topoleski L D and Payne G F (2000) Chitosan based water-resistant adhesive. Analogy to mussel glue. Biomacromolecules 1(2): 252-8.

YC F (1993). Mechanical Properties of living tissues, NewYork: Springer.

Young B K, Mackenzie A P, Roman A S, Stephenson C D, Minior V, Rebarber A and Timor-Tritsch I (2004) Endoscopic closure of fetal membrane defects: comparing iatrogenic versus spontaneous rupture cases. J Matern Fetal Neonatal Med 16(4): 235-40.

Young B K, Roman A S, MacKenzie A P, Stephenson C D, Minior V, Rebarber A and Timor-Tritsch I (2004) The closure of iatrogenic membrane defects after amniocentesis and endoscopic intrauterine procedures. Fetal Diagn Ther 19(3): 296-300.

Zisch A H and Zimmermann R (2008) Bioengineering of foetal membrane repair. Swiss Med Wkly 138(41-42): 596-601.

CURRICULUM VITAE

Personal Details

Name: Ajit Sankar Mallik

Date of Birth: 24th May 1977

Marital Status: Unmarried

Nationality: Indian

Languages known: English, Hindi, Oriya, Bengali

Education

MD PhD, University Hospital Zurich, Switzerland- Since 2005

I joined as a research scholar in the Tissue Engineering section of Department of Obstetrics in the University Hospital Zurich, under the supervision of Dr. PD. Andreas H. Zisch. The objective of my project is to develop a closure technique to repair the iatrogenic rupture of human fetal membrane using the modalities of regenerative medicine and biomechanics.

Masters in Medical Science & Technology, IIT Kharagpur, India- 2001 to 2004

This unique course, designed for medical graduates in the elite Indian Institute of Technology, Kharagpur in 2001. I was among the 10 students admitted through a nationwide selection examination.

1st Year
Physics for Medicine and Biology
Biomedical Mathematics
Biomaterial-I
Programming & Data Structure
Engineering Drawing & Graphics
Instrumentation & Control
Engineering Mechanics
Basic Electronics

2nd Year
Medical Imaging
Immunotechnology
Biomaterial-II, III
Telemedicine
Biomechanics
Recombinant DNA technology
Biomedical Instrumentation
Bioinformatics

3rd Year
Project Dissertation & Comprehensive viva voce examination

MBBS (Bachelor in Medicine & Bachelor in Surgery) from SCB Medical College Cuttack, India- 1994-2000

After my graduation in Medicine, I completed one year compulsory rotational clinical internship

1st MBBS	2nd MBBS	3rd MBBS
Anatomy	Microbiology	Medicine
Physiology	Forensic Medicine	Surgery
Biochemistry	Pathology	Orthopedics
	Social & Preventive Med	Otorhinolaryngology
		Obstetrics & Gynecology
		Ophthalmology

Scientific Experience & Projects

EPFL, Lausanne, Switzerland- August 2003 to March 2004

I worked under the supervision of Prof. Nikos Stergiopulos in the Laboratory of Hemodynamics & Cardiovascular Technology

1st Project

Endothelialization of decellularized porcine vascular xenografts with bovine aortic endothelial cells.

2nd Project

Effect of modified arterial compliance and gene therapy on ventricular function during cardiac failure provoked by myocardial infarction. In this project my animal model was rat and I worked in the Department of Cardiology in the University Hospital Lausanne.

AIIMS, New Delhi, India, December 2002

I worked in joint project between Department of Cardiology,AIIMS (All India Institutes of Medical Sciences), New Delhi and Center for Biomedical Engineering, IIT Delhi to detect the vulnerability of atherosclerotic plaques through the measurements of temperature by a thermistor tipped catheter.

AIIMS and IIT Delhi, India, December 2001

As a part of my winter internship during my Masters in IIT Kharagpur, I performed a review study on "Reversal of atherosclerotic plaques by life style management and yoga". My supervisors were Prof S.K Guha (IIT) and Prof. Rajiv Narang (AIIMS)

Semester Project

I developed an electronic stethoscope prototype using piezoelectric transducer as a part of my Masters thesis project in IIT Kharagpur.

Academic Achievements and Grants

* I obtained a grant from Zurich Center for Integrative Human Physiology (ZIHP) towards my MDPhD thesis for a period of 2 years 2006-2008

* MMST (Masters in Medical Science & Technology) from IIT Kharagpur, India with a grade point 8.04/10

* I was selected amongst 1000 medical graduates, through a nation wide entrance examination to get admission in to IIT Kharagpur in 2001,

* Scored 270/300 in TOEFL (Test for English as Foreign Language)

Oral Presentations & Posters

2008

A.S. Mallik, M. Jabareen, G. Bilic, D. Liekens, R. Zimmermann, J. Deprest, E. Mazza, A.H Zisch; "A Novel ex vivo platform to Develop Fetoscopic Closure Technique for Punctured Fetal Membranes"; TERMIS (Tissue Engineering International and Regenerative Medicine Society), Porto, Portugal; 22-26 June 2008; (Oral Presentation: A.S Mallik)

G. Bilic, S.M Zeisberger, **A.S Mallik**, R. Zimmermann, A.H Zisch; Comparative Characterization of Cultured Human Term Amnion Epithelial and Mesenchymal Stromal Cells for Application in Cell Therapy; TERMIS (Tissue Engineering International and Regenerative Medicine Society), Porto, Portugal; 22-26 June 2008; (Poster)

A.S Mallik, M. Jabareen, E.Mazza, A.H Zisch; "Comparison of Mechanical and Biochemical Properties of Human Fetal membranes"; EuroSTEC (European Soft Tissue Engineering for Congenital Birth Defects), Uppsala, Sweden, 5-6 June 2008 (Oral Presentation: A.S Mallik)

Jabareen, M, **Mallik, A**., Bilic, G., Mazza, E., and Zisch, A., "Mechanical and Histological Characterization of Human Fetal membranes", Reproductive Bioengineering, Wenns im Pitztal, Austria; April 1-5, 2008 (Oral Presentation: Jabareen, M.)

2007

A.S Mallik, G. Bilic, R. Zimmermann, A.H Zisch; "A novel ex vivo model for development of closure techniques for ruptured fetal membranes"; IFMSS (International Fetal Medicine and Surgery Society); Aruba, The Netherlands; April, 2007 (Oral Presentation: A.S Mallik)

2006

A.S. Mallik, M.A. Fiechter, S. Rieder, G. Bilic, S. Stergioula, J. Henke, K.T.M. Schneider, E. Biemer, R. Zimmermann, A.H. Zisch, N.A. Papadopulos; "Successful Closure of Fetal membrane defects using Manufactured Decellularized Human Amnion Membrane after fetoscopy in the Mid-gestational Rabbit model"; IFMSS (International Fetal Medicine and Surgery Society); Hawai, June, 2006 (Oral Presentation: G Bilic)

Publications

2009

Grozdana Bilic, Carrie Brubaker, Philip B. Messersmith, **Ajit S. Mallik**, Elisa Done, Leonardo Gucciardo, Steffen M. Zeisberger, D. Liekens, Jan Deprest, Roland Zimmermann, Andreas H. Zisch; Injectable sealants for fetal membrane repair: Bonding and toxicity in vitro; American Journal of Obstetrics & Gynecology; 2009 (Manuscript Accepted)

2008

Grozdana Bilic*, Steffen M. Zeisberger*, **Ajit S. Mallik**, Roland Zimmermann, Andreas H. Zisch; Comparative characterization of Cultured Human term Amnion Epithelial and Mesenchymal Stromal Cells for Application in Cell Therapy; Cell

Transplantation; 2008; 17; 1-14 (*****Co- first Authors)

Jabreen M*, **Mallik A.S***, Bilic G, Zisch A.H, Mazza E; Relation between mechanical properties and microstructure of human fetal membranes: An attempt towards quantitative analysis; Eur J of Obst & Gyne and Reproductive Biology (Submitted) (***** Co-first Authors)

2007

Mallik AS, Fichter MA, Rieder S, Bilic G, Stergioula S, Henke J, Schneider KT, Kurmanavicius J, Biemer E, Zimmermann R, Zisch AH, Papadopulos NA; Fetoscopic closure of punctured fetal membranes with acellular human amnion plugs in a rabbit model; Obstet & Gynecol. 2007 Nov; 110(5): 1121-9

Jegger D, **Mallik AS**, Nasratullah M, Jeanrenaud X, da Silva R, Tevaearai H, von Segesser LK, Stergiopulos N; The effect of a myocardial infarction on the normalized time-varying elastance curve; J of Appl Physiol. 2007 Mar; 102(3): 1123-9

2006

Jegger D, Jeanrenaud X, Nasratullah M, Chassot PG, **Mallik A**, Tevaearai H, von Segesser LK, Segers P, Stergiopulos N; Noninvasive Doppler-derived myocardial performance index in rats with myocardial infarction: validation and correlation by conductance catheter. American journal of Physiology. Am J of Heart and Circulatory Physiology; 2006 April; 290(4): H 1540-8

2005

Cornelia C. Weber, Hao Cai, Martin Ehrbar, Hisashi Kubota, Georg Martiny-Baron, Wilfried Weber, Valentin Djonov, Ernst Weber, **Ajit S. Mallik**, Martin Fussenegger, Karl Frei, Jeffrey A. Hubbell, Andreas H. Zisch; Effects of protein and gene transfer of the Ang-1 fibrinogen like receptor binding domain for endothelial and vessel organization. The Journal of Biological Chemistry; 2005 June 10; 280 (23): 22445-53